RECEIVED
LAWRENCE
RADIATION LABORATORY

FEB 26 1970

LIBRARY AND
DOCUMENTS SECTION

UCRL-19445

c.2

AN ELECTROPHYSIOLOGICAL AND SCANNING ELECTRON MICROSCOPIC INVESTIGATION OF INTERCELLULAR COMMUNICATION BETWEEN NORMAL AND BETWEEN CANCER CELLS IN TISSUE CULTURE

Paul Harris O'Lague
(Ph.D. Thesis)

November 1969

AEC Contract No. W-7405-eng-48

TWO-WEEK LOAN COPY

This is a Library Circulating Copy which may be borrowed for two weeks.
[redacted]

LAWRENCE RADIATION LABORATORY
UNIVERSITY of CALIFORNIA BERKELEY

UCRL-19445

DISCLAIMER

This document was prepared as an account of work sponsored by the United States Government. While this document is believed to contain correct information, neither the United States Government nor any agency thereof, nor the Regents of the University of California, nor any of their employees, makes any warranty, express or implied, or assumes any legal responsibility for the accuracy, completeness, or usefulness of any information, apparatus, product, or process disclosed, or represents that its use would not infringe privately owned rights. Reference herein to any specific commercial product, process, or service by its trade name, trademark, manufacturer, or otherwise, does not necessarily constitute or imply its endorsement, recommendation, or favoring by the United States Government or any agency thereof, or the Regents of the University of California. The views and opinions of authors expressed herein do not necessarily state or reflect those of the United States Government or any agency thereof or the Regents of the University of California.

TABLE OF CONTENTS

Page

INTRODUCTION 1

Electrical Coupling 3

1. Excitable Cells 3

2. Non-excitable Cells 4

A. Adult Tissues 9

B. Embryonic Tissues 10

C. Cells in Tissue Culture 12

The Role of Calcium and Magnesium in the Formation of Low-Resistance Junctions 16

Cell-Cell Tranfer of Molecules 19

Comments on Cell Interaction in Culture 23

A. Contact Inhibition of Movement 23

B. Density Dependent Inhibition of Cell Division. 25

MATERIALS AND METHODS 28

1. Cell Culture 28

2. Mechanical Setup 32

3. Optical Setup 33

4. Electrical Setup 34

5. Fixation and Scanning Electron Microscope 46

Page

RESULTS 49

Proliferation Rate of Fibroblasts in Culture 49

Electrical Coupling Between Secondary Fibroblasts.. 52

Formation of Low-Resistance Junctions 63

Estimation of the Specific Junctional Resistance between Isolated Fibroblasts 66

Coupling in Proliferating Cultures, Primary Cell Cultures and Cells Cultured on Bacterial Dishes ... 68

Loss of Coupling Following Cell Injury 73

Coupling in Cells Infected with Rous Sarcoma Virus. 80

Scanning Electron Micrographs of Coupled Fibroblasts 92

Scanning Electron Micrographs of Coupled Cells - One in Mitosis 111

Scanning Electron Micrographs of Rous Sarcoma Cells 119

Tight Junctions in Secondary Fibroblasts 134

Related Electrical Phenomena - Membrane Potentials of Secondary Fibroblasts 139

DISCUSSION 145

CONCLUDING REMARKS AND FUTURE OUTLOOK 160

SUMMARY 164

APPENDIX 167

BIBLIOGRAPHY 182

LIST OF FIGURES

		Page
1	Electrical circuit diagrams illustrating the steady state behavior of uncoupled and coupled cells.	6
2	Electrical setup used for junctional coupling measurements on cells in tissue culture.	38
3	Proliferation rate of secondary chicken embryo fibroblasts.	50
4	Phase contrast pictures of living normal secondary fibroblasts in culture.	53
5	Phase contrast photograph of two normal secondary fibroblasts in contact.	55
6	Phase contrast picture of two living normal secondary fibroblasts connected by a thin cytoplasmic process.	57
7	Two electrically coupled normal fibroblasts connected by a 50μ bridge.	59
8	The formation of junctional coupling between two secondary fibroblasts.	64
9	Coupled normal secondary fibroblasts within a confluent monolayer.	69
10	Normal chicken embryo primary cells (top) electrically coupled.	71
11	Normal secondary fibroblasts on bacterial dishes.	74
12	The loss of junctional coupling after cellular injury	76
13	Rous focus formation showing beginning morphological transformation of normal fibroblasts.	81

		Page
14	Coupling between two early Rous transforming fibroblasts.	85
15	Transforming fibroblast cells in a culture infected with Rous sarcoma virus.	87
16	Coupling between two transformed Rous sarcoma cells.	89
17	Two normal coupled fibroblasts.	94
18	Scanning electron micrographs of the coupled pair shown in the previous figure.	97
19	The establishment of junctional communication between fibroblasts.	100
20	Scanning electron micrographs of coupled cells shown in previous figure.	102
21	Coupled fibroblasts in a confluent monolayer	107
22	Scanning electron micrograph of the same field as shown in the previous figure.	109
23	Phase contrast picture of two normal fibroblasts impaled with microelectrodes.	114
24	Scanning electron micrographs of a coupled cell pair - one in interphase, the other in metaphase.	116
25	Scanning electron micrograph of a communicating cell pair.	120
26	Scanning electron micrographs of a mitotic fibroblast in junctional communication with an interphase cell.	123
27	Phase contrast picture of functionally coupled normal fibroblast cells.	125

		Page
28	Scanning electron micrographs of two coupled cells at an early stage of Rous sarcoma virus transformation.	128
29	Scanning electron micrographs of a Rous sarcoma transformed fibroblast in culture.	131
30	Transmission electron micrograph of two normal secondary cells.	135
31	Same as Figure 30.	137
32	Histograms of membrane potentials from normal chick embryo secondary fibroblasts.	140
33	High-input impedance Field Effect Transistor operational amplifier design.	168

ABSTRACT

Intercellular communication between normal chick embryo fibroblasts and between fibroblasts transformed with Rous sarcoma virus in culture was studied with intracellular microelectrodes. The results of this study show that coupling is present between normal chick fibroblasts (including cells in mitosis) in proliferating cultures and between cells in 'density dependent inhibited' cultures. In the case of cancerous (Rous transformed) fibroblasts, the results further show that coupling is present when the transformation appears in the Rous infected cells and remains present thereafter in these cells.

Coupling between cells in culture is not an artifact of the microelectrode technique but is shown to be due to cell's ability to form low-resistance junctions. In favorable cases, the specific resistance of the junctional membranes was approximated using a simple electrical equivalent circuit of a coupled cell pair. This specific resistance was found to be several orders of magnitude smaller than that of the non-junctional membranes ($0.12\,\Omega\text{-cm}^2$ as compared to $400\,\Omega\text{-cm}^2$). Possible effects

of low-resistance junctions on the behavior of cells in culture are discussed. The lability of the low-resistance junctions between fibroblasts in culture has been demonstrated by showing that injured fibroblasts readily uncouple from neighboring cells without interrupting coupling between healthy uninjured cells.

A method is presented to allow a study of the cellular morphology of previously electrically tested coupled cells with the scanning electron microscope. With this technique, it was possible to show that cellular processes which eventually reach neighboring cells, underlap them and form low-resistance junctions. In addition, during the course of Rous sarcoma virus transformation the cytoplasmic processes of the infected cells shrink, the number of processes decreases and become filamentous and eventually disappear. The surface of the completely transformed cancer cells exhibits invaginations not seen in normal cells. A transmission electron microscopic study on the contact area between tissue culture cells previously tested for coupling now appears feasible with this technique.

Preliminary studies on cellular membrane potentials of normal fibroblasts in culture as measured with intra-

cellular microelectrodes show that the potentials of isolated cells in proliferating cultures are significantly lower than those of cells within a confluent monolayer where cell division is inhibited. Possible permeability changes to specific ions are discussed as causes for the observed changes in the membrane potential values.

Finally, it is concluded that electrophysiological tools, combined with tissue culture techniques, autoradiography and electron microscopy offer new ways of attacking the problems of animal cell interactions.

ACKNOWLEDGEMENT

I would like to express my appreciation to Professors Cornelius A. Tobias and Harry Rubin for the use of their facilities, for their help and discussions during the course of this work.

The collaboration with and assistance of Dr. Helge Dalen in the scanning electron microscopic investigation was most valuable to me.

Appreciation is gratefully extended to Carol Hattié for her tolerant and capable assistance with the tissue cultures.

I wish to thank Werner Schlapfer and A. Megid Mamoon for their valuable criticism during the course of this work.

Special gratitude is extended to the members of the LRL staff, especially to Peter Dowling, Delbert Coleman and Victor Jensen of the Machine Shop; to E. L. Benjamin, John Gurule, Arnie Steinman, Frank Upham and A. L. Windsor in Electronics; to John Flambard and company in Drafting; and to Marjory Simpson and Dorothy Denney in the Library for all their kindness and assistance in the many aspects involved in the compilation of this work. And to Dewey D. Dean for his wit and other sundry services.

I thank Professors H. Rubin, C. A. Tobias and P. O. Vogelhut for their careful reading of this thesis and their helpful suggestions. However, I assume full responsibility for any errors found in the final copy of this thesis.

The author is grateful for support for the period September 1966 through September 1969 as the holder of a training fellowship under the Biophysics Training Section of the National Institute of Health, Grant No. 5-TI-GM-829.

INTRODUCTION

Cells of multicellular organisms interact in special and rather complex ways which distinguish them from populations of single-celled organisms, such as bacteria and protozoa. The growth and division of each differentiated cell type within a multicellular organism must be regulated separately. This is often accomplished by means of chemical factors, such as hormones and specific growth substances. These factors operating over large distances to modify cell behavior are often classified within a humoral system of cellular interactions. Other interactions involve chemical factors which act only over short distances, perhaps a few cell diameters away. These types of short range interactions are exemplified in the induction of cytodifferentiation and morphogenesis in embryonic organ rudiments, as studied by Grobstein (1964), Auerbach (1964), Lash (1963) and others. In this case, one tissue type induces differentiation in another tissue type growing in close proximity but without cytoplasmic contact between the two tissues.

Cell - cell contact also acts as a regulating mechanism *in vivo* and in tissue cultures of animal cells (Stoker, 1967;

Curtis, 1964). The effects of contact apparently are inhibitory in nature, acting on cell movement (Abercrombie and Ambrose, 1958; Abercrombie and Heaysman, 1963; Abercrombie and Ambrose, 1962; Barski and Belehraderk, 1965) and on cellular division (Abercrombie and Ambrose, 1958; Stoker, 1967). Over the last six years it has been established, mainly through the use of electrophysiological methods, that a wide variety of cells both in vivo and in vitro form intercellular contacts so structured as to allow direct flow of substances from one cell interior to the next (Loewenstein, 1966; Furshpan and Potter, 1968). The role played by this type of cellular communication, as yet undetermined, may be of importance in mediating these regulatory effects on cellular movement and growth.

One major objective of this thesis has been to investigate electrophysiologically ionic cellular communication between normal chicken embryo fibroblasts and between virus transformed fibroblasts, growing under tissue culture conditions and to attempt to draw some conclusions about the correlation between the electrophysiological findings and the behavior of these cells in tissue culture.

As general background, a review of the literature on ionic communication or electrical coupling between a variety of cells is given, along with some comments on the anatomical

description of various contact specializations; this is then followed by a brief consideration of the evidence for transfer of substances other than ions between cells in contact; and finally a brief description is given of some phenomena of cell interaction in culture which closely relates to the material in this thesis.

ELECTRICAL COUPLING

1. Excitable Cells

Low resistance junctions were first discovered between excitable cells and are referred to as electrical synapses or electrotonic junctions. Briefly, these electrotonic junctions, unlike chemical synapses, permit the passive spread of potential changes directly from one cell to the next. These junctions are known to exist in a variety of excitable cells, both nerve and muscle. The most familiar is perhaps the vertebrate heart, where most muscle cells have extensive low-resistance connections with their neighbors. Electrical coupling also exists in several types of smooth muscles.

Electrotonic junctions have been studied in the nervous systems of annelids, molluscs, arthropods, fishes, amphibians and birds (Bennett et.al., 1967). On an anatomical basis,

much evidence has accumulated from electron micrographs which strongly suggests that tight junctions, i.e., contact areas between cells where the extracellular space has been occluded, are the structural basis for low resistance coupling between excitable cells (however, see later). For a more detailed account on both the anatomical and electrophysiological basis for electrical coupling between excitable cells the reader is referred to excellent reviews by Bennett et.al.(1967) and Furshpan and Potter (1968).

2. Non-excitable Cells

Before electrophysiological coupling measurements had been applied to non-excitable cells, electron microscopists were discovering tight junctions, strongly implicated as sites of electrical transmission between excitable cells, in a variety of non-excitable cells. Farquhar and Palade's now classical survey of junctional complexes in mammalian epithelia in 1963 showed that tight junctions (or zonula occludente as they defined them) are a constant feature of these complexes (Farquhar and Palade, 1963). Shortly after, investigators began accumulating evidence for low-resistance junctions between a variety of non-excitable cells.

The low-resistance junctions of non-excitable cells, like those of excitable cells, are sites at which potential changes spread passively and directly from one cell to the next. The mechanism of this electrical transmission can best be understood by first considering the case where two cells are closely opposed and where electrical transmission does not occur as in the case of the chemical synapse. It is experimentally known that the spread of ionic current along an axon is interrupted at a chemical junction. No direct electrical spread of current across a synapse can be detected even though the two cells are separated by less than 500Å (del Castillo and Katz, 1954; Hagiwara and Tasaki, 1958).

Two important factors contribute to this as can be seen with reference to the circuit diagram in Figure 1a. The first is that the two opposed cell membrane resistances Rc_1, Rc_2 act as a strong barrier to the flow of ionic current from one cell interior to the next. The second is that the ionic resistance (Figure 1a, R_s) of the synaptic cleft between the cells is low compared to the cell membranes bordering it. Ionic current passing through the presynaptic terminals leaves by way of the low-resistance pathway between the cells and essentially none travels through the parallel

FIGURE 1

Electrical circuit diagrams illustrating the steady state behavior of uncoupled (a) and coupled (b) cells. The microelectrodes (ME) are used either to inject intracellular pulses of ionic current or to measure the potential difference V_1 and V_2 across the membranes of cells 1 and 2.

In (a) an electrical equivalent circuit is shown of two cells separated by a low-resistance (R_s) extracellular space of 200-500Å as is the case at a chemical synapse. The electrical circuit for two coupled cells is shown in (b). In this case coupling arises because the junctional membranes have fused, occluding the extracellular space and hence eliminating the low-resistance pathway R_s (shown in (a)) as a current pathway. The junctional membrane resistance Rc is several orders of magnitude smaller than the non-junctional cell membrane resistances R_2 and R_1. Further details are described in the text.

a

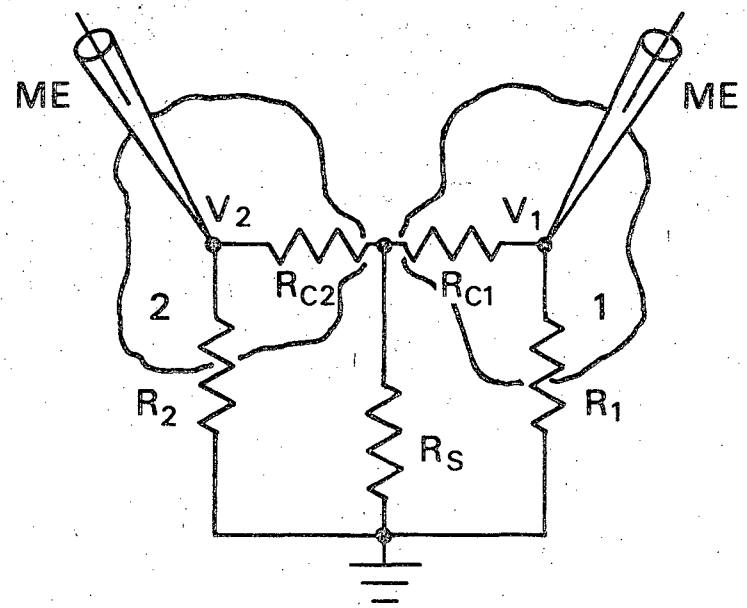

b

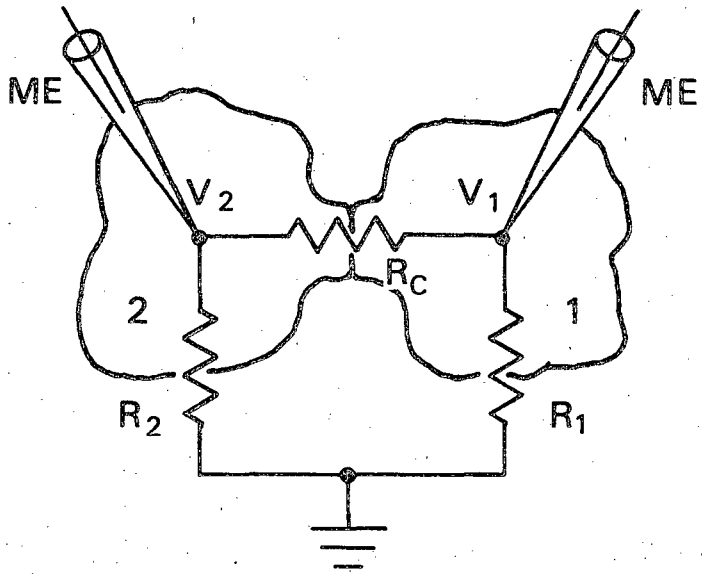

DBL 698-5009

pathway (Rc_1 and R_1), twice through the high resistance membrane of the post synaptic cell.

Both of the above two factors which prevent electrical transmission at a chemical synapse are altered in cells which are electrically coupled. This can be seen with reference to the circuit diagram in Figure 1b. The low ionic resistance pathway (R_s in Figure 1a) has been eliminated with the formation of a specialized contact between the cell membranes which occludes the extracellular space between them. The opposed cell membrane resistances Rc_1, Rc_2 in the junction region become several orders of magnitude smaller than either R_1 or R_2 (see Rc in Figure 1b); for instance, Rc may be as small as $1\Omega\text{-cm}^2$ as compared to $1000\text{-}3000\Omega\text{-cm}^2$ for R_1 and R_2 (Payton et.al., 1969). Now when current is supplied to Cell 2, the potential change in Cell 1 depends only on the resistances Rc and R_1. For example, if $Rc = R_1$, the voltage in Cell 1 would differ from that in Cell 2 by a factor of only two.

This mechanism of electrical transmission or electrical coupling as described above has been found to operate between non-excitable cells in a variety of tissues, including adult and embryonic and in tissue culture.

A. Adult Tissues

Kuffler and Potter in 1964 reported electrical coupling between glia cells in the leech. These cells are known to be electrically inexcitable (Kuffler and Potter, 1964). Loewenstein and Kanno at about the same time demonstrated tight coupling between salivary gland cells of *Drosophila* (Loewenstein and Kanno, 1964).

A variety of cells in adult vertebrate tissues are now known to be electrically coupled. These have been found in toad urinary bladder (Loewenstein et.al., 1965) mammalian liver (Penn, 1966) and amphibian skin (Loewenstein and Penn, 1967). Electrical junctions exist between amphibian glia cells (Kuffler et.al., 1966), between cells in rabbit gall bladder, amphibian meningial membranes and between cells in the epithelium of the small intestine of the mouse (Furshpan and Potter, 1968). Tight junctions have been observed in most of these cases and although other junctions are present in epithelia, evidence on coupling in excitable cells suggests that here also, coupling is a result of tight junctions (however, see Revel and Sheridan, 1968, for a possible exception). "Septate desmosomes" which may be responsible for coupling in some invertebrates such as *Drosophila* and the

midge Chironomus Thummi (Bullivant and Loewenstein, 1968) have not been observed in vertebrates. For excellent reviews on the morphology of junctional contacts between non-excitable cells the reader is referred to Fawcett (1961, 1966), Farquhar and Palade (1963) and Furshpan and Potter (1968).

B. Embryonic Tissues

Low resistance junctions are now known to have wide distribution during development, as well as widespread occurrence in adult tissues. Coupling measurements have been made in various embryos including squid, chick and amphibian.

In the squid embryo where cleavage is meroblastic Potter et.al. (1966) found that from stage 10, the earliest studied, through stages 25-26 (numbering system after Arnold, see Potter et.al., 1966), all cells tested (450) are electrically coupled to the yolk cell. These include cells in the epidermis of tentacle, mantle, fin, funnel, gills, outer yolk-sac membrane and anal papillia; deep, presumably medodermal cells in the tentacle, gill and fin; developing receptor cells of the retina; cells in the otocyst, in visceral

and optic ganglia, blood vessels, and in two layers of the beating heart. They conclude that "...the cytoplasm of the embryo is a continuous compartment for the current - carrying ions, a compartment isolated from extracellular space by the high resistance of the non-junctional cell membrane...." This statement appears to be true up to stage 25, since during stage 25-26 coupling between the yolk cell and all the tissues tested is lost. However, there is evidence that like cells of some tissues remain coupled to one another as is the case in gill epithelium (Potter et.al, 1966).

Sheridan (1966, 1968) has likewise demonstrated the presence of widespread coupling in the early chick embryo. Low-resistance connections found in the same tissue are ectoderm, notochord, neural plate, mesoderm and Hensen's node; in different tissues, coupling exists between notochord and neural plate, between notochord and neural tube, between notochord and mesoderm. Parallel studies with the electron microscope carried out by Trelstad et.al., (1967) on the chick detected only two morphological specializations, close junctions (apposed plasma membranes closer than 100Å) and tight junctions.

Ito and Hori (1966) and Ito and Loewenstein (1969) have shown that cells of <u>Triturus</u> embryos are tightly coupled

from early cleavage through morula stages. The latter investigators have demonstrated quite strikingly that even cells (macromeres) isolated from the morula and from each other, when manipulated into contact rapidly form a coupled system in which the plasma membranes in contact differentiate into a low-resistance junction.

Cells of cleavage stages and blastulae (Slack and Palmer, 1969) and cells in later (neurula) stages (Sheridan, unpublished observation) of the amphibian Xenopus Laevis are known to be electrically coupled, as are the blastomeres of Rana pipiens eggs (Woodward, 1968). And, finally, extensive coupling has been demonstrated in a few lobster embryos at about the 100-cell stage (Furshpan and Potter, 1968).

It appears from the above findings that low-resistance junctions are not exclusively a property of adult tissues, for evidently a large proportion, if not all, of the cells in early embryos of the invertebrate and vertebrate species studied are coupled.

C. Cells in Tissue Culture

Electrical coupling between normal cells of established mouse and hamster lines 3T3 and BHK in tissue culture was

first reported by Potter et.al (1966). Cells of the same lines transformed by polyoma and SV40 viruses were also shown to be effectively coupled by these workers. Since their first report, Furshpan and Potter (1968) have performed coupling experiments on cells in tissue culture to include among "normal" cells; (1) primary cells from the spleen, kidney, and heart of newborn mice and from spleen and kidney of newborn rats; (2) two serially propagated lines of diploid human lung fibroblasts (WI-26 and a line obtained from Baltimore Biological Labs); (3) a line of diploid minnow fibroblasts also obtained from BBL; (4) serially propagated fibroblasts from baby hamster kidney BHK 21/13. In all cases the results were the same, whenever two cells appeared to be in contact they were effectively coupled, whether or not the cells were sparsely or densely packed. It is know that tight junctions frequently occur between fibroblasts in culture (Devis and James, 1964; Martinez-Palomo et.al., 1969). This suggests that in tissue culture cells, as well as those in vivo, coupling is probably a result of tight junctions.

Among the cells transformed with carcinogenic viruses that these workers tested were baby hamster kidney cells (BHK) transformed by polyoma virus (Dulbecco's Py cells; Stoker's PyY) and mouse embryo cells (3T3) transformed

either by Polyoma or SV40 viruses, or both. Electrical coupling in these cells was indistinguishable from that of the untransformed parent. Coupling was also found between BHK cells and their polyoma-transformed derivative (Py19), between normal mouse embryo cells (3T3) and transformed hamster cells (Py19); and between BHK and Py3T3.

Two cell lines (S-180I, S-180-II) derived from the Crocker mouse sarcoma (S-180), a transplantable sarcoma adapted to grow in culture were also tested for electrical coupling. In both cell lines nearly all cells remaining in the same medium for more than 4 or 5 days were well coupled. However, replacing the old medium by fresh medium caused a large decrease in coupling between cells. This loss of coupling was first detected at about 15 hours after the medium change and was maximal between about 24 and 28 hours. Coupling recovered progressively over a few days, depending on cell density (Furshpan and Potter, 1968).

It is of interest to note that *in vivo* cancerous cells which have been tested by Loewenstein and his colleagues lack coupling. Loewenstein and Kanno (1967) tested both primary and transplatable hepatomas in which the tumor was excised and impaled with microelectrodes *in vitro*. Coupling was not detectable between cells in any of the tumor nodules, whereas normal liver cells were well coupled. (However, coupling

between cells in liver tumors *in vivo* has been found by Sheridan, 1968a). These results have been extended to cancerous thyroid epithelium (Jamakosmanovic and Loewenstein, 1968) and cancerous human stomach epithelium (Kanno and Matsui, 1968); as well as two lines of liver cancer cells and certain X-ray transformed embryonic epithelioid cells in tissue culture (Loewenstein, 1968). In no case was coupling detected in the cancerous cells, whereas their normal counterparts were tightly coupled. Recently, Higashino, Borek and Loewenstein (unpublished) have found coupling between cultured fibroblasts transformed by X-radiation.

Thus, electrical coupling between cancer cells has been observed in some cases and not in others. These results suggest that even with the supposition that low-resistance junctions play a role in growth regulation, there is no reason to assume that there exists a simple relationship between the lack of coupling and the defective growth control generally found among cancer cells. (Furshpan and Potter, 1968).

THE ROLE OF CALCIUM AND MAGNESIUM IN THE FORMATION OF LOW-RESISTANCE JUNCTIONS

The available information on the formation of low-resistance junctions between various types of cells is scant. The only systematic study on this problem was carried out by Loewenstein (1967). He investigated the formation of junctional communication between isolated sponge cells, Microciona prolifera and Haliclona occulata. He found that within minutes after two dissociated sponge cells were brought into mechanical contact, a low-resistance junction was formed between them. Ca^{++}, Mg^{++} and an organic factor, the same elements which are required for cellular adhesion (Galtsoff, 1925; Humphreys, 1963; Moscona, 1963) were found to be necessary in this junction formation. In the absence of either Ca^{++} (and Mg^{++}) or the organic factor, coupling failed to be established; and upon withdrawal of the former, established coupling was broken.

Loewenstein has proposed the following hypothesis to account for the permeability differentiation during junctional formation between cells (Loewenstein, 1967a): Ca^{++} and Mg^{++} are detached from the junctional membranes once these are incorporated into the intracellular compartment wherein Ca^{++}

and Mg^{++} activities are below 10^{-5} (see Hodgkins and Keynes, 1957). The driving force maintaining the low intracellular Ca^{++} and Mg^{++} activities is some form of continuous energy dependent active transport of these ions, out of the cytoplasm across the non-junctional membrane surfaces; and the starter of the differentiation processes is the formation of perijunctional insulation, i.e., the sealing around the low-resistance junction.

Support for this hypothesis has been reported in one cell system (Politoff et.al., 1967; Loewenstein et.al., 1967) but not in another (Payton et.al., 1969). Consistent with this hypothesis are the findings of Politoff et.al (1967, 1968) which show that junctional membrane permeability between salivary gland cells of Chironomus depends on a supply of metabolic energy. Exposure of these cells to low temperature or to various chemical metabolic inhibitors, such as dinitrophenol, cyanide, oligomycin and N-ethylmaleimide causes uncoupling, whereas ouabain, the specific inhibitor of Na^{+} and K^{+} -activated ATPase does not. Moreover, intracellular injection of ATP prevents uncoupling in the case of dinitrophenol.

Also consistent with the above hypothesis are the observations by Loewenstein (1966) and Loewenstein et.al. (1967) that raising the cytoplasmic Ca^{2+} concentration by injecting Ca^{2+} ions into salivary gland cells of Chironomus with a fine micropipette causes sealing of the junctional membranes (equivalent injections of other ions such as K^+ produce no sealing).

However, in another cell system evidence for an energy dependent junctional permeability was not observed. At the electrical synapses located at the septum of the lateral giant axon of crayfish (Procambarus) Payton et.al. (1969) have shown that lowering the temperature from 20° to $5^{\circ}C$ rapidly causes a four-fold increase in junctional membrane resistance. This effect differs from that observed in Chironomus salivary gland cells, where uncoupling has a slow onset and is associated with considerable depolarization of the cells (Politoff et.al., 1967). Payton et.al. (1969) state that the relatively rapid time course in the septate axon suggests that there is a direct effect on the junctions themselves, (i.e., such as membrane structure at the junction being affected by temperature) rather than an indirect action through a reduction of metabolic pumping, as postulated for the Chironomus cells.

At present too few experiments have been reported to critically evaluate Loewenstein's hypothesis.

CELL - CELL TRANSFER OF MOLECULES

That substances other than inorganic ions might also diffuse between cells by way of low-resistance junctions was suggested early in 1964 by Kuffler and Potter and by Loewenstein and Kanno.

Physiological tests for cell-to-cell transfer in a number of cell systems have been made by injecting fluorescent substances intracellularly through micropipettes. Fluorescein (mol.wt. 332) has frequently been used as a tracer for these tests because it can be detected at very low concentrations by fluorescent microscopy. At these low concentrations this water soluble dye does not appear to be highly toxic to the cells tested, though this dye may bind, to some extent, to components of cytoplasm (Gurr, 1960). Cases in which coupled cells exchange fluorescein rather rapidly are those in the salivary gland of *Drosophila* (Kanno and Loewenstein, 1964); at the electrical synapse of the crayfish (Pappas and Bennett, 1966) and at the same synapse in the lobster (Furshpan and Potter, 1968). Cells in tissue culture which have been tested and have been found to transfer the dye include BHK 21/13, the transformed cells PyY and the sarcoma cells (S-180II) (Furshpan and Potter, 1968).

One exception to the spread of fluorescein between coupled cells has recently been reported by Slack and Palmer (1969). In cleavage stages and blastulae up to stage 7 in Xenopus Laevis eggs, fluorescein injected into a cell spread to the margins of the injected cell but no further. Coupling was present and was unaffected by the presence of fluorescein. The possibility that fluorescein may bind strongly to some cytoplasmic component in this case must, as the authors themselves suggest, be considered as one explanation for the dye's inability to diffuse across the junctions. Another possibility, however, is that only very small amounts of fluorescein diffused through the junction and was not detected. Whatever the explanation, this case is the only exception among those cells tested with fluorescein to date. In the above cases in which transfer of the dye occurs it is not know if the dye passes from one cell to the next through low-resistance junctions or by other routes.

The experiments demonstrating rapid cell-to-cell transfer of fluorescein complement recent experiments on intercellular transfer of molecules using a genetic method. Both Subak-Sharpe et.al. (1969) and Stoker (1967a) have

demonstrated metabolic cooperation between cells in culture. Metabolic cooperation is defined as the process whereby the metabolism of cells in contact is modified by exchange of materials (Subak-Sharpe et.al., 1969).

Subak-Sharpe et.al. (1969) have demonstrated that cells of a genetic variant of the hamster fibroblast line BHK 21 which lack inosinic pyrophosphorylase activity (termed IPP^- cells) and, therefore, cannot normally incorporate ^3H - hypoxanthine in culture, do in fact incorporate this substance when these deficient cells are in direct or indirect contact with cells of BHK 21 sublines which have inosinic pyrophosphorylase activity (IPP^+ cells) and do incorporate ^3H- hypoxanthine in culture. Cell-to-cell contact appears to be essential for this gain of a metabolic function by IPP^- cells, for IPP^- cells not in contact with IPP^+ cells but in the same dish do not gain this function. The transferred molecules participating in this are not known but may have been nucleotide, nucleic acid, the enzyme or substances involved in its synthesis (Subak-Sharpe et.al., 1969)

Stoker (1967a) has now shown that the defective hamster cells (IPP^-) also incorporate label when they are

in contact with normal mouse embryo cells. Again, increased incorporation does not occur in IPP$^-$ cells in the same dish which are not in contact with normal mouse cells.

Both of the above results suggest direct transfer of substances (possibly including growth regulating molecules) between cells in contact. However cells add and remove a variety of molecules in their immediate environment and there must exist a series of concentration gradients which extend outwards from the cell membranes. If these gradients fall off rather abruptly then another explanation of what appears to be direct transfer between contacted cells in culture may be the release and absorption of substances between cells whose cell membranes are closely opposed but not in contact (Stoker and Rubin, 1967). Further experiments are needed to determine what role each mechanism plays in the transfer of substances between cells. Also, if direct transfer of metabolic substances does occur it still remains to be shown whether these substances pass through the low-resistance junctions studied by the electrophysiologists.

COMMENTS ON CELL INTERACTION IN CULTURE

Mammalian cells in culture affect their neighbors in various ways. The phenomenon of inhibition of movement associated with cell contact in culture has been well documented (Abercrombie and Ambrose, 1958) and that of cell division somewhat less (Stoker, 1967). The sensitivities of normal cells and tumor cells to both of these phenomena differ.

A. Contact Inhibition of Movement

Abercrombie and Heaysman (1953, 1954) and Abercrombie and Ambrose (1958) studied contact inhibition of movement of cells in culture a number of years ago. These workers demonstrated that in the case of normal fibroblasts their movement is regulated by cell contact. These contacts occur when ruffled membrane of one cell meets a neighboring cell. Time-lapse cinematography has shown that actual "contact" between the cells is required for inhibition of movement (Abercrombie and Ambrose, 1958). The films show that at points of contact the active ruffled border of cells is immobilized and the cells then cease to move toward, or over, each other. Contacts between the cells

usually break after a period of time. However, these intercellular adhesions appear to be very stable since they do not break rapidly. Cells appear to be only able to rupture them as a result of a very active membrane movement on the solid substrate in a region of the cell which is not attached to another cell. Considerable distortion in the shape of the cell occurs in the region of contact before rupture takes place (Ambrose and Forrester, 1968).

The making and breaking of cell contacts and regulation of movement between cells as described above was observed in many isolated secondary fibroblasts which were tested for low-resistance junctions(this thesis). As will be shown in the results, coupling was found between these cells at all stages of contact which were tested.

In contrast to the contact behavior between normal cells, it was shown that certain mouse tumor cells are not inhibited by contact but move over one another and also over normal cells (Abercrombie et.al., 1957). In general, cells derived from tumors or transformed by carcinogenic viruses are contact-inhibited to a lesser or undetectable degree. However, some tumor cells appear

to be subject to contact inhibition of movement when in contact with normal cells, but not with one another (Stoker, 1964; Barski and Belehradek, 1965).

B. Density Dependent Inhibition of Cell Division

It is known that normal cells are commonly limited in their multiplication in surface cultures to a saturation density which is characteristic of the cell type. When fibroblasts that are sensitive to contact inhibition of movement approach saturation density, their proliferation rate decreases and eventually approaches zero, provided they remain in the same medium (Green and Todaro, 1967). This appears not to be caused by any limitation of ordinary nutrients, as transfer of the population by trypsinization (Levine et.al., 1965) into the same medium (Todaro and Martin, 1967), will result in the resumption of cell division of "density dependent inhibition" (Stoker and Rubin, 1967) and appears to be another contact-promoted regulation process.

A permanent decrease in sensitivity to this type of inhibition occurs in many types of tumor cells (Stoker, 1967). Rous and polyoma-transformed fibroblasts, unlike their parent cells, are known to grow into multi-

layers of cells, indicating the absence of inhibition in completely surrounded cells (Temin and Rubin, 1958; Vogt and Dulbecco, 1960; Stoker and Macpherson, 1961). Release from density dependent inhibition has been recently demonstrated on chick embryo fibroblasts infected with Rous sarcoma virus (Rubin and Colby, 1968).

In light of the differences between Rous sarcoma cells and normal chick embryo fibroblasts with relation to the regulation processes described above, the study presented in this thesis was undertaken to determine if ionic communication in some way reflects these differences. Moreover, the only electrical measurements on coupling between normal and transformed fibroblast cells in culture were done on cells many generations removed from the cells originally transformed (Potter et.al., 1966; Furshpan and Potter, 1968). The physiological measurements on cellular coupling during the early phase of fibroblast transformation are presented in this thesis.

In addition, this thesis includes a study at the scanning electron microscopic level of the contact

morphology between pairs of cells in tissue culture which have previously been checked for junctional coupling with standard electrophysiological techniques.

MATERIALS AND METHODS

1. Cell Culture

Falcon plastic tissue culture dishes of 60mm outside diameter (approximately 21 cm^2 bottom surface area) were used in all experiments unless otherwise indicated.

The basic medium used throughout the experiments was medium 199 obtained from Grand Island Biological Company. This medium was supplemented with 2% tryptose phosphate broth (Difco), 1% calf serum and 1% chicken serum (Microbiological Associates), and was designated medium 2-1-1. Medium 2-1-1 was augmented with 10 units/ml of Penicillin G (Lily), 5 mg/ml dihydrostreptomycin sulfate (Pfizer) and 0.5 γ /ml fungizone (Squibb).

The balanced salt solution used for all cell washes and resuspensions was tris-saline with the following composition per liter: 3.0 g Sigma Trizma Base; 8.0 g NaCl, 0.38 g KCl; 0.10g Na_2HPO_4: 1.0 g glucose; 10^4 units pencillin; 5.0 mg dihydrostreptomycin. The pH was adjusted with concentrated HCl to 7.4. This solution had a final osmotic pressure of 305 milliosmoles as measured with a Fiske osmometer. A Difco 1:250 trypsin made tris-

saline was used to detach cells from the bottom of the dish for counting (see below).

Chicken cells designated as "primary" and "secondary" cells were used in all experiments. Primary cells are obtained directly from the embryo and are plated once, whereas secondary cells are once replated primary cells.

Primary cells were prepared as follows: ten day old White Leghorn Strain 813 chicken embryos were used. The embryo was carefully removed from the shell, its head and viscera removed and discarded, the remainder of the embryo was then rinsed with tris-saline, minced with a scoopula and stirred magnetically in 10 ml of 0.25% trypsin for approximately 10 minutes. Following this period, large clumps of cells were allowed to settle to the bottom of the flask and the remaining trypsin cell suspension was poured into a 40 ml centrifuge tube containing 16 ml of cold 199, plus 4 ml calf serum. Six ml of 0.25% trypsin was added to the flask and stirred continually for a five minute period. The resulting clumps were again permitted to settle out and the remaining solution was added to the centrifuge tube. The cell suspension was then centrifuged for five to ten minutes at 200x g and the cell pellet re-

suspended in 20ml of warm 2-1-1 medium. This solution was allowed to stand for five minutes or so to permit any large clumps to settle out and the top fluid was then pipetted into a sterile test tube. This suspension was counted in a hemacytometer and approximately 8 x 10^6 cells in 1.5ml or less were seeded into 10ml of 2-1-1 in a 100mm diameter plastic dish. These dishes were incubated in a 5%-10% CO_2 air atmosphere (pH 7.4-7.6) at a temperature of 37°C. After three to four days the medium was removed and the dishes overlayed with 2-1-1 medium containing 0.36% agar (Difco).

These primary cultures were then processed in the following manner to obtain what are called secondary cells: primary cultures with initial seeding of 8 x 10^6 cells per plate were used after four to five days of incubation. The medium was removed from the primary cells which were then twice washed with warm tris-saline. Five ml of 0.5% trypsin was added and the dishes incubated at 39°C for from eight to ten minutes. The cells were then gently agitated with a rubber policeman, pipette-rinsed once or twice and then pipetted into a 12ml centrifuge tube. This cell suspension was centrifuged for three minutes at 200 x g and resuspended in 5 ml of warm fresh

medium 2-1-1. A 1:100 dilution of this suspension was counted on the Model B Coulter Counter (Coulter Electronics, Inc.) and appropriate dilution was made to seed 2×10^{-5} cells into 60mm-diameter tissue culture plates containing 5ml of 2-1-1. All experiments were done with secondary cells unless otherwise indicated. Nearly all cells appeared to be fibroblasts. Rous sarcoma transformed cells were obtained by adding 5×10^{6} focus forming units of the Bryan strain of Rous sarcoma virus (RSV) per 60mm plate to freshly plated normal secondary cells in 2-1-1 (Temin and Rubin, 1958; Rubin, 1960).

The number of cells on a plate was determined by the following procedure: the medium was removed and the plate was washed with 5 ml tris-saline. This saline was then removed and 0.5 ml of 0.25% trypsin was added and agitated to assure complete coverage of the bottom of the dish by the trypsin solution. The dishes were then incubated for 15 minutes at 39°C and 2ml of tris-saline was then added and agitation was continued by repeatedly pipetting the cell suspension over the bottom of the dish with a hand pipette. Depending on the number of cells expected, the suspension was either counted undiluted in

glass vials (Kimble #60930) or diluted with 7.5ml tris-saline and then counted with a Model B Coulter Counter (Coulter Electronics, Inc.).

2. Mechanical Setup

To insure minimum vibration of the microelectrodes in these experiments, a large heavy wooden table was mounted on specially designed shock mounts (Barry Isolators Y94-AB-150, Barry Controls, Inc.). A heavy metal plate which was mounted on four shock absorpent pads at each corner (Kinetics Corporation) was placed on the table top. Next, a layer of ordinary packaging insulation wire mesh padding was placed on the large metal plate. Another metal plate on which was mounted the micromanipulators, Tiyoda microscope plus both cameras (see below) and lead bricks (150 lbs.) were placed on the padding. A shelf near the bottom of the table was loaded with approximately 500 lbs. of lead bricks.

The electrodes were held and positioned at an angle of 45° with single and double Narishigo Manipulators MM3 and MMD4, respectively (Eric Sobotka, Inc.) which were bolted to the upper metal plate. All positioning of the microelectrodes near the cell membranes was accomplished by a transmission

cable attachment to the fine horizontal adjust of the Narishigi Manipulators and turned manually at the front of the table. With this arrangement, movements as precise as a micron or so appeared possible. All joints on the structure carrying the manipulators were covered with duxseal (Johns-Manville Co.) which aided in reducing the vibration.

The above mechanical arrangement reduced vibrations of the microelectrodes satisfactorily as determined with a gravity accelerometer. A pulse vibration on the floor was reduced by more than 500 times at the microscope stage.

3. Optical Setup:

A basic Tiyoda Microscope #20200 was used throughout these experiments. Zeiss Phase Optics (condenser, x40 and x10 objectives) were added to the microscope to improve the optical image. Two of the three photographic ports contained cameras, a Polaroid in the left port and a 35mm Leitz camera in the right. The optical image could be switched from one port to another by moving the internal prisms of the microscope. All photographs of the cells were taken within a few minutes after microelectorde penetration.

4. Electrical Setup

It was necessary to take great care in the production of high resistance glass microelectrodes which had low tip potentials and which did not exhibit erratic behavior when current was passed through them. (Therefore, the steps in the microelectrode production will be described in detail.)

Long pieces of Kimble Glass #46485 of 0.7-1.0mm inside diameter were cut into approximately 11cm. segments and were washed thoroughly in a 1% solution of 7X detergent (Limbro Chemical Co.). The pieces of glass were then rinsed well in distilled water. They were boiled in distilled water for 10 minutes, and then boiled in 0.12 N HCl for an additional 10 minutes. The capillary glass segments were then rinsed once again in distilled water, boiled in triple distilled water for the same period of time and then boiled in ethyl alcohol (approximately 90°C). The ethyl alcohol was poured off and the segments were put in a covered petri dish and placed in the oven to dry. The cleaned glass tubes were stored in a stoppered test tube.

The glass micropipettes were formed on a conventional horizontal microelectrode puller. (John Keefe, Assoc., Cambridge, Massachusetts). The resulting microelectrodes had a tip diameter of 0.1 μ as determined by the scanning electron microscope. They were filled (see below) with a solution of 3MKCl which was freshly prepared and millipore filtered (0.2 μ size filter) for each new batch of microelectrodes. The pH of the filling solution was adjusted to 7 by adding freshly millipore filtered KOH as it was found that this gave electrodes with low tip potentials and the desired resistance.

The electrodes were filled in the following manner: after being pulled, the electrodes were placed tip down into the filling solution in a polystyrene container. After approximately 15 minutes to one-half hour the filling solution had moved into the tips by capillary action, filling approximately 10-20 μ of the electrode cylinder from the tip. Triple distilled water was injected into the back of the microelectrode with a #31 guage needle and syringe. The resulting distribution of liquids in the microelectrode was 3MKCl filling the tip region and triple distilled water filling the rest

of the cylinder, except for an air space, which separated the two solutions. The container with the microelectrode tips still in the 3MKCl was then covered and placed under an infrared heat lamp for from six to eight hours.

Due to the established heat gradient resulting from the heat lamp and the difference in vapor pressure between 3MKCl and triple distilled water, water in the pipette evaporated from its bottom surface and condensed on the top surface of the 3MKCl in the tip region. This in effect caused the air space or "bubble" to apparently move up the narrow tip region to near the shoulder of the micropipette. After six to eight hours of this action the bubble was expelled from the micropipette by sticking a finely flame etched tungsten wire down the pipette and poking it around the bubble.

After this air space had been expelled, 3MKCl was injected into the pipette replacing the distilled water. The pipettes were left with their tips in the 3MKCl for approximately one hour before being used. Microelectrodes produced in this way usually had tip potentials of about -5mv and resistances of 50 to 80MΩ. They were stored for no longer than one day after being made, since after

this period the majority of electrodes were unusable. Only microelectrodes produced by the above procedure were used in the experiments reported here.

During the course of any experiment if either the noise recorded by the microelectrode increased or the tip potential changed, the microelectrode was discarded and replaced by a fresh one. The resistance of the microelectrodes was necessarily high, because it was found that penetration of the fibroblasts with electrodes of resistance 30MΩ or under caused irreversible cell damage, presumedly due to the larger tips associated with low resistance electrodes, and this prevented later processing of the cells for the scanning electron microscope. It is unlikely that leakage of 3MKCl from microelectrode tips into cells caused any cell damage through osmotic effects, since in similar situations leakage is known to be in the order of 10^{-14} moles/second (Eccles, 1957). In these experiments cell penetrations lasted no more than one minute, thus the increase in intracellular KCl due to leakage is insignificant.

A schematic diagram of the electrical setup is shown in Figure 2. The filled microelectrodes were connected to

FIGURE 2.

Electrical setup used for junctional coupling measurements on cells in tissue culture. The recording amplifiers are high input impedance field effect transistor amplifiers. Vcal is a low impedance voltage source connected to the reference electrode to introduce calibrating pulses. Switch S is used to simultaneously connect the recording microelectrode (ME-1) to a constant current stimulator I (after Baird, 1967) and connect the recording amplifier to ground. The microelectrode current pulse is measured as a voltage drop across the 1MΩinput impedance of a Tektronix oscilloscope.

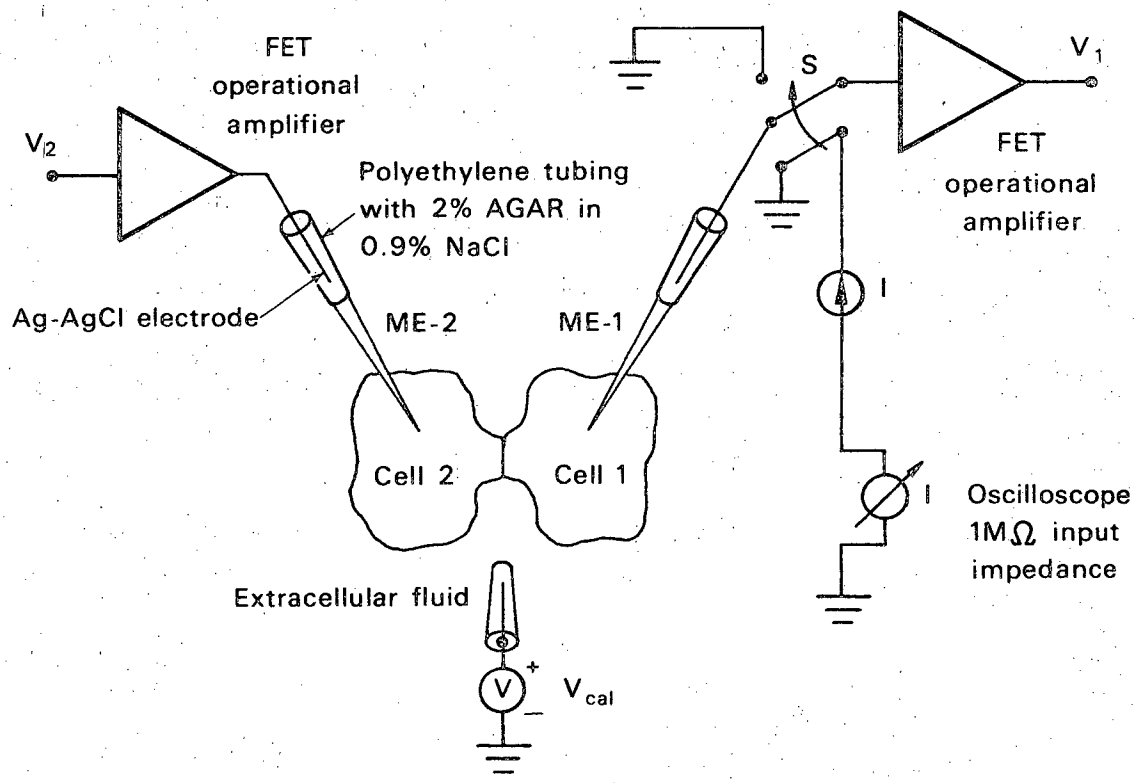
FET
operational
amplifier
V_2
Polyethylene tubing
with 2% AGAR in
0.9% NaCl
Ag-AgCl electrode
ME-2
ME-1
Cell 2
Cell 1
Extracellular fluid
V
+
−
V_{cal}
S
V_1
FET
operational
amplifier
I
I
Oscilloscope
1MΩ input
impedance

DBL 698-5008

segments of polyethylene tubing which fit over the top end of the pipette and were filled with a 2% agar (Difco) in 0.9% saline solution (physiological saline). This agar solution made contact with the 3MKCl inside the electrode forming a liquid-liquid junction. The other end of the tubing with the agar solution was inserted into a ¼cc. plastic syringe which acted as a reservoir containing physiological saline. Reversible Ag-AgCl electrodes were inserted into the saline reservoir and connected to the inputs of the recording amplifiers or the current stimulator (see below).

The reversible electrodes used in these experiments were made in the following way: 25 mil diameter silver wires of 5 cm lengths were cleaned by first sanding with medium grade emery cloth, then dipping in hot concentrated nitric acid and finally rinsing in distilled water. The wire segments were connected to the anode of a 1.5 V battery in series with a 500 Ω potentiometer which limited the current density to approximately 5 ma/cm^2 (see below). The potentiometer was connected to a platimun plate which acted as the cathode. Both the silver wire and the platinum plate were dipped into 0.1N HCl which

was essentially bromide free as tested with the fluorescein method (fluorescein turns red in solutions with minute concentrations of bromide). The polarity of the battery was reversed through three complete cycles of one minute periods. Current densities of approximately 5 ma/cm^2 gave the stablest low resistance reversible Ag-AgCl electrodes. These electrodes were kept in physiological saline until used.

The reference electrode system consisted of a 2% agar physiological saline solution filling a segment of polyethylene tubing, one end of which was placed in the medium within the culture dish and the other end placed into a reservoir containing physiological saline and a reversible Ag-AgCl electrode. This silver-silver chloride electrode was connected to a grass stimulation isolation unit and a grass Model S4 stimulator which delivered a calibration pulse into the recording system (see Vcal, Figure 2).

The voltage recording amplifiers were specially designed for the electrophysiological measurements reported in this thesis and are described in detail in Appendix I. Briefly, they were negative capacity compensated (see

Appendix II), unity-gain, high input impedance ($10^{12}\Omega$) operational amplifiers with gate current $< 10^{-11}$ amperes and low drift <5 mv per ½ hour. The electrode resistance was easily monitored at any time by a specially designed circuit used to apply a triangular wave through a 2pF capacitor at the input of each amplifier (see Appendix I and III).

Two microelectrodes were used in the electrical coupling measurement, one in each cell. The output of one microelectrode could be switched from the recording input of one amplifier to a photo diode coupled constant current stimulator (after Baird, 1967) (see switch S in Figure 2). This current stimulator was used to apply a pulse of current of varying duration and amplitude into or out of the cells through one microelectrode. The microelectrode in the other cell detected any voltage response due to the applied current in the first.

The current pulse was measured as a voltage drop across the $1M\Omega$ input impedance of the oscilloscope. Both the current through and the voltage recorded by the microelectrodes were displayed on a dual beam Tektronix 502A and four trace storage Tecktronix RM 564 oscillo-

scope and photographed with a Polaroid camera. The oscilloscope beam sweeps were triggered by a pulse from a Tektronix 162 wavefrom generator. This pulse preceeded in time and was synchronized with the constant current pulse. The calibration pulses from a Grass Model S-4 stimulator were also synchronized to this pulse. Cellular membrane potentials were recorded on a Hewlett Packard-Moseley 7100 BM two channel strip chart recorder.

The whole electrical setup was isolated from electrical interference by placing it in a large Faraday cage. Any interference from the Tiyoda light source was also eliminated by sheilding to ground the entire light source. With this arrangement, interference voltage fluctuations of no more than 10μ were present.

The chamber containing the cells to be investigated electrophysiologically was the same 60mm outer diameter tissue culture dish in which the cells were incubated beforehand. All experiments were done at room temperature 25°-27°C. The experimental procedure for both the electrophysiology and subsequent fixation were as follows: the culture dish containing the cells was removed from the

the incubator and the bottom portion (top removed) was attached by metal hooks along its rim to the stage of the Tiyoda microscope. A gentle flow of gas (10% CO_2 - 90% air bubbled through water) was established across the culture medium which maintained the pH in the range 7.4-7.6. Evaporation was minimal. The microelectrodes which had already been placed near the culture dish were coarsely positioned near the bottom of the dish under x100 magnification. They were then positioned by the transmission cable arrangement onto the cell membrane at x640 magnification and the final introduction of the electrodes into the cells was done by gently tapping the metal columns holding the micromanipulators. Entry into a cell was signalled by a "stable" negative resting potential with respect to the reference electrode system. In the experiments reported here a "stable" membrane potential was defined as one which remained constant at its original value for five or more seconds.

For coupling measurements one electrode was introduced into a cell and the resting potential was noted as being stable or not: if stable, the other microelectrode was

then introduced into another cell; if not, another cell was found. If both membrane potentials remained approximately constant, a pulse of current was passed through one cell by switching the microelectorde to the constant current stimulator. The voltage response was detected by the other microelectrode in the connected cell.

Early in the course of this work it was observed that the membrane potentials of coupled cells are interdependent. With an electrode already inserted into one cell, penetration of a neighboring cell with a second microelectrode caused an instantaneous and transient fall in the membrane potential of the first cell. This results from slight damage to the surface membranes of the second penetrated cell. "Sealing" in of the second electrode was accompanied by a rise of both potentials to the same level. In the voltage records for coupled cells presented in this thesis resting potential of the first cell penetrated did not change by more than 2mv by the introduction of the second electrode into the other cell. In one respect this interdependence of cell membrane potentials which was observed in all coupled cells was taken as support for the validity of the coupling measurements. Experiments lasted as long

as three hours or more without there being detectable decreases in either cellular membrane potentials or coupling potentials. No experiment was carried out for more than three hours.

Fixation and the Scanning Electron Microscope

After the electrophysiological measurements were made on the fibroblasts, the microelectrodes were removed and the microscope objective was rotated out of the way and a Zeiss diamond marker was brought to the bottom of the plastic petrie dish and a ring of approximately 1mm in diameter was inscribed around the cell pair which were shown to be coupled the moment before. This ring permitted the relocation of the cell pairs at every stage in the fixation process.

Within one to two minutes after the electrical measurements were made, the dish was removed from the microscope stage. The cells were then fixed for later viewing in the scanning electron microscope in the following way: the medium was aspirated off and the cells were carefully washed in room temperature tris-saline buffer for approximately two minutes. The buffer was then carefully

aspirated off and the bottom of the plastic dish on which the cells were attached was inverted over a drop of 1% OsO_4 in buffer solution. The osmium vapor was allowed to fix the cells for 10 minutes. These cells were then washed once in buffer solution and 5 ml of a 2% glutaraldehyde buffer solution was added to the dish. The cells were kept at 4°C for 24 hours.

After this period the cells were carefully washed twice in buffer for five minutes and then post fixed in 5 ml of 1% OsO_4 buffer solution for one hour. The cells were then washed twice in triple distilled water for five minutes each. At this stage a two cm. diameter circle containing the cells was removed from the bottom of the dish. This was accomplished by using a heated metal circular die. The temperature, checked with a sensitive thermocouple, on the top surface of the circle containing the cells did not rise above 25°C as the circle was burned out. As judged by a comparison between the phase contrast photographs and the late scanning electron micrographs, no cellular damage resulted from this procedure.

The cells on the plastic circle were then serially dehydrated in 50%, 70%, 80%, 95% and absolute ethyl alcohol for 10 minutes each and were then left to air dry for 24 hours in the refrigerator at $4^{o}C$. After this period a thin layer (approximately 500Å) of either pladium/platinum alloy or gold metal was vacuum evaporated onto the plastic disk containing the fibroblasts. The coated disk was then viewed under a microscope at low power and an arrow was scribed with fine forceps pointing to the coupled cell pair. The arrow tip was located approximately 50-100 μ from the cell pair. The arrow, and subsequently, the cell pair were located in the scanning electron microscope with relative ease. A Jeolco Model JSM scanning microscope with a 45° inclined stage was used at an accelerating potential of 25KV and a specimen current of 2×10^{-11} amperes. Secondary electrons were used to form the image and pictures were taken on Polaroid film.

RESULTS

Proliferation Rate of Fibroblasts in Culture

Figure 3 shows the proliferation rate of secondary chick fibroblasts. After an initial fall in cell number due to the failure of many cells to adhere to the dish at plating, the number of cells increases at a constant rate with a doubling time of approximately 18 to 24 hours. The cells continue to divide at this rate until about 90 to 120 hours in culture, at which time they form a confluent monolayer. Further division of the cells is inhibited (saturation density about 10^5 cells/cm^2). This inhibition is not due to depletion of nutrients in the medium since the same medium is found to support dividing cells. Also, it can be temporarily overcome with replacement of old medium by new which causes a burst of cell division to a greater saturation density. This inhibition of cell proliferation in confluent cultures occurs in many cell cultures and is thought to be a process involving contact promoted regulation (Stoker, 1967).

FIGURE 3.

Proliferation rate of secondary chicken embryo fibroblasts plated at an initial concentration of 2.5×10^5 cells into 60mm outside diameter Falcon plastic tissue culture dishes containing 5 ml of medium 2-1-1 (see Materials and Methods). The cells were trypsinized and counted at the indicated intervals. Ordinate: number of cell; abscissa: hours in culture.

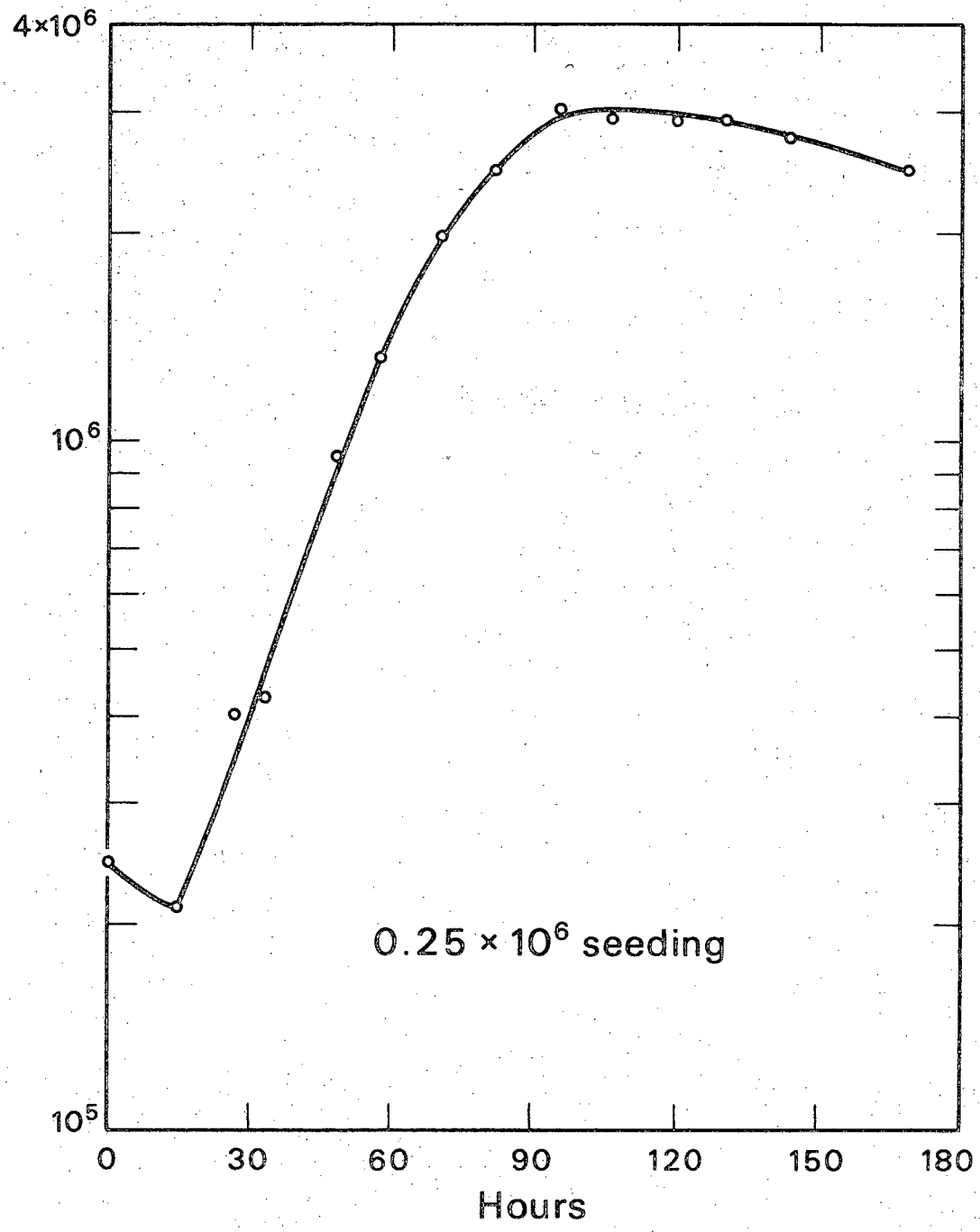

DBL 698-5007

Figure 4a shows cells with the typical fibroblast morphology in an actively proliferating culture (48 hours in culture). The cells are flat (no more than 1-5μ in thickness) and many, if not all, cells at this stage exhibit locomotory behavior. Similar cells are shown in Figure 4b somewhere between 90 and 120 hours in culture. The cells are closely packed with apposition of their lateral surfaces and many cells lie parallel to one another due to their geometry (see also Figure 9). This regular arrangement of these cells in a confluent monolayer is believed to be a consequence of contact inhibition of movement (Abercrombie and Heaysman, 1953).

Electrical Coupling Between Secondary Fibroblasts

Coupling measurements between fibroblasts were made as early as 12 hours and at various stages up to 120 hours in culture.

Figures 5, 6 and 7 show examples of coupling between cells 24 hours in culture. Over 200 cells were tested at this stage and in every case whenever two isolated cells appeared to be in contact, some degree of coupling

FIGURE 4

(a) Phase contrast picture of living normal secondary fibroblasts in culture two days. The typical spindle fibroblast morphology is evident. One mitotic cell with its chromosomes separated is clearly visible in the field.

(b) Normal secondary cells between three and four days in culture. The cells have approximately reached a confluent monolayer in which further cell division is arrested ("contact inhibition of cell division"). The fibroblasts line up in a parallel fashion with some overlap. (Phase contrast).

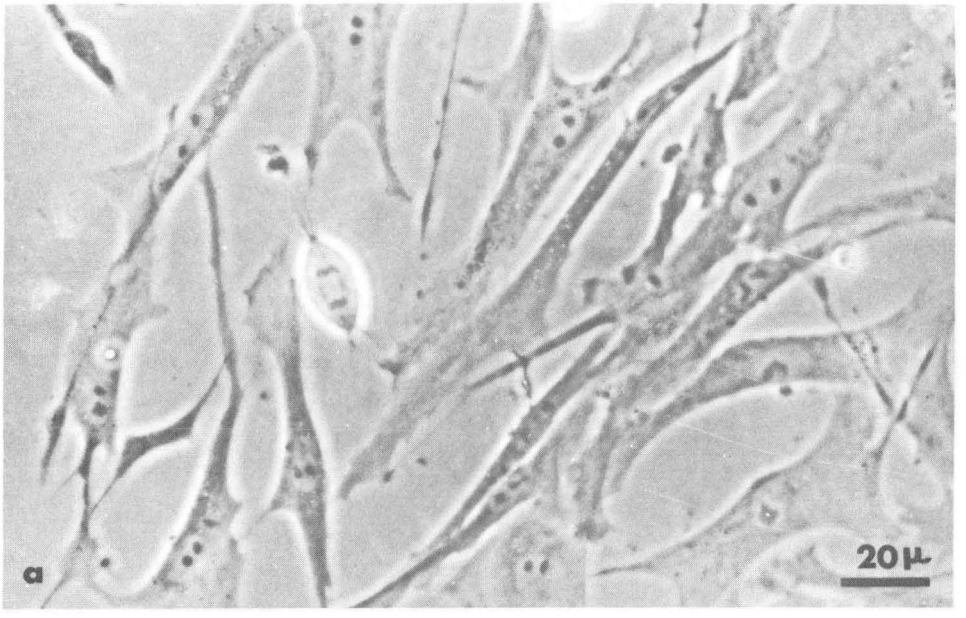

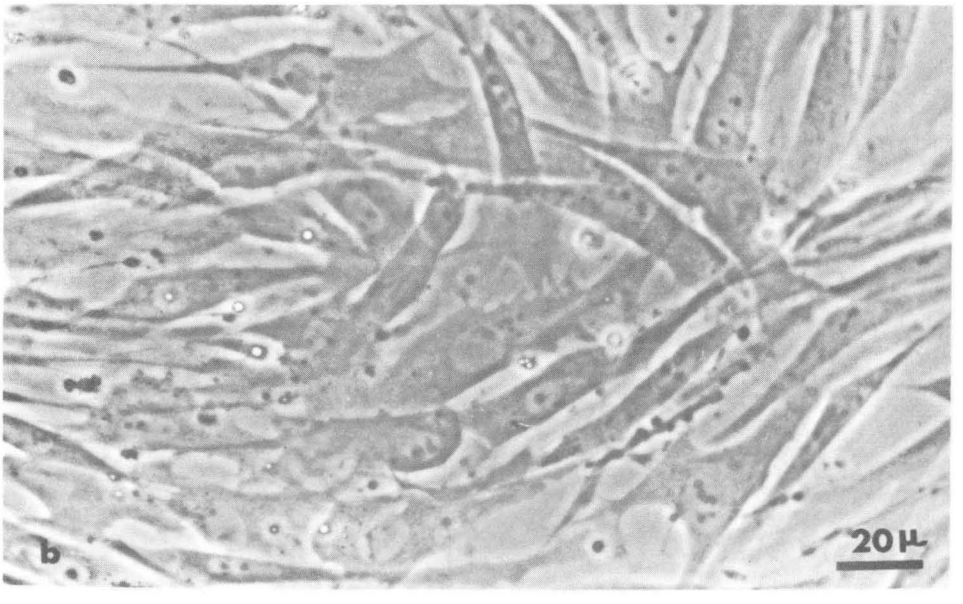

XBB 698-5023

Fig. 4

FIGURE 5.

Phase contrast photograph of two normal secondary fibroblasts in contact (one day *in vitro*). Two micropipettes (ME) are shown in the field. The electrical records (bottom) indicate that the two cells are in electrical communication. The positive calibrating pulses at the left of the top two traces are 10 millivolts in amplitude and 10 milliseconds in duration. These positive calibrating pulses are the same for all subsequent figures. The white vertical bar in the electrical record represents 20 millivolts for the top two traces and 20×10^{-9} amperes for the bottom current trace. Hyperpolarizing current is positive up in this and all subsequent electrical records.

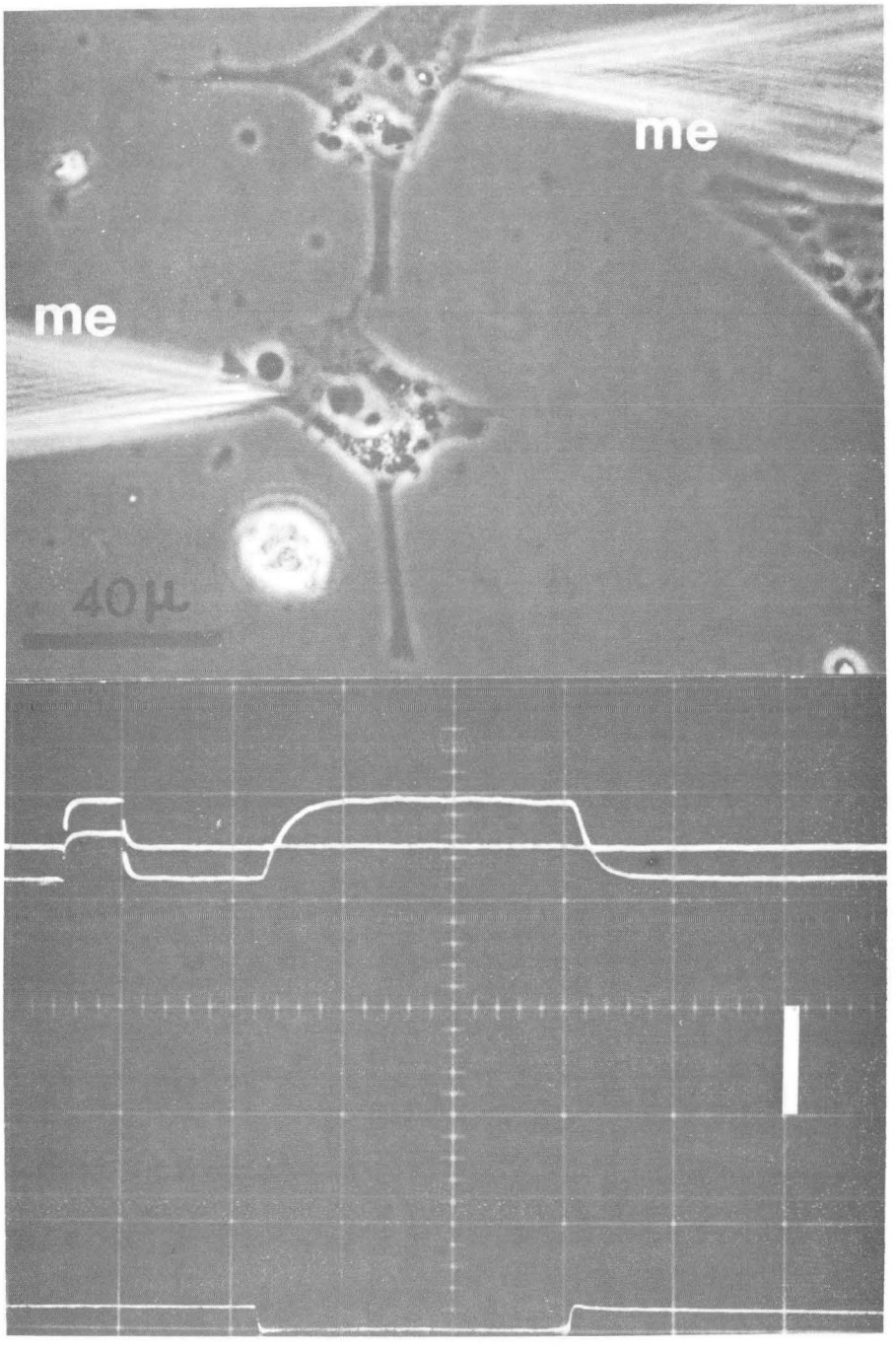

XBB 697-4796

Fig. 5

FIGURE 6.

Phase contrast picture of two living normal secondary fibroblasts (one day *in vitro*) connected by a thin cytoplasmic process. These cells are eletrically coupled as is shown in the electrical record insert. The white vertical bar is 20 millivolts for the top two traces and 20×10^{-9} amperes for the bottom trace. The top (control) and middle traces are voltage recordings from the bottom microelectrode (me) placed just outside and within the cell membrane, respectively, while a current pulse of 5×10^{-9} amperes in amplitude and 56 milliseconds in duration was passed into the left cell by the top microelectrode. Positive calibrating pulses: 10 millivolts and 10 milliseconds.

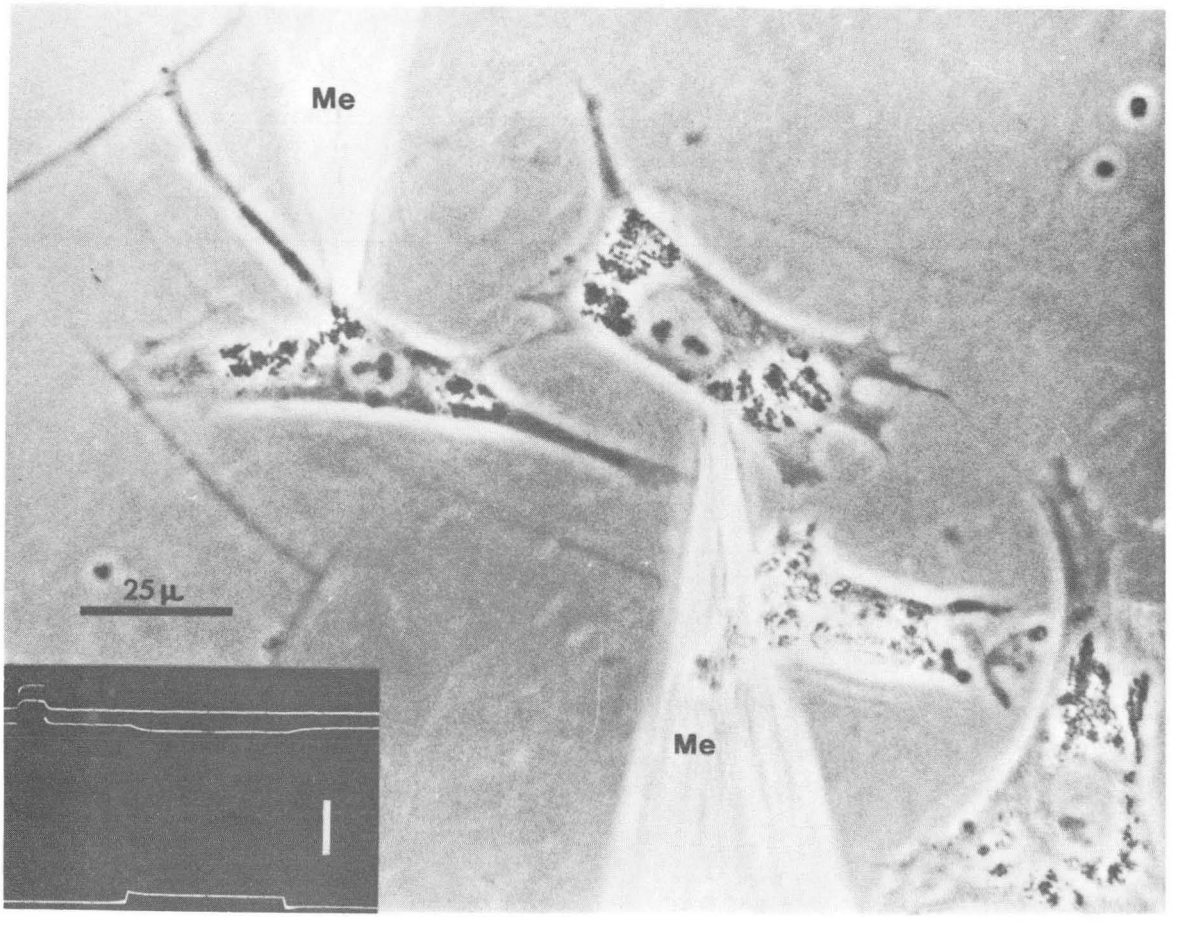

XBB 697-4810

Fig. 6

FIGURE 7.

Two electrically coupled normal fibroblasts connected by a 50 μ bridge. Electrical record inset is the same as in the previous figure. Middle trace shows voltage response of the bottom cell due to a hyperpolarizing current pulse of approximately 5×10^{-9} amperes and 56 milliseconds in duration passed into the upper cell by the top microelectrode (ME). Top control trace in electrical inset shows no response due to the passage of the same current pulse. Vertical white bar: 20 millivolts for top two traces, 2×10^{-8} amperes for the bottom current trace. Positive calibrating pulses: 10 millivolts, 10 milliseconds.

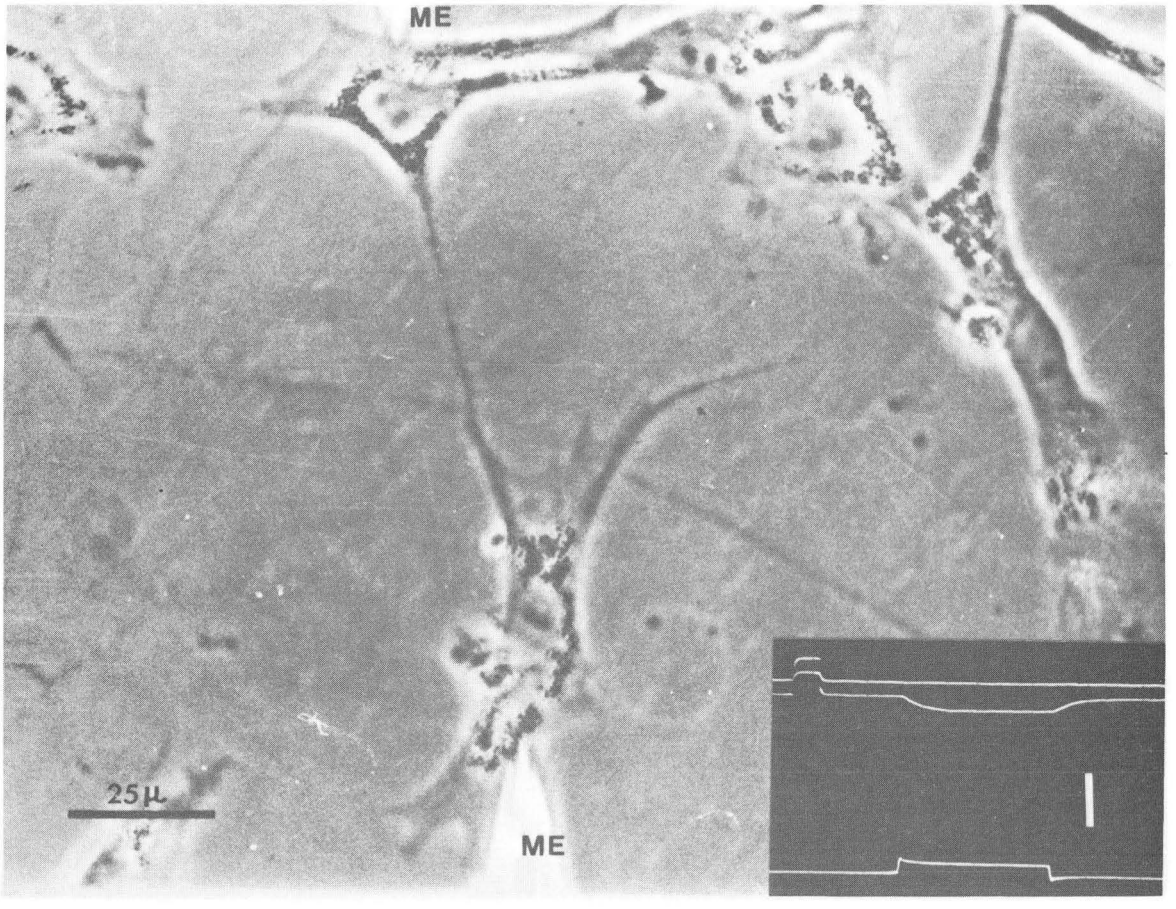

XBB 697-4809

Fig. 7

was demonstrable. Figure 5 is a typical example of two isolated cells which are coupled and appear in contact. As is illustrated by the electrical record at the bottom of Figure 5, when a 5×10^{-9} amperes - 56 millisecond depolarizing current pulse (bottom trace) was supplied to the inside of the lower of the two cells, the second microelectrode recorded an electrotonic potential (middle trace) when it was inside the upper cell, but not (top trace) when it was just outside this cell. The membrane potential (6 millivolts in this case) is seen as the displacement of the middle trace from the top trace in all electrical records. The top trace in Figure 5 and in all subsequent figures is called the control trace and was important for the following reason: it showed the voltage response due to an intracellular current pulse in one cell detected by the recording electrode placed just outside the other cell. Thus, any voltage drop due to the ionic current through the resistive medium was shown in the control trace and this could be compared to the voltage response due to the passage of this this current through the cell membrane plus the resistive medium.

The wave form of the cell response (middle trace) in Figure 5 has a rise and fall time of about four milliseconds and is similar in appearance to the response of a parallel RC circuit frequently used to model cell membranes where the time constant is τ =RmCm and Rm and Cm are membrane resistance and capacitance, respectively. In this case, however, the time constant of the waveform is complex and includes the two non-junctional membrane capacitances and one junctional capacitance all in parallel with their respectives resistances shown in the circuit of Figure 1b. Thus the time constant is not simply τ =RC.

Similar coupling measurements are shown in the subsequent figures. Coupled cells in the process of separating are shown in Figure 6. The cells are connected by only a thin cytoplasmic process and the ruffled membranes which point in the direction of movement of each cell are directed away from the area of contact. Figure 7 shows coupled fibroblasts connected by a cellular process over 50 μ in length.

The current density due to the ionic pulses of current shown in Figures 5, 6 and 7 (bottom traces) is well within physiological limits. A simple calculation shows that

in the case shown in Figure 5, the current density $J = 0.25\ ma/cm^2$. (Cell area = $2 \times 10^{-5} cm^2$). This is about one-tenth of the magnitude of the ionic current density observed during an action potential in the squid (Hodgkin and Huxley, 1952). In no coupling measurement reported in this work was the current density above $1\ ma/cm^2$.

Formation of Low-Resistance Junctions

It is impossible to determine from Figures 5, 6 or 7 whether the coupled cells are in fact daughter cells connected by a cytoplasmic process due to an incomplete mitosis or whether they are cells which have moved into contact forming a low-resistance junction between them. The experiment shown in Figure 8 was one of five experiments demonstrating the formation of a low-resistance junction between isolated fibroblasts in culture. Figure 8a shows two normal fibroblasts apparently unconnected and, as the electrical record indicates, uncoupled. Figure 8b shows the same cells one hour and a half later. The cells have moved together and within

FIGURE 8.

The formation of junctional coupling between two secondary fibroblasts. Phase contrast picture of (a) two living normal secondary fibroblasts (one day in culture) which appear to be unconnected and which are uncoupled. The middle trace in the electrical record to the right shows no voltage response in the right cell due to a current pulse of depolarizing current 8×10^{-9} amperes and 56 milliseconds in the left cell. White bar represents 20 millivolts in top two traces and 40×10^{-9} amperes for bottom current trace. Positive calibrating pulses in (a) and (b) 10 millivolts and 10 milliseconds. Photograph of cells taken after the withdrawal of the microelectrodes (me).

(b), same cells as in (a) but one hour and a half later. In the electrical record the top control trace and middle voltage response are at the same d.c. level due to the decline of the cellular membrane potential. A considerable voltage deflection detected by the right electrode (me) due to the same depolarizing current as in (a) indicates that the cells are now junctionally coupled. White bar and calibrating pulses same as in (a).

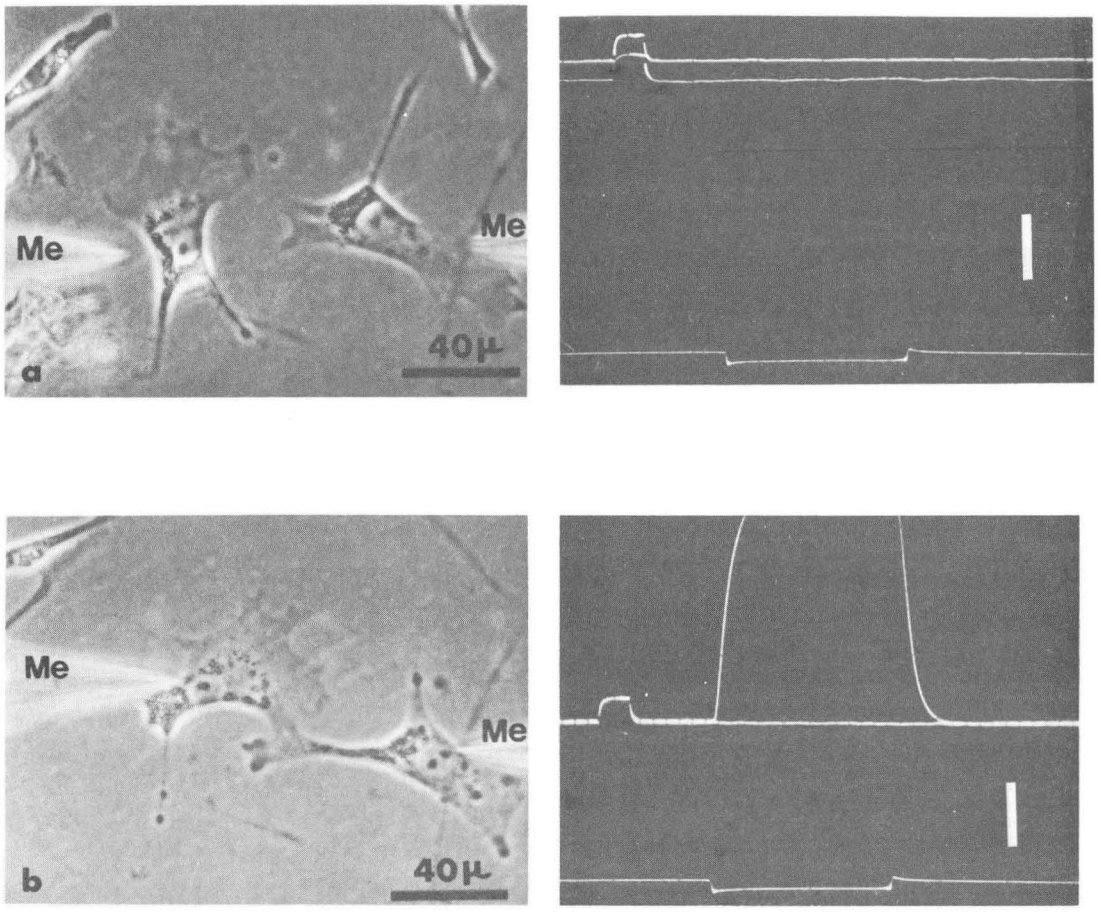

XBB 698-5066

Fig. 8

minutes after connecting have become very tightly coupled. Note that in Figure 8b the ruffled membranes are in the direction of cell contact (compare this with Figure 6 where the cells are in the process of separating).

Estimation of the Specific Junctional Resistance between Isolated Fibroblasts

In a few cases where both surface area of the cell pair and the contact area between them can be estimated from the photographs, the specific resistance of the junctional membranes can be approximated using the circuit in Figure 1b. One such cell pair is that of Figure 8. For the calculation, Figure 1b is reproduced here in Figure 8a. The values of the current $I = 8 \times 10^{-9}$ amperes and the voltage $V_2 = 75 \times 10^{-3}$ volts are taken

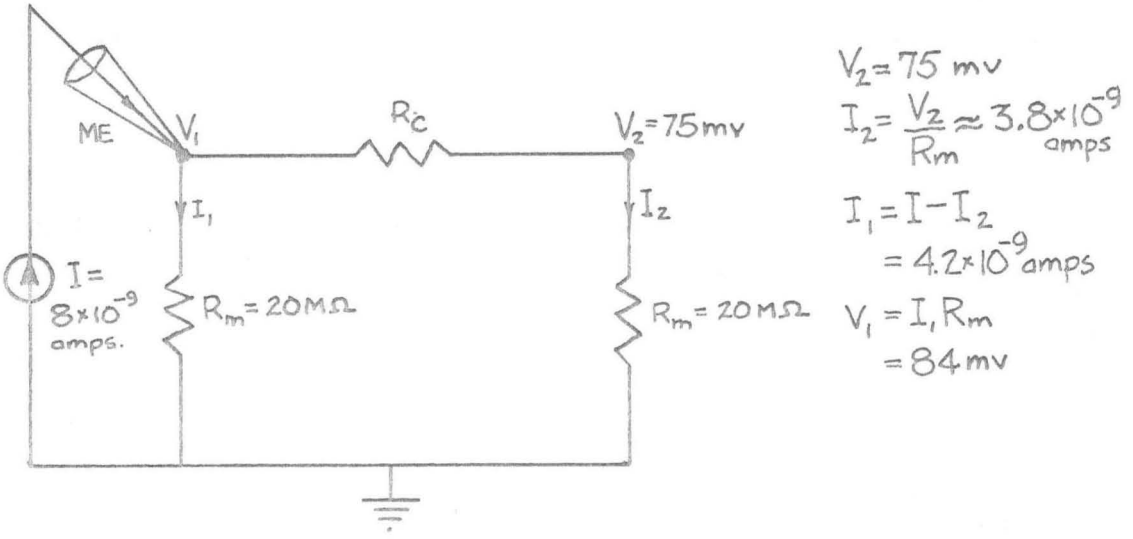

FIGURE 8a.

directly off the electrical record in Figure 8. The non-junctional membrane resistance value $R_m = 20M\Omega$ of each cell (shown in Figure 5a) are assumed to be the same and are the upper values found in input resistance measurements (range $2.7M\Omega$ - $20M\Omega$) on approximately fifty single isolated fibroblasts one day in culture. For these measurements both the current electrode and recording electrode were inside the same cell and the ratio V_2/I was computed as the cell input resistance. The values V, I, and I_2 shown in Figure 8a were computed from Ohm's law. The junctional membrane resistance R_c is given by:

$$R_c = \frac{V_1 - V_2}{I_2} = \frac{(84 - 75) \times 10^{-3} \text{ volts}}{3.8 \times 10^{-9} \text{ amperes}} = 2.4M\Omega$$

The specific junctional membrane resistance r_c can be obtained by multiplying R_c by the area of the contact which in this case is estimated at $5 \times 10^{-8} cm^2$, giving:

$$r_c = 2.4 \times 10^{+6} \cdot 5 \times 10^{-8} cm^2 = 0.12\Omega\text{-}cm^2$$

The specific membrane resistance r_m is:

$$r_m = 20 \times 10^6 \cdot 2 \times 10^{-5} = 400\Omega\text{-}cm^2$$

where $2 \times 10^{-5} cm^2$ is the approximate area of the cell.

It can be seen that r_c is several orders of magnitude smaller than r_m. The resistance of the process between the two cells in Figure 8 was not included in the calculation. However, assuming normal ionic composition within this process and a specific core resistance of 50 Ω-cm (see Hodgkin and Rushton, 1946), its value is less than one-tenth of the junctional resistance.

Coupling in Proliferating Cultures, Primary Cell Cultures and Cells Cultured on Bacterial Dishes

Extensive coupling was detected between normal cells at every stage (24, 48, and 72 hours) and between cells which had proliferated into a confluent monolayer (Figure 9). Coupling between cells within a monolayer but separated by as many as 8 to 10 cells could be detected. That coupling is not particular to secondary cultures of chicken fibroblasts was shown by the fact that primary cultures of the same cells were also well coupled (Figure 10).

Coupling has also been observed between secondary fibroblasts cultured on different substrates. Cells plated on bacterial dishes in standard medium 2-1-1 adhere to one another more than to the plastic substrate on which they move, subsequently, the pattern of cells assumes the form of discrete clumps of cells scattered over the bottom

FIGURE 9

Coupled normal secondary fibroblasts within a confluent monolayer in which the cells have stopped their proliferation - 96 hours *in vitro*. Current microelectrode on the left (me). Middle trace of the electrical record shows the voltage response of cell impaled on the right due to current pulse of 11×10^{-9} amperes and 56 milliseconds in duration passed into the other cell. Top trace is the control trace. Vertical white bar 20 millivolts for top two traces and 20×10^{-9} amperes for bottom current trace. Positive calibrating pulses; 10 millivolts, 10 milliseconds.

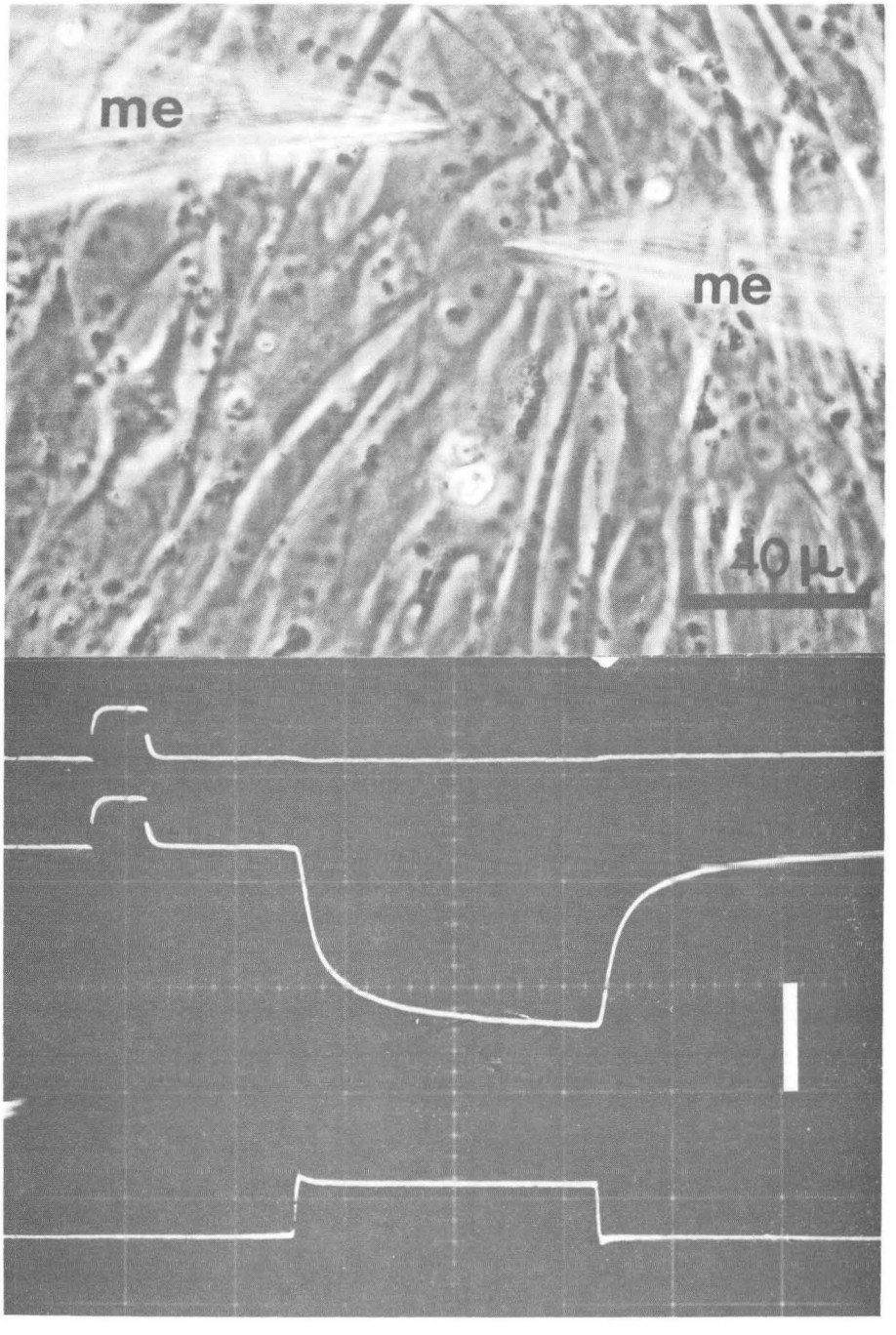

XBB 697-4803

Fig. 9

FIGURE 10.

Normal chicken embryo primary cells (top) electrically coupled. Electrical records (bottom). Top trace is control. Middle trace shows voltage response of cell impaled by the electrode (Me) at the right due to 4×10^{-9} amperes and 56 millisecond hyperpolarizing current pulse passed intracellularly through the left microelectrode. Vertical white bar 20 millivolts for top two traces. 20×10^{-9} amperes for bottom current trace. Positive calibrating pulses: 10 millivolts, 10 milliseconds.

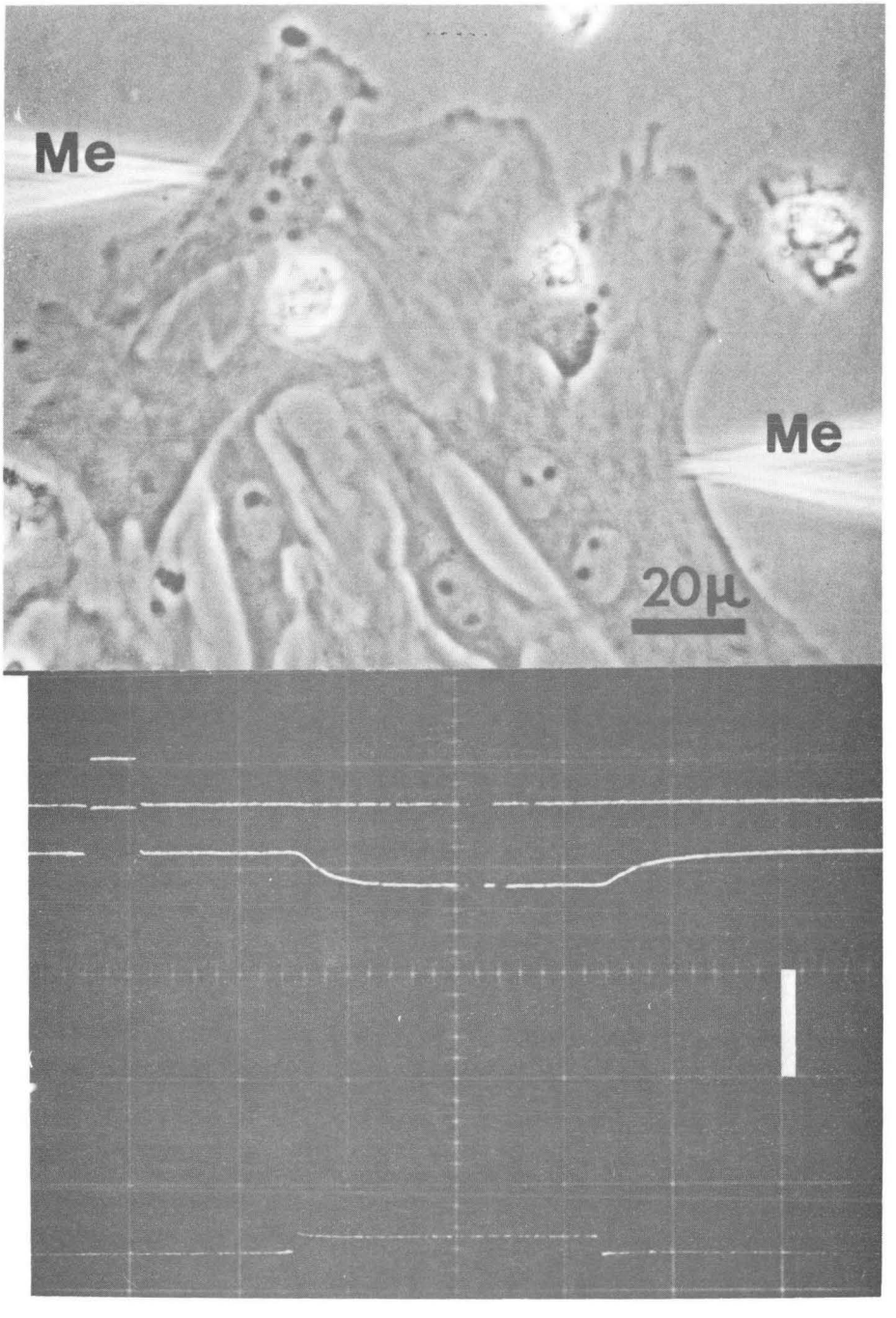

XBB 697-4799

Fig. 10

surface of the dish. The electrical records of Figure 11 (a),(b) show that cells within these clumps have low resistance junctions between them. Figure 11a is particularly dramatic in that it shows that two cells impaled with microelectrodes within a clump are tightly coupled even though they are connected through 10 to 15 cells. This suggests the likelihood that all cells within a clump share a continuous compartment of current-carrying ions.

Loss of Coupling Following Cell Injury

Since the coupling evidence strongly suggested the possibility that coupled cells in culture might share a continuous compartment of current-carrying ions, it was of some interest to inquire whether the injury of one cell in a coupled system might lead to the short circuiting of the rest of the cells. This was not found to be the case.

An example of uncoupling of an injured secondary cell from its neighbors is shown in Figure 12. In (a) three isolated cells are seen in apparent contact, and from the electrical evidence in (c) they are all coupled. The microelectrode in cell 1 was the recording electrode.

FIGURE 11.

(a), (b) Clumps of normal secondary fibroblasts in medium 2-1-1 on falcon plastic bacterial dishes 60mm in outside diameter (three days in culture). Cells separated by as many as 10 to 15 cell diameters (a) within these clumps are well coupled as indicated in the corresponding electrical records. Top traces in each record are control traces. Middle traces show the voltage response of left electrode (me) to an intracellular pulse of anodal current in the right microelectrode (me). In (a) the pulse of current was 28×10^{-9} amperes and 90 milliseconds and was passed in both directions; in (b) 12×10^{-9} amperes and 90 milliseconds. Vertical white bar in each record is 30 millivolts for the top two traces and 20×10^{-9} amperes for bottom current traces. Positive calibrating pulses are 10 millivolts, 10 milliseconds.

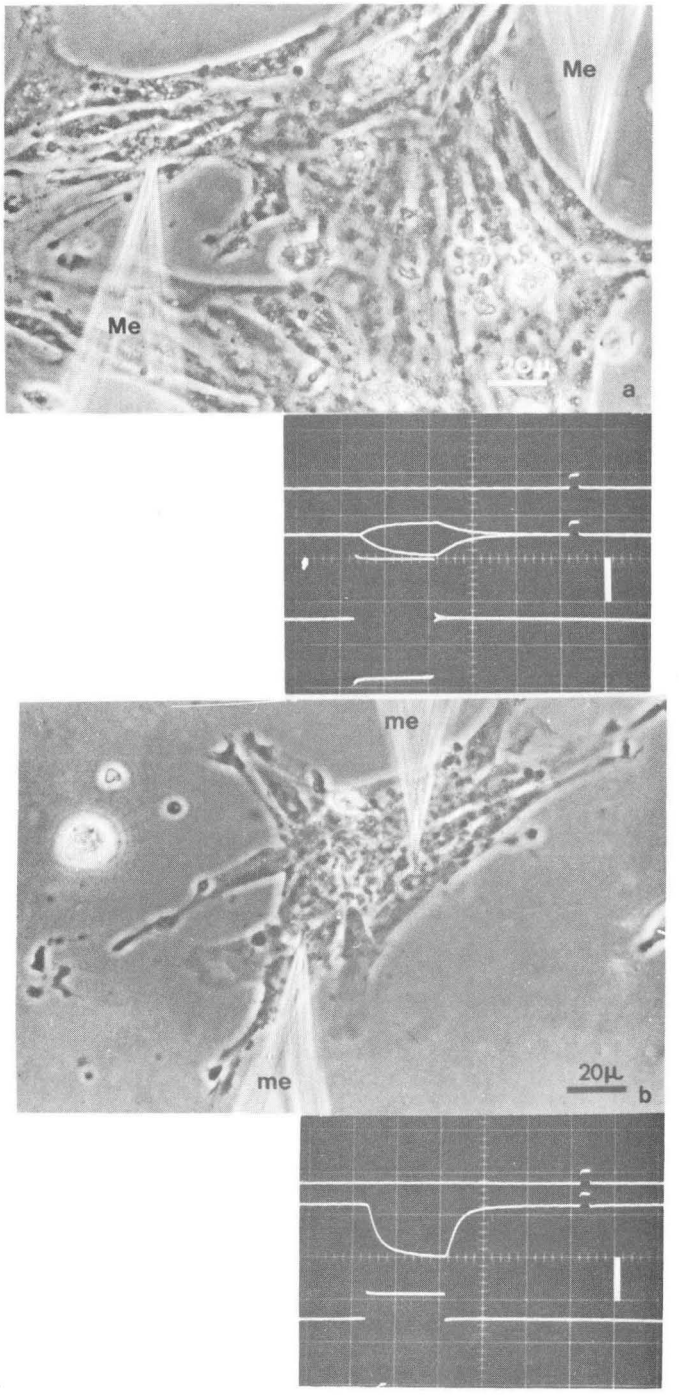

XBB 698-5019

Fig. 11

FIGURE 12.

The loss of junctional coupling after cellular injury. (a) Phase contrast picture of three normal fibroblasts one day in culture each in electrical communication with the others as seen in (c). V_{12_b}(before) shows the traces of coupling between cell 2 and cell 1 before the destruction of cell 2 with microelectrode (me -2). V_{13_b}(before) shows the electrical coupling between cell 1 and cell 3 also before the injury to cell 2. Note that microelectrode position two and three show the same microelectrode in two different positions at different times. (b) Approximately two minutes after the destruction of cell 2, the contact morphology betweeen cell 2 and cell 3 has changed and both cell 1 and cell 3 are no longer in junctional communication with cell 2 (see V_{12a} in (c), however, they continue to communicate with each other the same as before destruction of cell 2, compare V_{13_a} after (coupling after) to V_{13_b} before (coupling before).

(c) Electrical records of coupling. The hyperpolarizing current pulse is identical for each set of records, 5×10^{-9} amperes and 56 milliseconds. The top trace of each group of records, (i.e., V_{12b}, V_{13b}, etc.) is the control trace while the trace immediately below each control trace is the voltage response of cell 1 due to the current pulse in either cell 2 or cell 3. Positive calibrating pulses are 10 villivolts and 10 milliseconds. Vertical white bar is 20 millivolts for the voltage traces and 20×10^{-9} amperes for the bottom current trace.

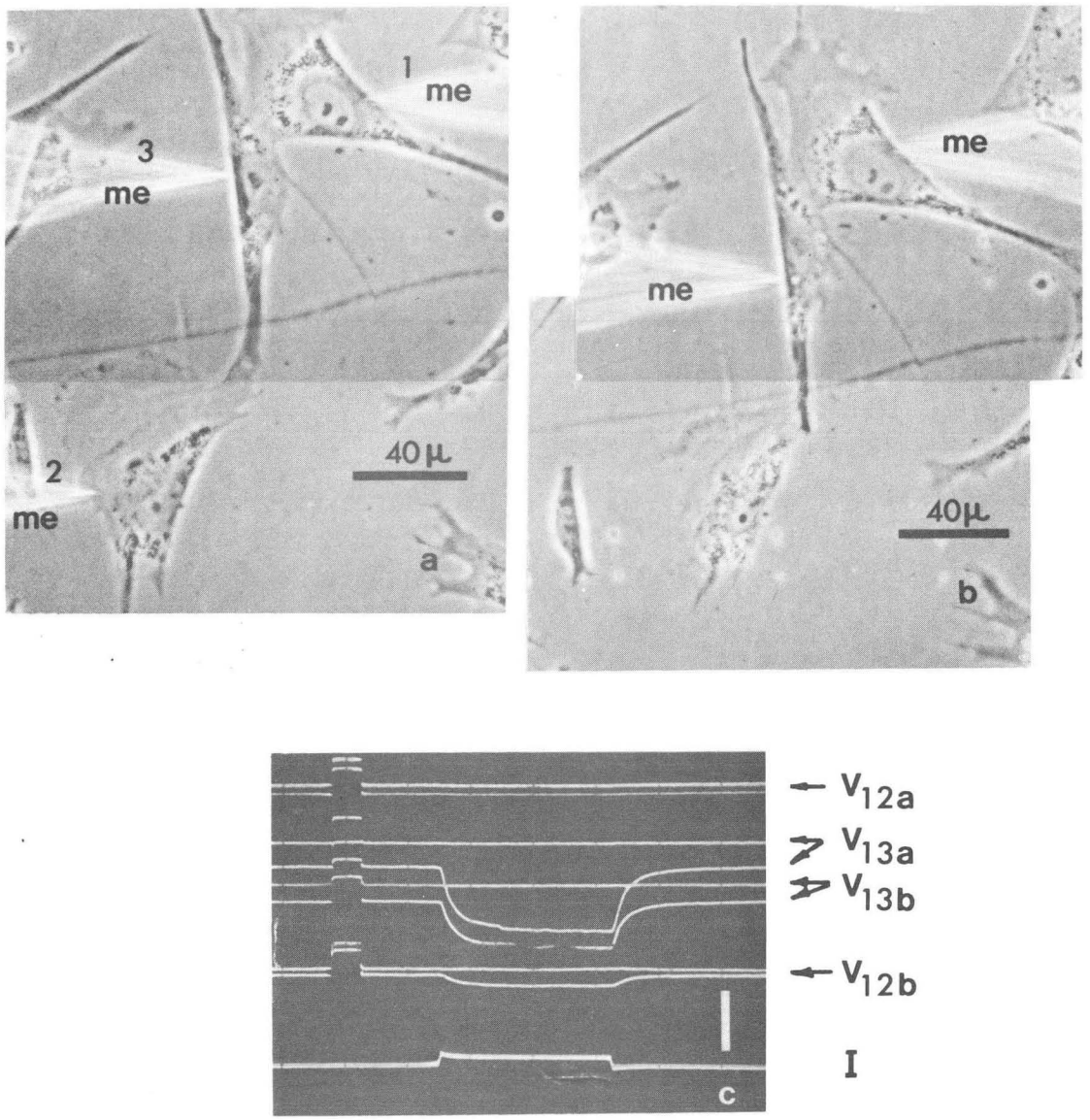

XBB 698-5025

Fig. 12

That in cell 3 or cell 2 was the current passing electrode. Within minutes after cell 2 had been destroyed by mechanical rupture with the microelectrode (Figure 12b), the coupling between it and cell 3 was no longer detectable. The junctional contact morphology between cell 2 and cell 3 had changed drastically, however, the coupling between the two uninjured cells was unaffected just seconds after uncoupling of the injured cell. In fact, the voltage response in cell 1 due to a current pulse in cell 3 is seen in Figure 12c to be greater than before (compare V_{13a} (after) with V_{13b} (before) in Figure 12c). This is consistent with the fact that before its destruction, cell 2 acted as a pathway for the current injected into cell 3.

The above results suggest that the loss of cells from their coupled neighbors does not lead to any short-circuiting of the remaining intact cells. Thus it appears that normal low-resistance junctions in this case are quite labile, sealing off folowing injury. This finding differs from that found in the case of junctional sealing after wounding in urodele epidermis (Loewenstein and Penn, 1967).

There, a fringe around the wound several cells deep has subnormal communication ratios when probed a few minutes after wound production.

Coupling in Cells Infected with Rous Sarcoma Virus

The concentrations of Rous sarcoma virus used in these experiments usually produce characteristic foci of Rous sarcoma cells (Temin and Rubin, 1968, Rubin, 1967) at around three to four days after infection of the secondary fibroblast cells. Two examples of focus formation showing early stages of morphological transformations of normal secondaries are shown in Figure 13. The chief characteristics observed at this early stage of transformation are the alteration of cellular morphology from the typical elongated spindle geometry of normal fibroblasts to a more spherical shape and the distinctly wider separation between cells as compared to normals. Cells at this stage in an infected culture are frequently observed to be heavily vaculated and the nuclei are usually distorted and located near the extreme margins of the cells. As this transformation continues, cells within the foci are easily distinguishable from the surrounding normal cells

FIGURE 13.

Two examples of focus formation showing beginning morphological transformation of living normal secondary fibroblasts infected 72 hours prior with Rous sarcoma virus. The spindle morphology characteristic of the normal fibroblasts is easily distinguishable from the more spherical geometry of the early transformed cells within the focus. (Phase contrast).

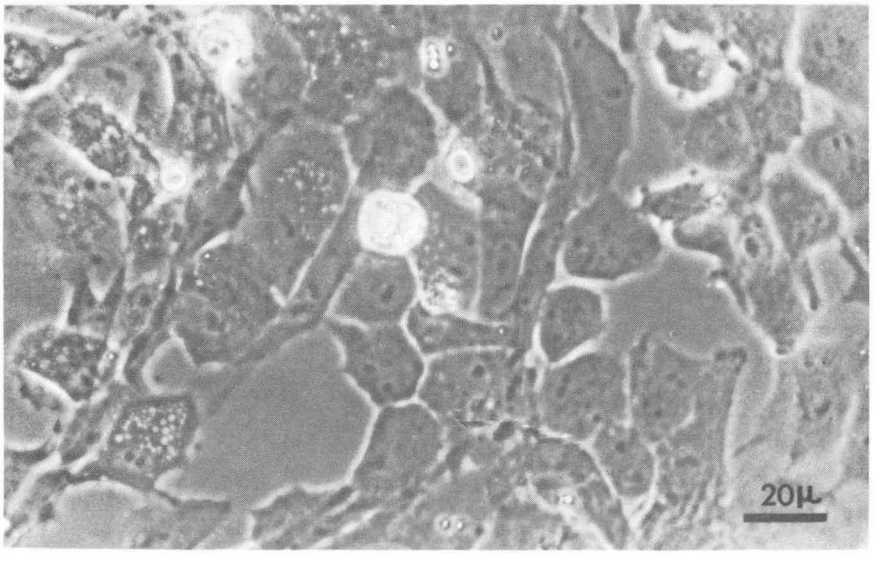

XBB 697-4811

Fig. 13

by their rounded, highly refractile appearance and their tendency to heap up on top of one another.

Infected cells were tested for coupling on the first and second day in culture when the cellular geometry was still that of normal fibroblasts; and on the third day and thereafter where foci were apparent and cells at various stages of morphological transformation were present.

In the majority of experiments some degree of coupling was detected between cells at all stages of virus induced transformation. "Normal" appearing cells in cultures infected with virus two days prior were well coupled. "Normal" cells surrounding foci were found to be coupled to cells within the foci whether those cells were partially or fully transformed and finally, transformed cells were coupled to transformed cells. Sometimes it was not possible to demonstrate the existence of coupling between completely transformed cells. However, mechanical disturbance due to electrode penetration might account for these cases, especially since transformed cells were observed to detach from the plate after penetration and to

remain attached to the electrode tip upon withdrawal of the microelectrode. Transformation of chick embryo fibroblasts by Rous sarcoma virus is known to cause a decrease in adhesiveness between these cells (Rubin, 1966). In any case, coupling between virus transformed cells at various stages of transformation was the rule rather than the exception.

Coupling between infected cells at different stages of transformation are shown in Figures 14, 15 and 16a, b. Two adjacent infected cells at an early stage of transformation are shown in Figure 14 to be tightly coupled. As shown by the electrical record (inset) when current was supplied to the inside of the lower cell (bottom trace), the top electrode recorded an electrotnic potential when it was inside the top cell (middle trace) but recorded no potential change right outside the upper cell (top trace). A resting membrane potential of 22-millivolts is indicated by the displacement of the middle trace from the top trace.

Figure 15 shows two transforming cells which are somewhat round and highly refractile but still possess

FIGURE 14.

Electrical coupling between two early transforming fibroblast cells infected with Rous sarcoma virus three days prior. Me-microelectrodes. Inset: top trace is the control; middle trace shows the voltage recorded by the top electrode due to a 5×10^{-9} amperes and 56 millisecond hyperpolarizing current pulse (bottom trace) in the other electrode (Me) within the lower cell. Vertical white bar 20 millivolts for top two traces, 20×10^{-9} amperes for bottom current trace. Positive calibrating pulses 10 millivolts, 10 milliseconds.

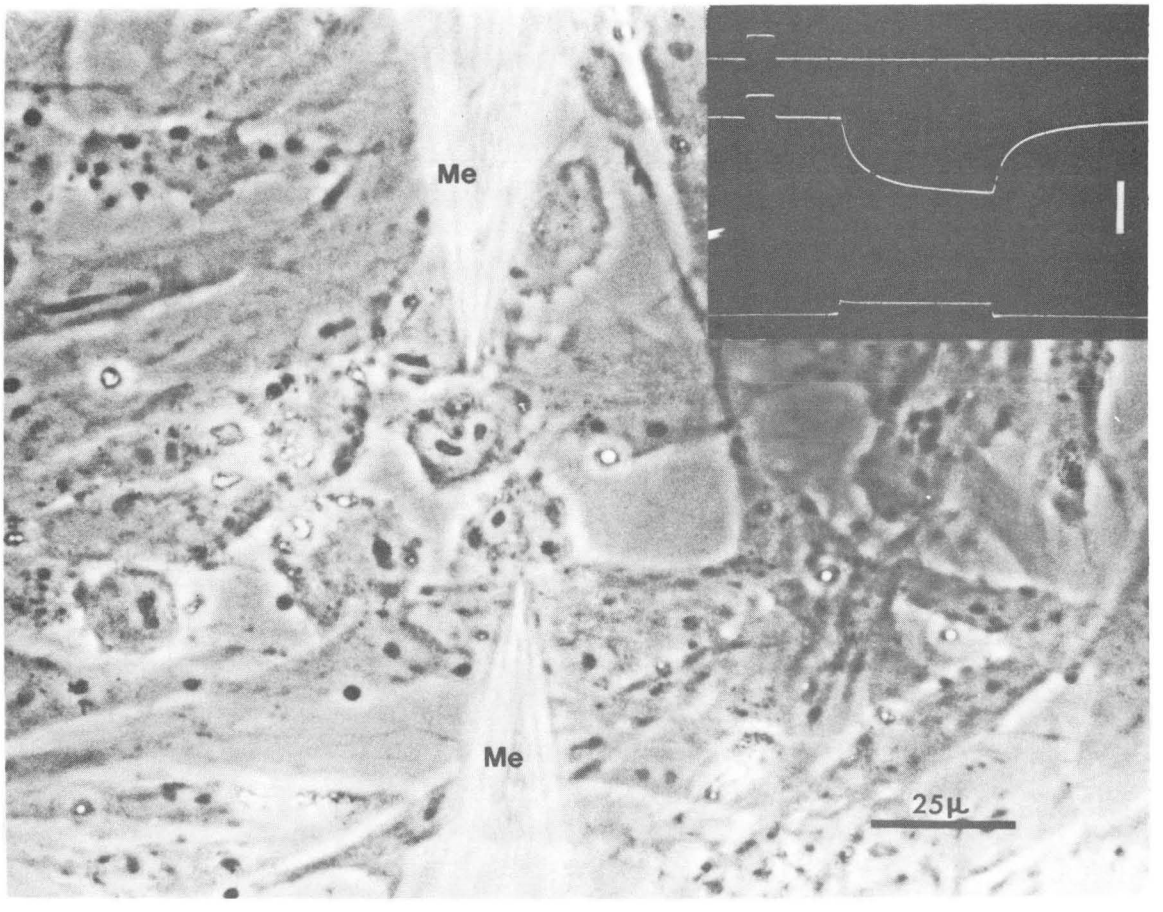

XBB 697-4813

Fig. 14

FIGURE 15.

Transforming fibroblast cells in a culture which was infected with virus four days prior to the electrophysiological experiment. Two cells are seen impaled with microelectrodes (Me) and the electrical data (inset) indicates that the cells are coupled. Top trace is the control trace; middle trace shows voltage response of upper cell due to 5×10^{-9} amperes and 56 millisecond current pulse passed in both directions through the lower cell. White bar 20 millivolts for voltage traces, 20×10^{-9} amperes for bottom current trace. Positive calibrating pulses 10 millivolts, 10 milliseconds.

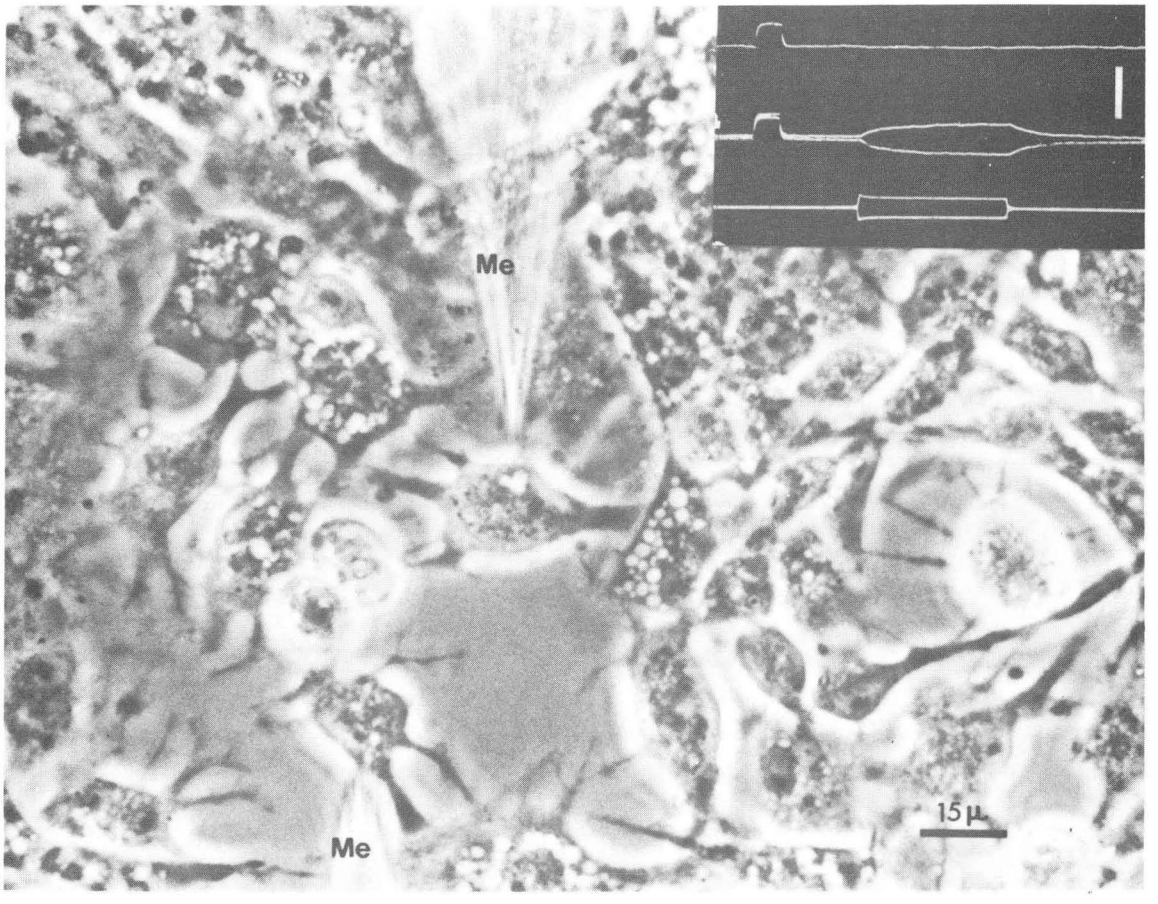

XBB 697-4808

Fig. 15

FIGURE 16.

(A), (B) Phase contrast photographs of living Rous transformed fibroblast cells in a culture which was infected nine days prior to the experiment. The following description applies for both (A) and (B). Two transformed cells are seen impaled by microelectrodes (me). The electrical data indicates that the cells are coupled. Top electrical trace is the control; middle is the voltage response in the right intracellular electrode due to a 6×10^{-9} amperes, 56 millisecond hyperpolarizing pulse passed intracellularly through the left microelectrode. Vertical white bar is 20 millivolts for voltage traces and 20×10^{-9} millivolts for voltage traces and 20×10^{-9} amperes for bottom current trace. Positive calibrating pulses, 10 millivolts, 10 milliseconds.

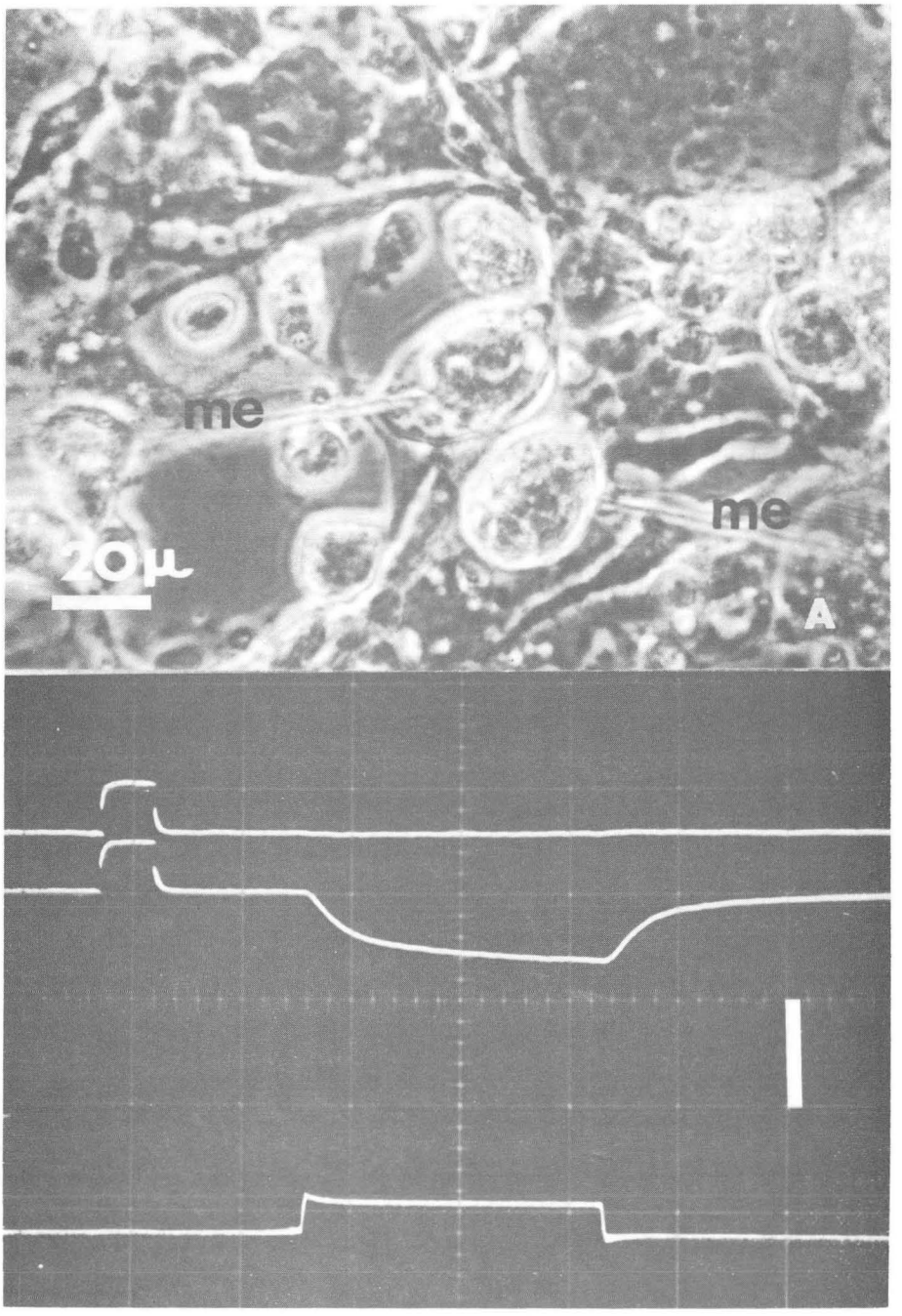

XBB 697-4801

Fig. 16A

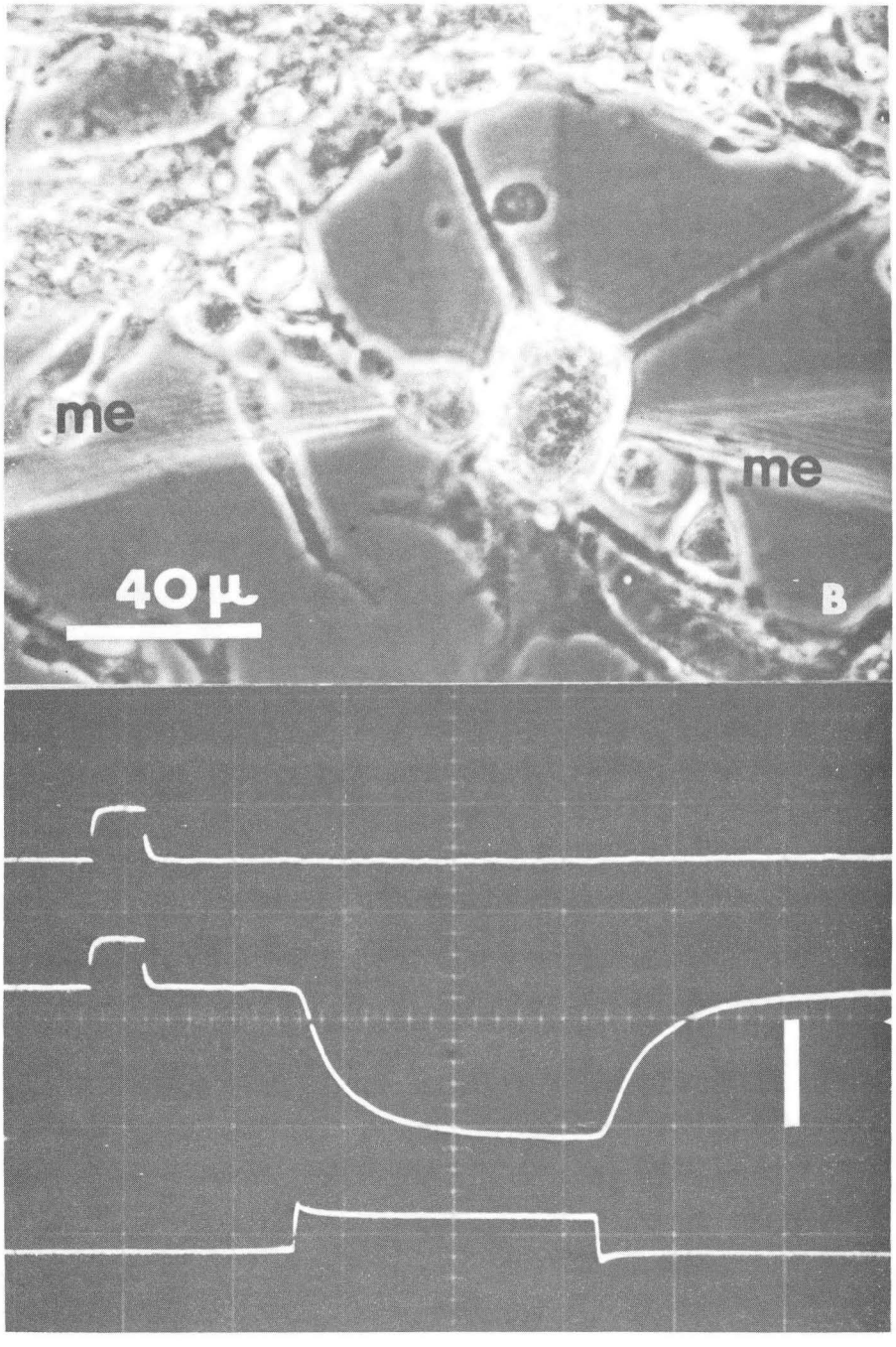

XBB 697-4802

Fig. 16B

long cytoplasmic processes which are not usually characteristic of the final transformed state (see Figure 16). The electrical evidence (inset of Figure 15) indicates that the cells are coupled. In this experiment a current pulse was passed through a microelectrode in eith direction from the inside of one cell and the other electrode recorded a symmetrical response which indicates that the transfer of ions between the cells is the same in either direction.

Fully transformed cells which are coupled are shown in Figure 16a, b. The rounded, refractile appearance of the cells is characteristic of Rous sarcoma cells (Rubin, 1967). Entry of the microelectrodes into these cells was done as gently as possible for the adhesion of these cells for each other and the substrate appeared to be weak; in more than one case cells of this type detached from the bottom during an attempted coupling measurement. However, inspite of this problem, coupling was found in a majority of the transformed cells tested.

Scanning Electron Micrographs of Coupled Fibroblasts

The passage of small ions and presumedly low molecular weight molecules through low-resistance junctions has been

well documented (see introduction). However, in most cases concrete evidence for the site of membrane contact at which this passage of particles occurs is lacking. This situation has arisen mainly from the technical difficulty of histologically studying all the junctions between a cell pair which has previously been tested for coupling or for the transfer of molecules between them.

Cells in tissue culture may prove to be a favorable preparation to circumvent this difficulty. As a preliminary step in this direction, a study of the contact morphology between pairs of coupled cells (previously checked electrophysiologically), was undertaken by H. Dalen and the author utilizing the scanning electron microscope. This is the first study of this type and the first study on chick embryo fibroblasts, transformed with Rous sarcoma virus, using the scanning electron microscope.

Two normal fibroblasts as viewed with phase microscopy are shown in Figure 17. Electrical evidence (bottom) indicates coupling between the cells. These cells were fixed within minutes after the coupling measurement and subsequently prepared for viewing in the scanning electron

FIGURE 17.

Phase contrast photograph of two normal fibroblasts after one day *in vitro*. The microelectrodes (me) are shown withdrawn from the cells after the coupling measurement. These cells are in junctional communication as evidenced by the bottom electrical record. Hyperpolarizing current pulse 4×10^{-9} amperes and 56 milliseconds in duration. Left microelectrode, current electrode. White vertical bar is 20 millivolts for top two traces and 20×10^{-9} amperes for bottom current traces. Positive calibrating pulses 10 millivolts, 10 milliseconds.

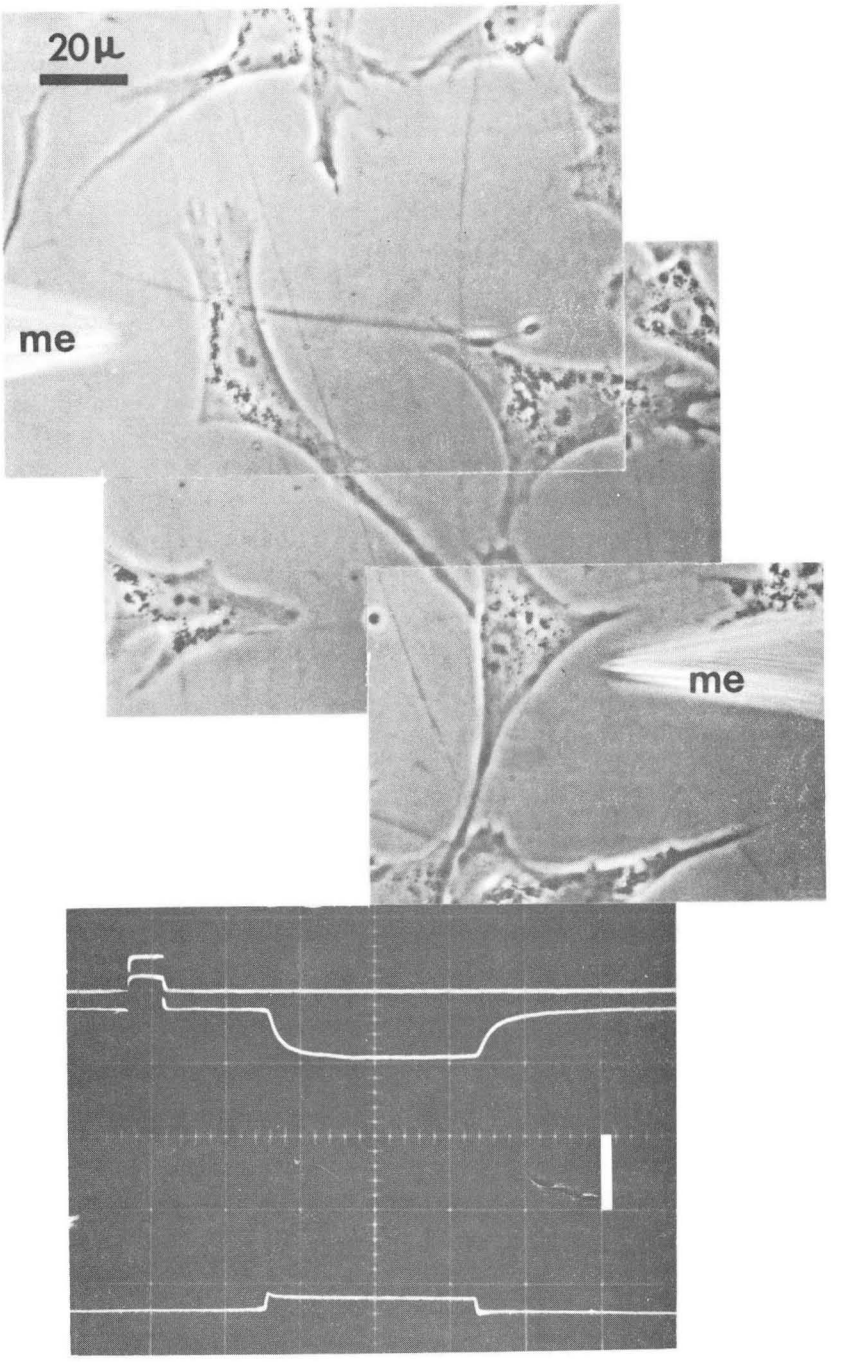

XBB 697-4786

Fig. 17

microscope. Scanning electron micrographs of these same cells are shown in Figure 18.

These cells show no visible damage due to the previous microelectrode penetrations and the small contact area appears to have remained intact throughout the fixation procedure. Other morphological features possessed by the living cells also appear little changed in the scanning micrographs. The nuclei of the cells are quite visible. The round structures seen scattered in the area of the cell's cytoplasm and also seen in the contact regions shown in the upper micrograph of Figure 18 are frequently observed in these cells one or two days in culture. They appear not to be mitochondria (see later), but are probably pinocytotic vacuoles. These structures are, in general, absent from cells within confluent monolayers (see later, Figure 22). The nature of these structures is not known at present.

As seen in this upper photograph, the junctional contact between the two cells is restricted and since the cells were coupled, the low-resistance junction and its

FIGURE 18

Scanning electron micrographs of the same coupled pair shown in the previous figure (Figure 17). The photograph in the upper right is a higher magnification of the junctional contact area between the two electrically coupled cells. See text for further discussion.

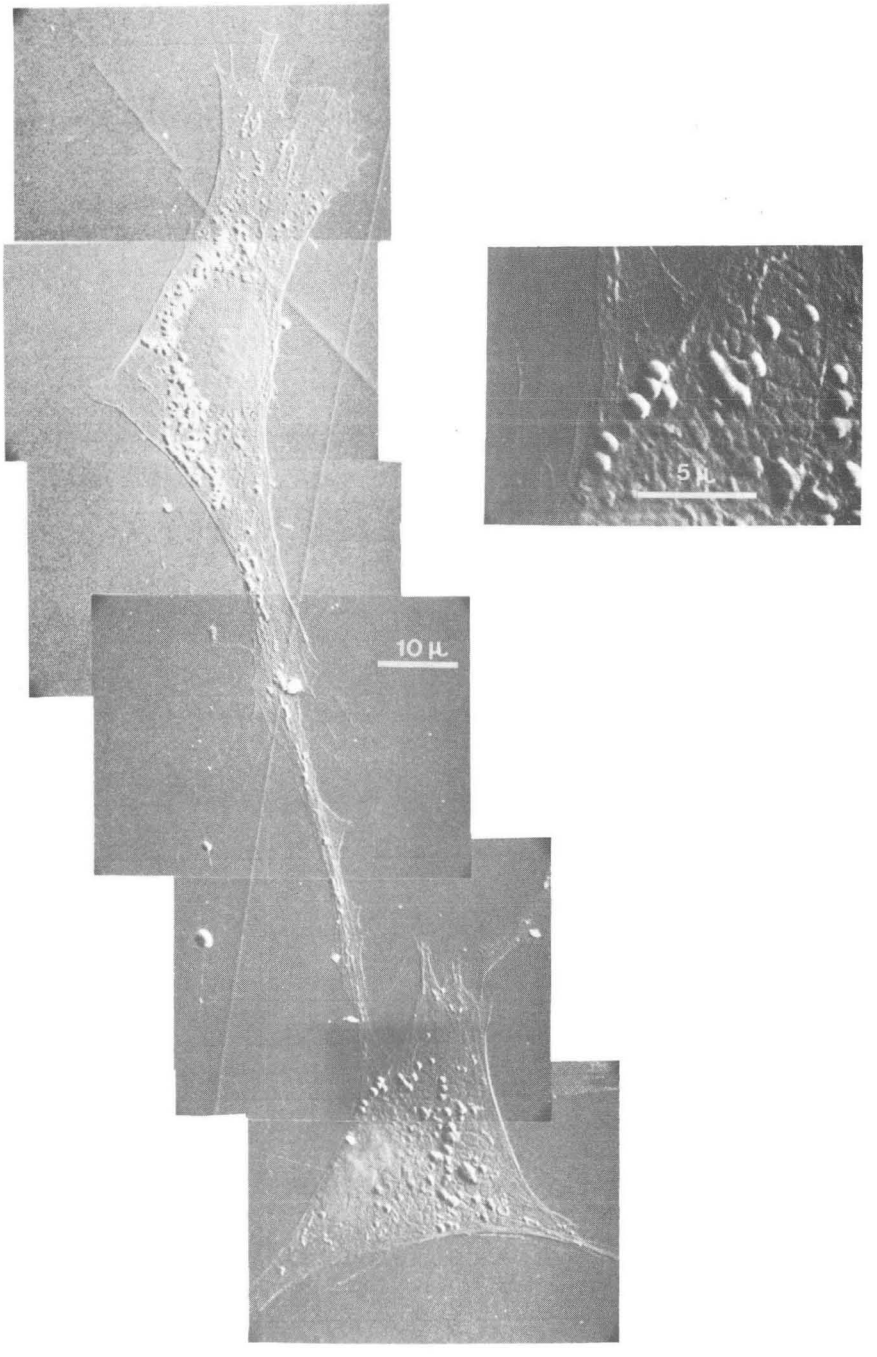

XBB 697-4793

Fig. 18

corresponding morphological structure must exist somewhere within this one and only contact region.

Figure 19 shows the formation of a low-resistance junction between two normal cells as viewed with phase optics. The corresponding scanning electron micrographs of the contact regions are shown in Figure 20a, b, and c. In the upper left photograph of Figure 19 cell A and cell B first approach and then make contact (middle right photograph) forming a low-resistance junction (electrical record, bottom left). Contact between cells C and D also occurred and presumedly they formed a low-resistance junction, however, this was not checked electrically.

The scanning micrograph in Figure 20a shows cells A, B, C, and D. The junction between cells A and B (Figure 20b) reveals an interesting aspect of cell contact which was frequently observed in other micrographs: when one fibroblast (cell A in this case) advances towards and makes contact with another cell, its leading ruffled membrane passes beneath the encountered cell (cell B in this case). Thus the advancing ruffled membrane appears to retain contact with its substrate and to either detach or to

FIGURE 19

The establishment of junctional communication between fibroblasts. The phase contrast photograph in the upper left shows four normal fibroblasts. Cells A and B are not visibly connected. Electrophysiological measurement at that time indicated that the cells were not functionally coupled. After two hours the cells had moved into positions as shown in the picture at the right. Cell A has formed a visible connection with Cell B. At this stage the cells were coupled as is shown in the electrophysiological record at the lower left of the figure. Current electrode was in cell A and recording electrode in cell B (both electrodes are not shown). White vertical bar is 20 millivolts for top two voltage traces, 20×10^{-9} amperes for current trace. Middle trace: voltage response of cell B to a 4×10^{-9} amperes and 56 millisecond hyperpolarizing current pulse in cell A. Positive calibrating pulses: 10 millivolts, 10 milliseconds.

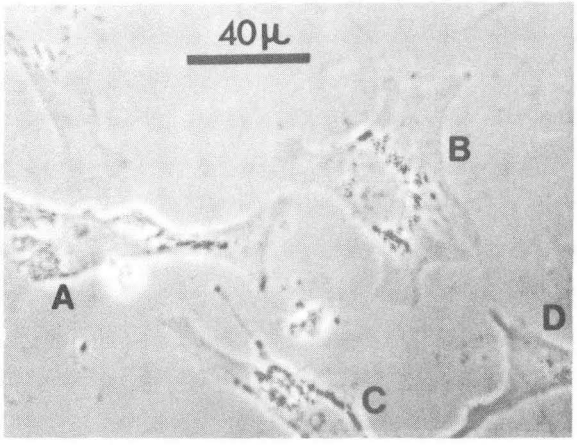

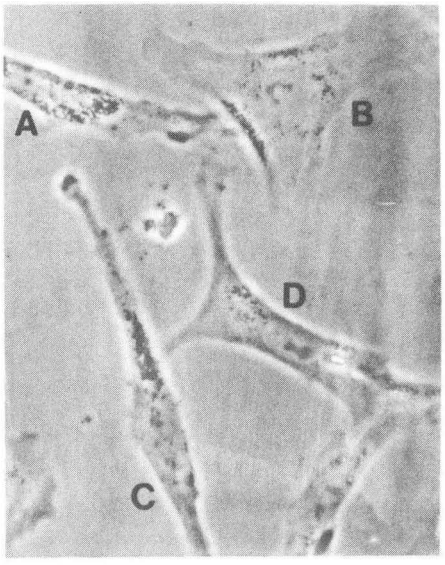

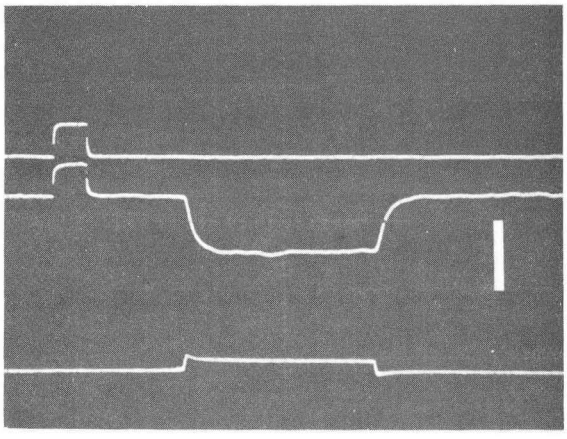

XBB 697-4791

Fig. 19

FIGURE 20 a, b, c.

Scanning electron micrographs of the same coupled cells as shown in previous Figure 19.

(a) Photograph showing the junctional contact areas between cell A and cell B and between cell C and cell D. Junctional contact area between cells A, B contains elements of high permeability; that between cells C and D presumedly of high permeability.

(b) Higher magnification of junctional area between coupled cells A and B. Note that the fan-like cell process from cell A dips under the cell membrane of cell B. For further discussion, see text.

(c) Higher magnification of junction between cell C and cell D. The diffuse looking white particle below the contact area is probably debris not associated with the cell surface.

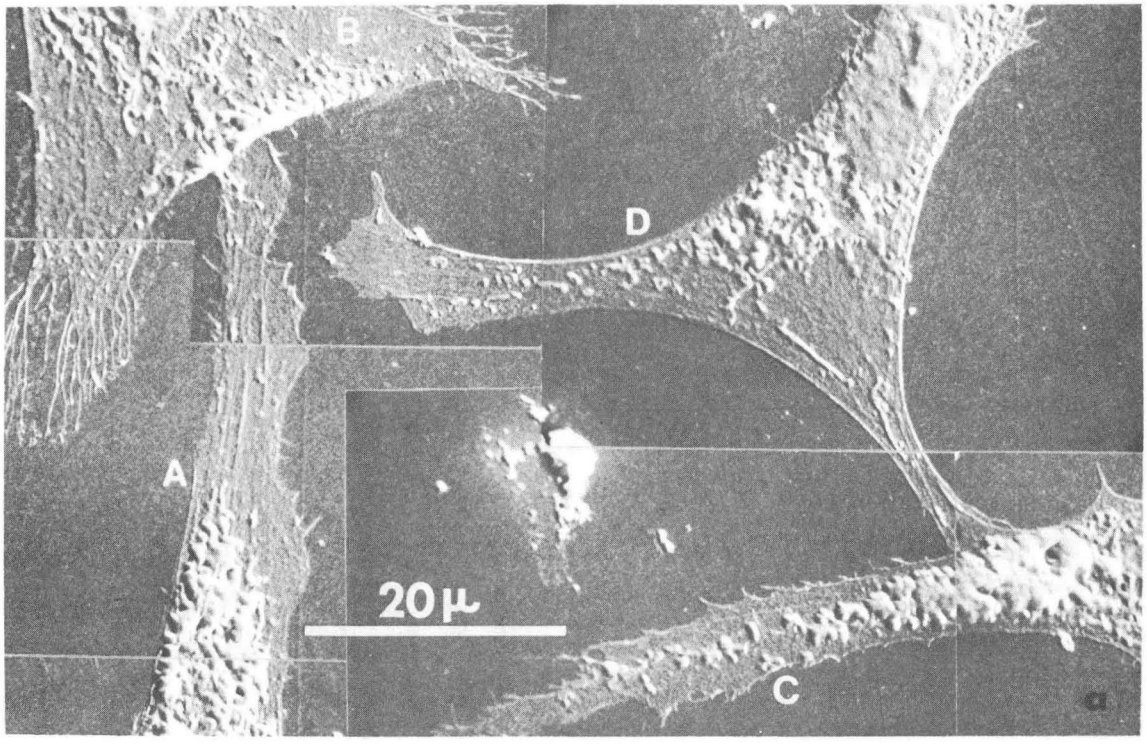

XBB 698-5334

Fig. 20A

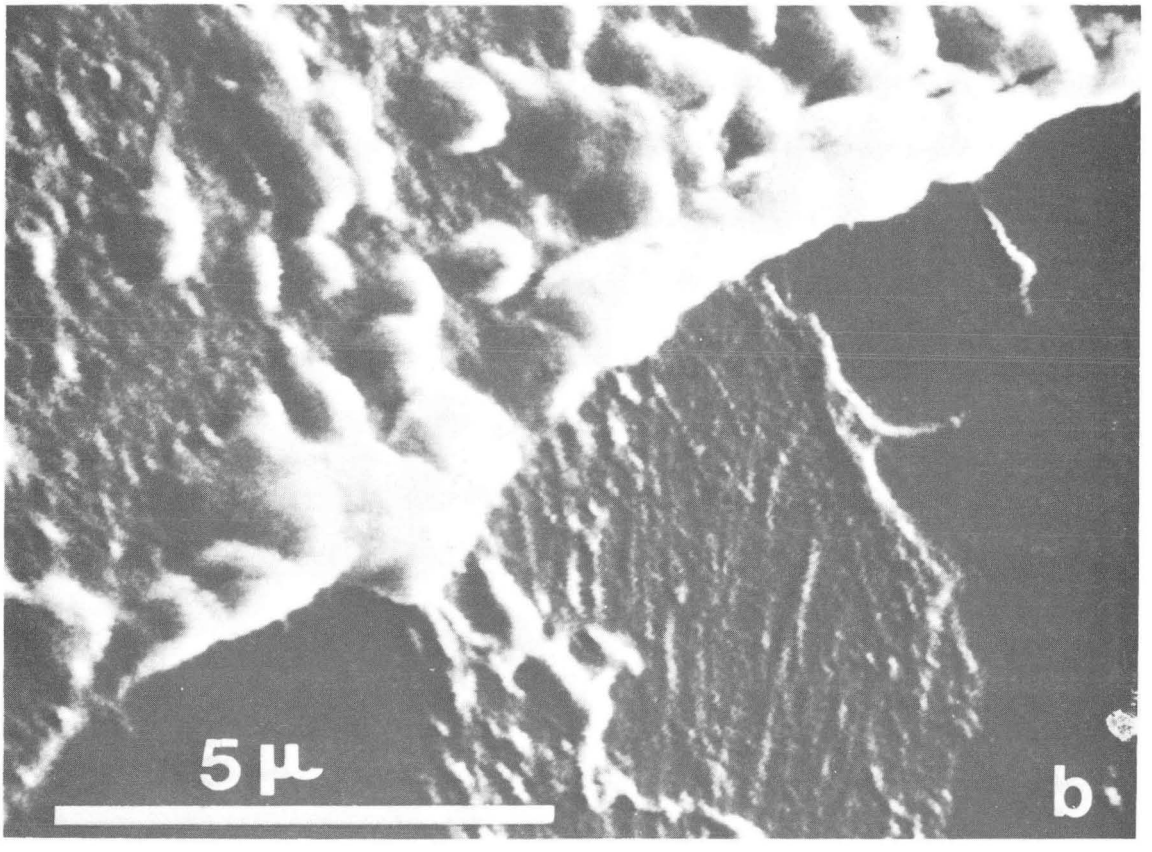

XBB 698-5332

Fig. 20B

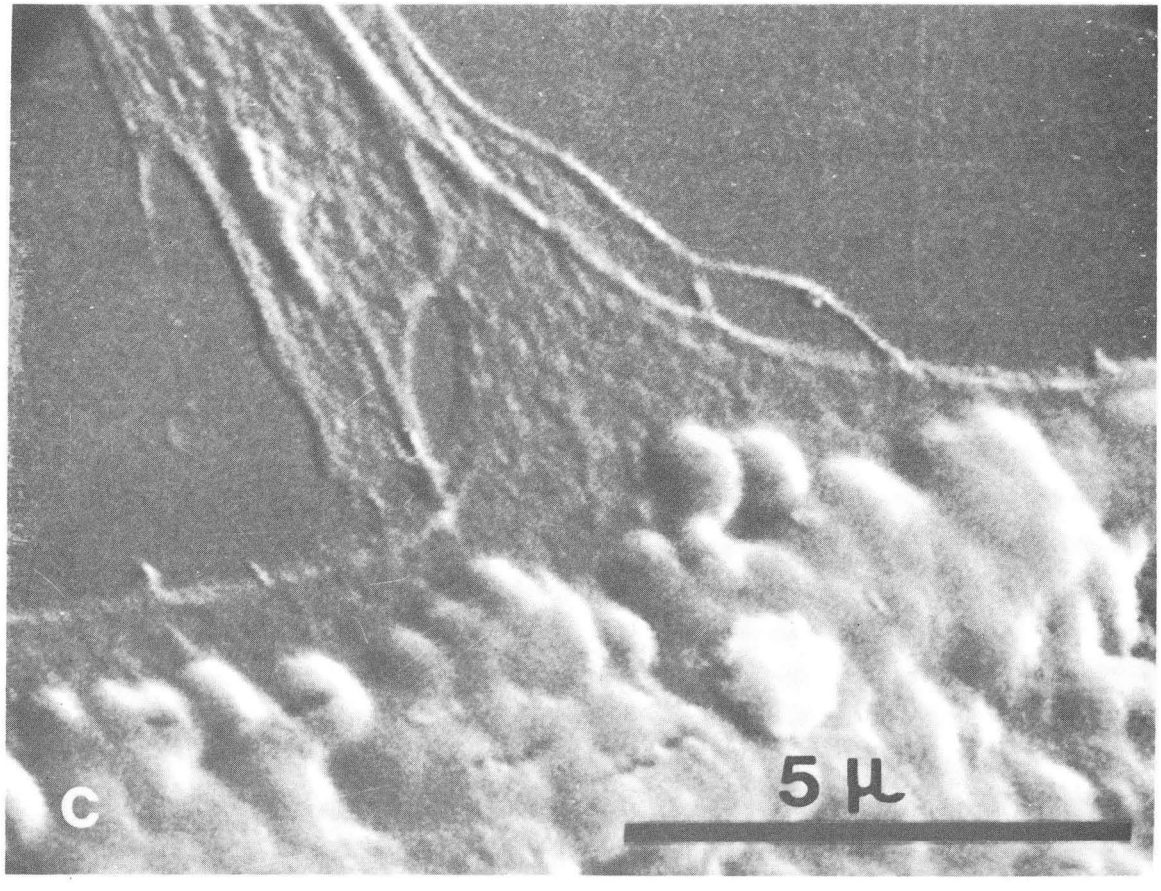

XBB 698-5333

Fig. 20C

pass beneath an already detached part of the cell it encounters. This phenomenon has been studied by Boyde et. al, (1969) and the results presented here are consistent with their observations. The relevance of these results to a hypothesis on the role of cell adhesion in contact inhibition of movement proposed by Carter (1965) is discussed later (see discussion). Figure 20c shows the more complicated contact between cells C and D. It appears that parts of the process from cell D have passed beneath the advancing membrane of cell C, while parts of cell C may be "underlapping" cell D.

Figure 22 shows a scanning electron micrograph of part of a confluent monolayer of fibroblasts containing two coupled cells A and B shown in Figure 21 as viewed with phase microscopy. The cells at this stage had stopped growing. In the scanning micrograph note the abundance of cellular microextensions interconnecting all the cells. It would be of interest to know whether these microextensions play any role in "density dependent inhibition". The structures presumed to be "vacuoles"

FIGURE 21

Phase contrast picture of normal living secondary fibroblasts forming a confluent monolayer in which the cells are in a state of "contact inhibition" of growth (four days in culture). Two cells ("a" and "b") are seen impaled by the microelectrodes (me). The electrical records indicate that cell a and cell b are functionally coupled. The 4×10^{-9} amperes and 56 millisecond hyperpolarizing current pulse is shown on the bottom trace. The intracellular voltage response of cell 'b' to this current in cell 'a' is shown in the middle trace. Top trace is the control trace. Positive calibrating pulses are 10 millivolts and 10 milliseconds.

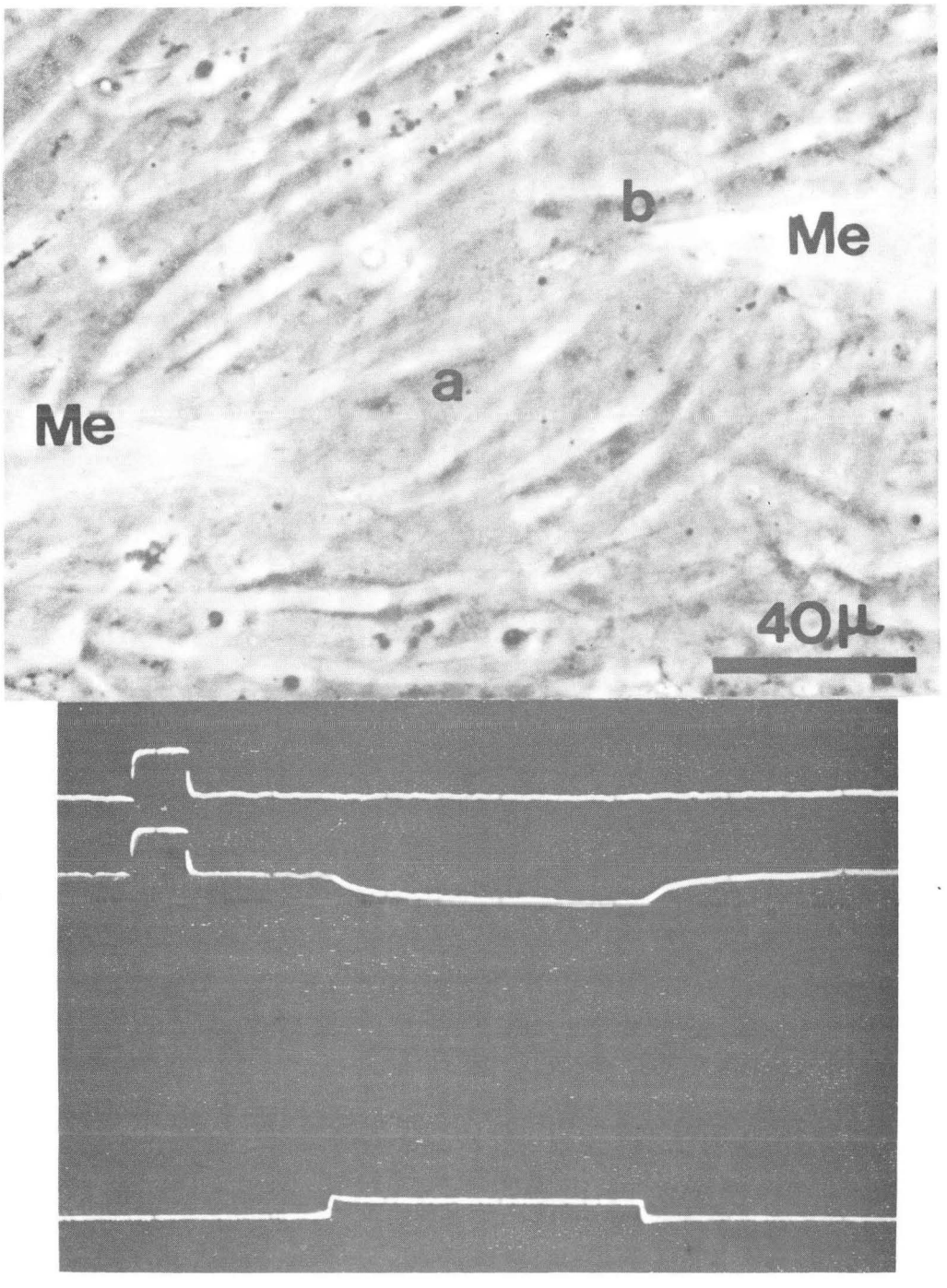

XBB 698-5020

Fig. 21

FIGURE 22

Scanning electron micrograph of the same field as shown in the phase contrast picture of the previous Figure 21. Cells A and B were shown to be electrically coupled. Both the nuclei and nucleoli of cells A and B are visible. Note the abundance of thin processes between the cells. The structures described as vacuoles frequently seen in one day cultured fibroblasts (see Figures 18 and 20) are not seen in this micrograph. See text for further discussion.

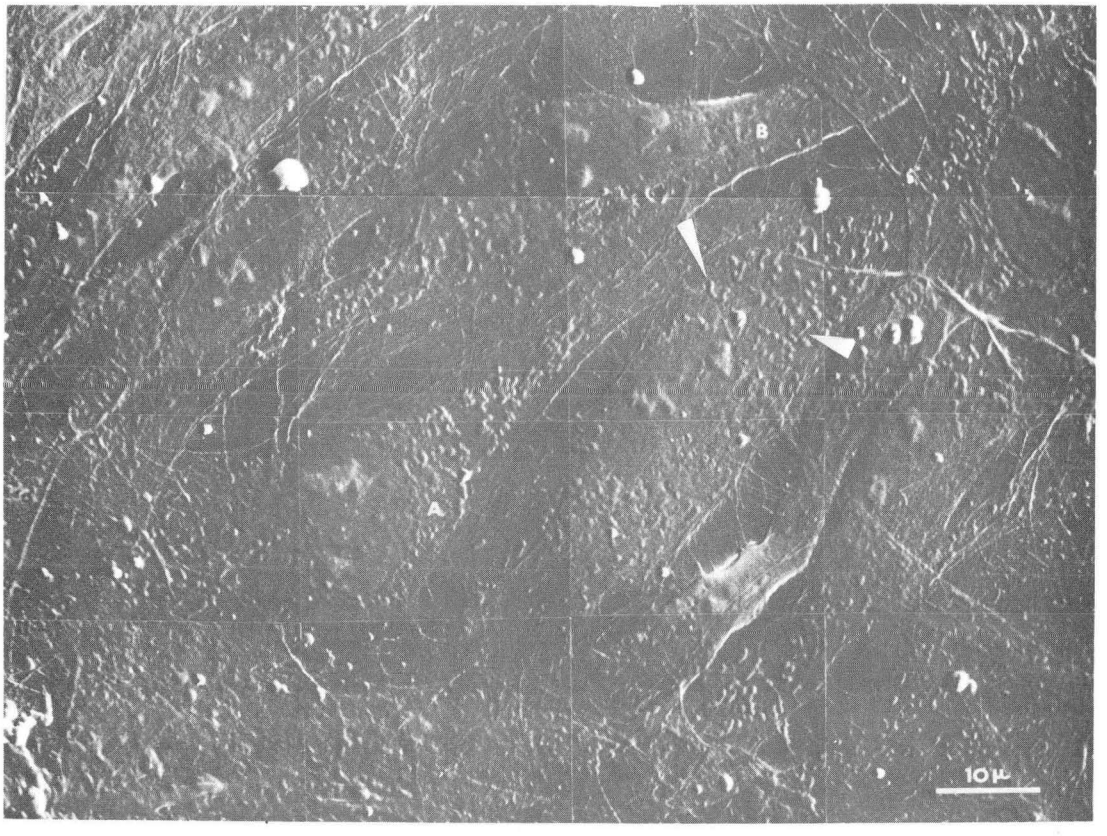

XBB 698-5022

Fig. 22

and frequently observed in one day cultured fibroblasts (see Figures 18 and 20) are in general not present in cells within confluent monolayers. The absence of these structures is evident in Figure 22. The rod-like structures (arrows) seen the these cytoplasmic areas of the cells have been observed by Boyde et.al. (1969) and are thought to be mitochondria.

Scanning Electron Micrographs of Coupled Cells - One in Mitosis

The surface morphology of cultured fibroblast cells in beginning mitosis was always observed to change rather drastically, progressing from a flat appearance at interphase to a rather spherical shape at early metaphase. A priori, it seemed likely that during this process the low-resistance junction would also change, possibly uncoupling the cells. Therefore, during the course of these experiments it was rather surprising to find that some degree of coupling was always detectable between interphase cells and cells in various stages of mitosis. It was not possible to keep cells impaled with microelectrodes through the course of cellular mitosis and

therefore it was not ascertained whether the mitotic cell broke coupling for a short period before, during, or after division. In some cases where a mitotic cell was completely rounded up and appeared to be connected to its neighbor by fine cytoplasmic processes, electrotonic potentials spread from one cell to the next as well as they did between normal interphase cells which were coupled. Mitotic cells were recognized under the phase contrast microscope by (1) possessing a halo indicative of the rounding up process of cells during mitosis, (2) by being connected to its interphase neighbors and the substrate by many fine cytoplasmic microextensions from the mitotic cell surface, and (3) by their chromosomes being in various stages of separation (from being lined up along a cellular axis to their being separated into two complete sets located at opposite ends of the cell).

Figures 23 - 26 show typical examples of mitotic cells coupled to normal interphase fibroblasts and corresponding scanning electron micrographs. The three-dimensional pattern of radial microextensions from the mitotic cells and connections between the mitotic cell and its

coupled interphase cell neighbor are clearly seen in the scanning micrographs.

Figure 23 shows a phase contrast photograph of two cells impaled by microelectrodes (Me), with one mitotic cell (M) apparently connected to the interphase cell by two thin processes. The electrical records (bottom) indicate that the cells are coupled. The dark gray area in the middle of the mitotic cell was actually seen under the microscope to be chromosomes lined up in an axial manner.

The scanning pictures of the above cells are shown in Figures 24 a, b. The cells appear to be little distorted from the morphology seen in the phase contrast picture. Both the nucleus and the nucleoli of the interphase cell are clearly seen in (a). The rod-like structures (arrows) seen in the cytoplasmic area of the interphase cell have been observed in other fibroblastic cells and are thought to be mitochondria (Boyde, et.al., 1969). Many mitotic microextensions occur around the mitotic cell and two definite areas of contact occur between the mitotic and interphase cells (arrows in Figure 24b).

FIGURE 23

Phase contrast picture of two normal fibroblasts impaled with microelectrodes (me). One cell (M) is in mitosis while the other is in interphase (one day in culture). The electrical record indicates that the cell pair are functionally coupled. Current pulses (4×10^{-9} amperes and 56 milliseconds) were passed in either direction through the cell membrane of the mitotic cell (M) and symmetrical voltage changes were recorded within the interphase cell. Positive calibrating pulses: 10 millivolts, 10 milliseconds. Vertical white bar: 20 millivolts for top two electrical traces, 20×10^{-9} amperes for bottom current traces.

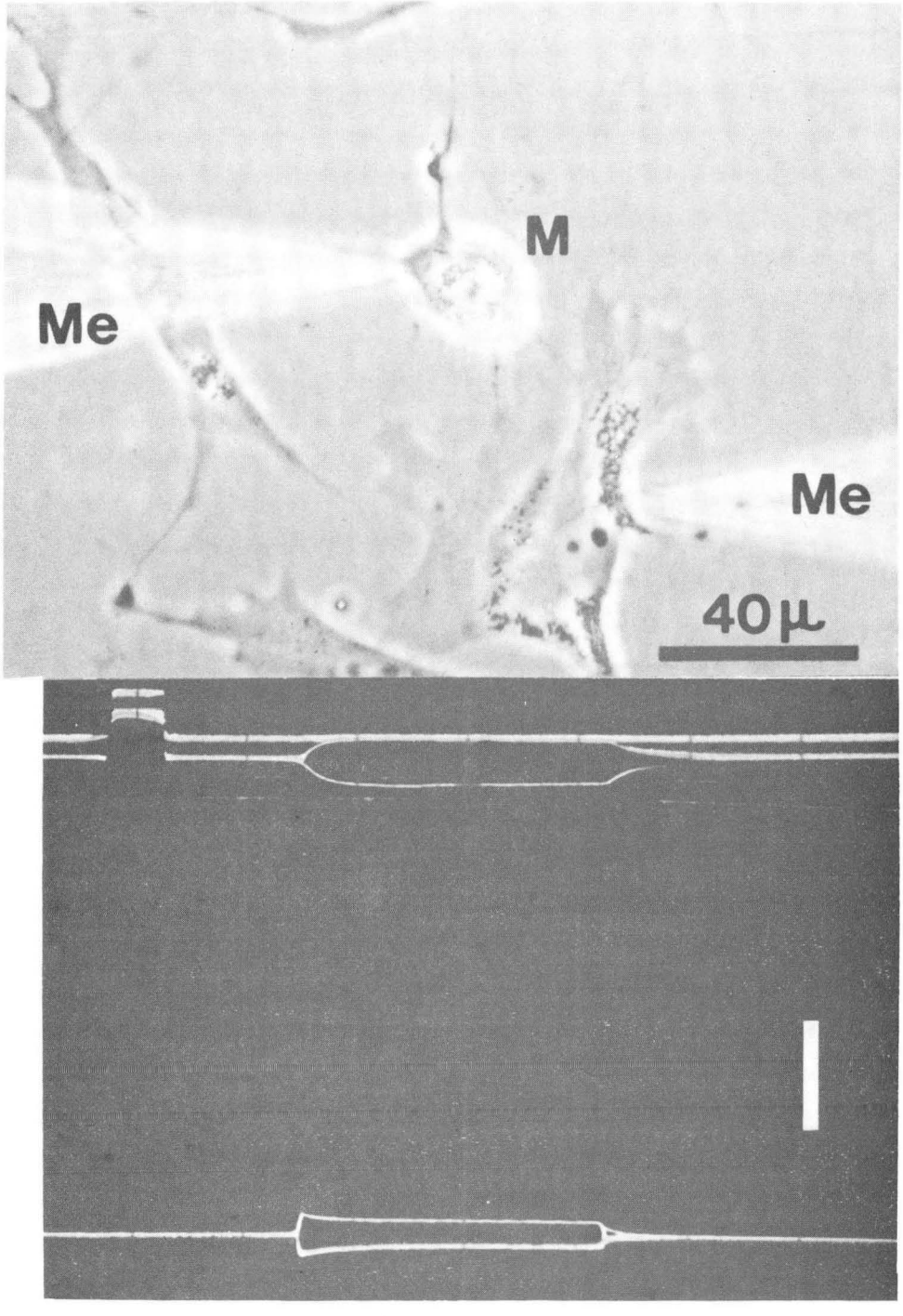

XBB 698-5024

Fig. 23

FIGURE 24a, b

(a), (b) Scanning electron micrographs of the same coupled cell pair as shown in the previous Figure 23.

(a) Many mitotic retraction filaments are seen eminating radially from the mitotic cell (M). Several areas of contact between the mitotic and interphase cell are also evident. The rod-like structures (arrows) seen in the interphase cell resemble the fibroblast mitochondria reported by other investigators (Boyde, et.al, 1969). Both nucleus and nucleoli are clearly visible. The large white round structures on the interphase cell are most likely pinocytotic vesicles seen in the other micrographs.

(b) Higher magnification of the contact areas (arrows) between the mitotic and interphase fibroblasts.

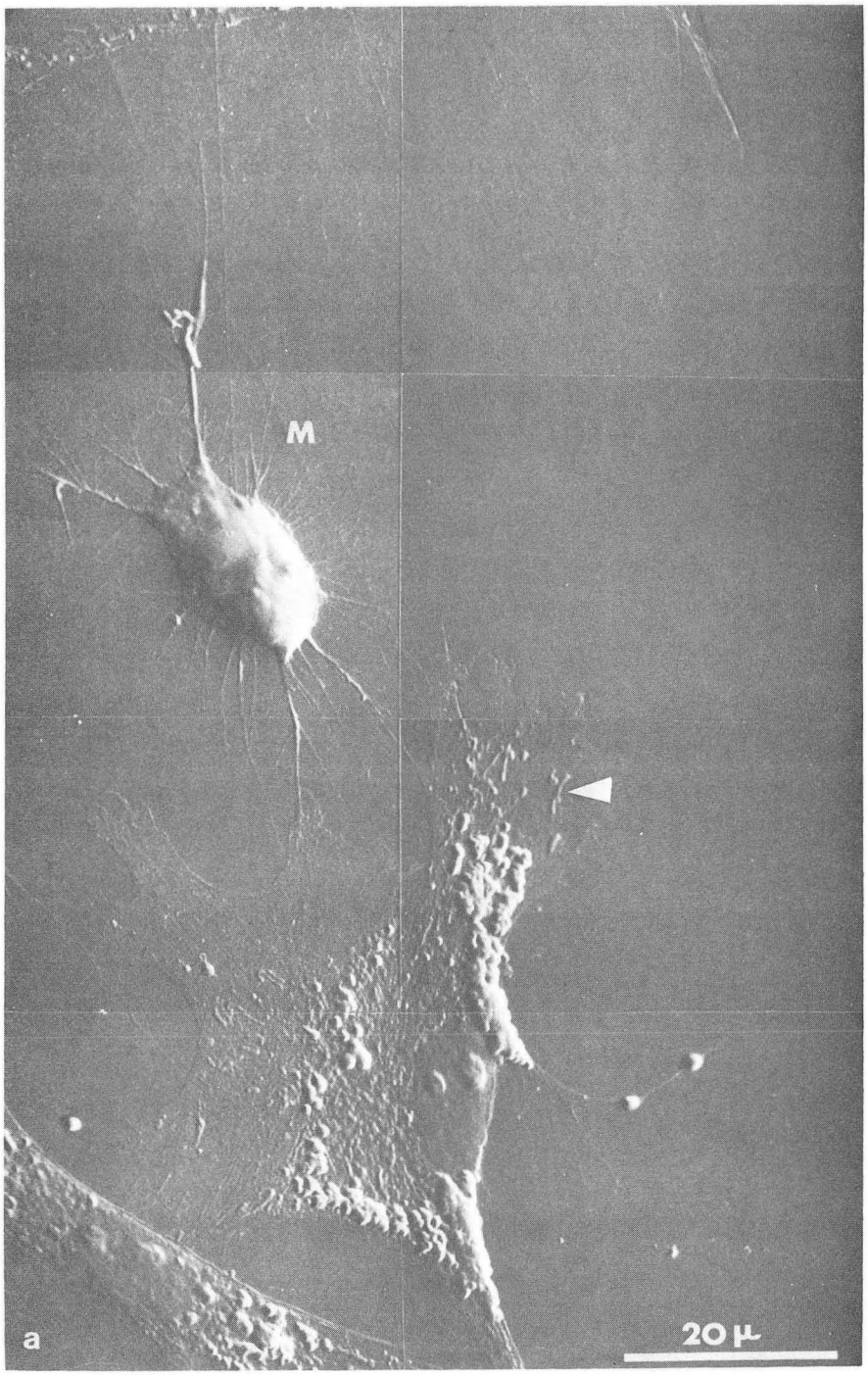

XBB 698-5065

Fig. 24A

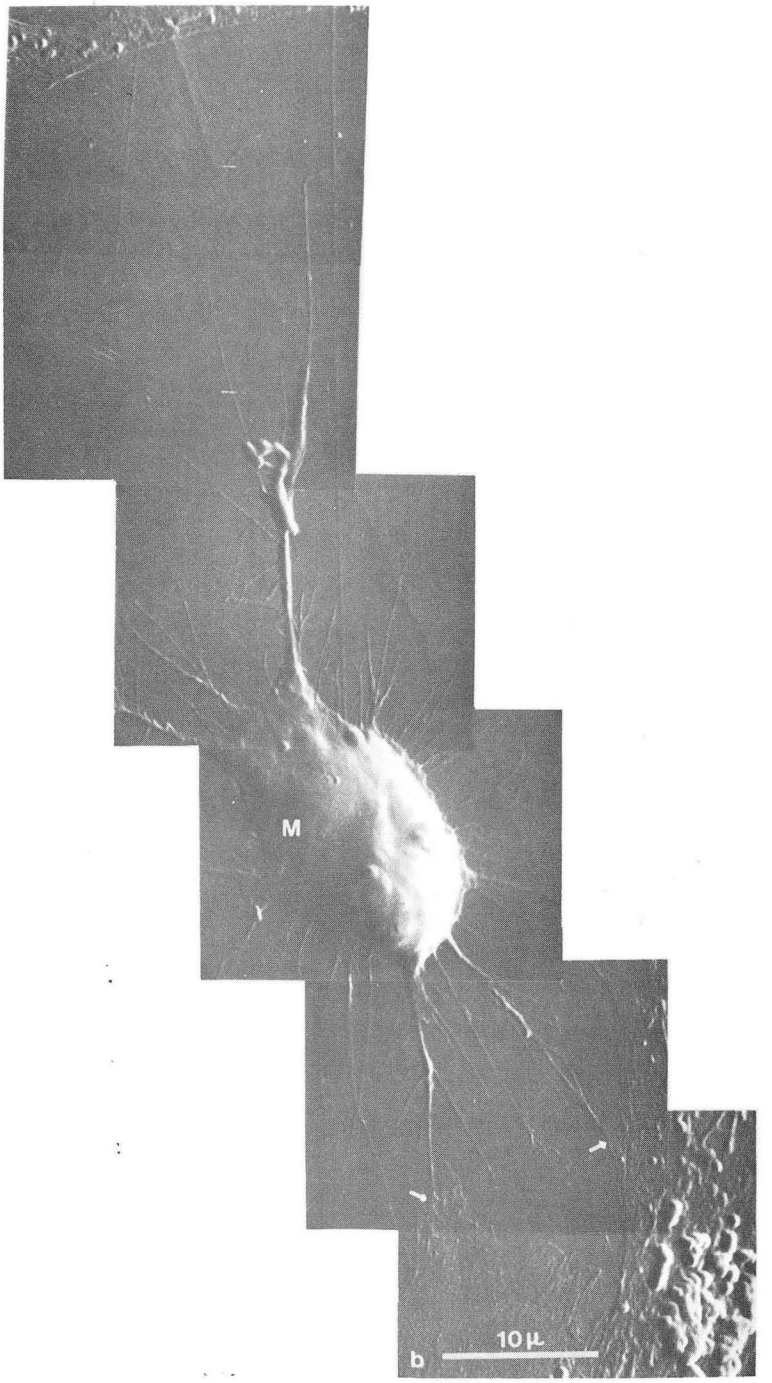

XBB 698-5064

Fig. 24B

Two other scanning electron micrographs of a mitotic cell coupled to an interphase cell are shown in Figures 25 and 26 (see Figure captions for details).

Finally, one example of coupling between a daughter cell of a cellular division and an interphase cell with corresponding scanning micrographs is seen in Figure 27. Current pulses were passed into the daughter cell and electrotonic potentials were recorded from inside the interphase cell but not outside (see electrical record).

Scanning Electron Micrographs of Rous Sarcoma Cells

Scanning electron micrographs of two cells in the early stages of transformation in an infected culture are shown in Figure 28. The electrical recrods (B) demonstrate the presence of coupling between the two apparently unconnected cells impaled with microelectrodes (Me) (shown in A). The abundance of overlapping cells is evident both in the phase pictures and the scanning micrographs. The micrographs in (C) and (D) demonstrate the presence of many cytoplasmic extensions from the coupled cells a and b. These extensions are

FIGURE 25

Scanning electron micrograph of a communicating cell pair, where one cell is undergoing mitosis. The photograph (upper left) shows a phase contrast picture (top) of two fibroblasts, one in mitosis connected to one in interphase (one day in culture). The linear arrangement of chromosomes along an axis is clearly seen in this mitotic cell. Two microelectrodes (me) used for the electrical measurement are shown. The electrical record demonstrates that the cells are coupled. Top trace is control trace which shows no response to the applied current pulse (bottom trace). The middle trace is the intracellular voltage response of the mitotic cell to a 6×10^{-9} amperes and 56 millisecond hyperpolarizing current pulse applied through the cell membrane of the interphase fibroblast. Positive calibrating pulses: 10 millivolts, 10 milliseconds. Vertical white bar 20 millivolts for top two traces, 20×10^{-9} amperes for bottom current trace. (Right) Scanning electron micrograph of the same cell pair shown in the phase contrast picture at left. Cellular processes are seen connecting the mitotic cell

to the interphase fibroblast. A dimpling of the central portion of mitotic cell may indicate the beginning of a division furrow.

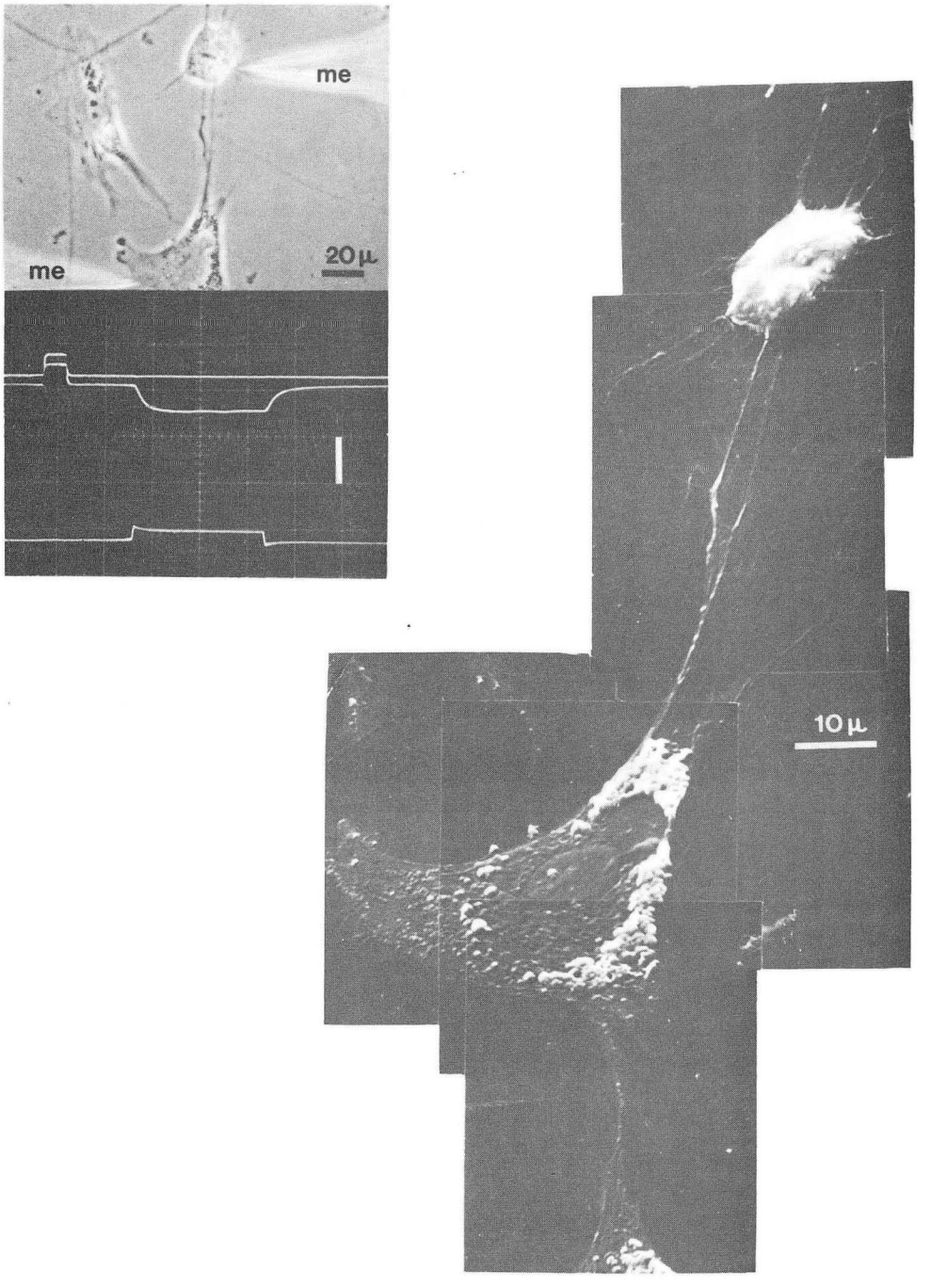

XBB 697-4790

Fig. 25

FIGURE 26

Scanning electron micrographs of a mitotic fibroblast in junctional communication with an interphase cell (one day *in vitro*). Picture at lower left shows phase contrast photographs of a cell rounded up in mitosis joined to an interphase cell. Two microelectrodes (me) are shown. The electrical data indicates that the cells are coupled. Current pulse (bottom trace) is 6×10^{-9} amperes in amplitude and 56 milliseconds in duration. White vertical bar: 20 millivolts for top two traces and 20×10^{-9} amperes for bottom current trace.

The scanning electron micrographs are shown at the right. The higher magnification of the mitotic cell shows the abundant number of small processes radiating from the round cell body. These processes were seen in every mitotic cell studied.

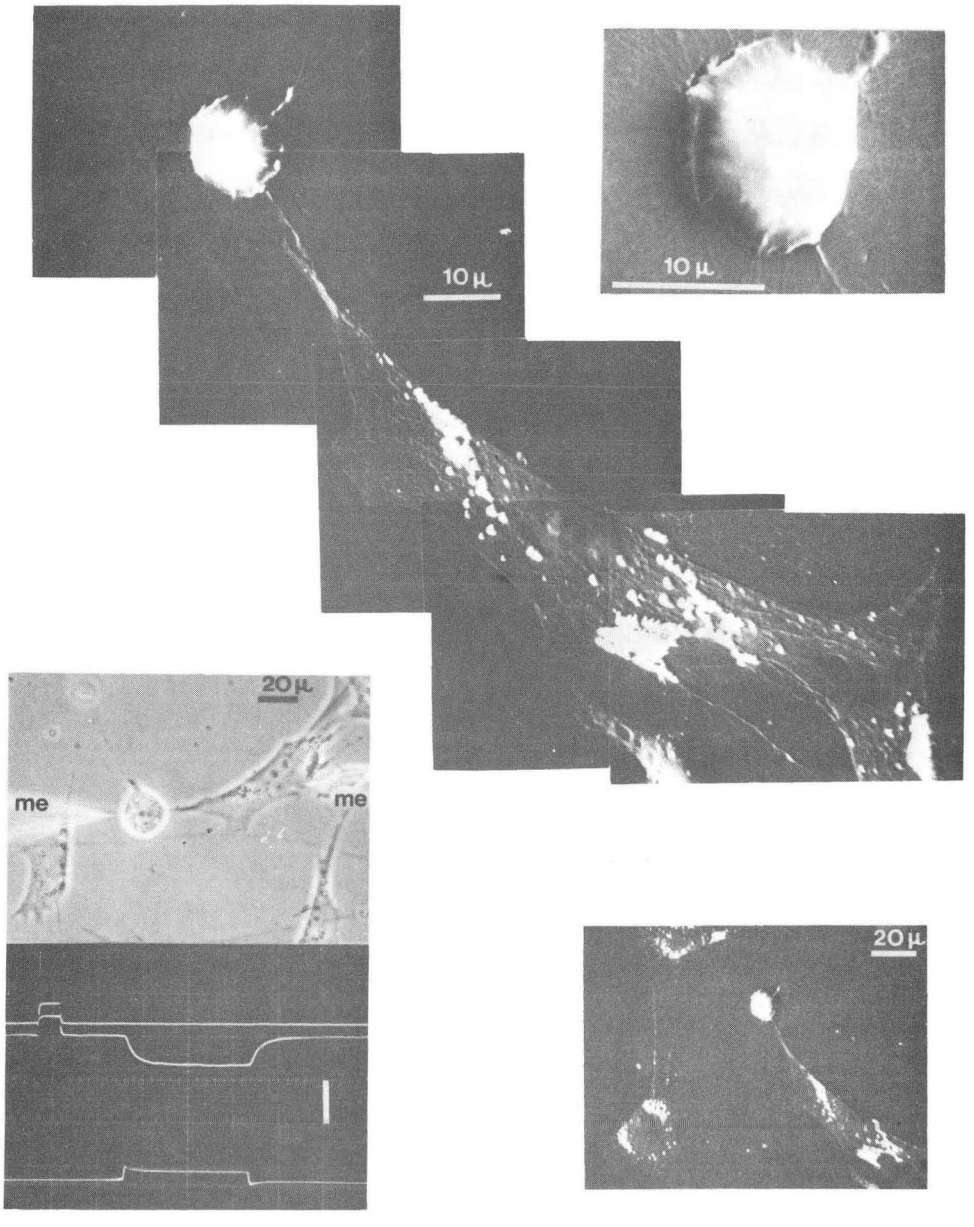

XBB 697-4785

Fig. 26

FIGURE 27

(A) Phase contrast picture (top) of functionally coupled normal fibroblast cells. One member of the coupled pair is a daughter cell of a mitosis, the other an interphase cell. Electrical record: 4×10^{-9} amperes and 56 millisecond hyperpolarizing current pulse passed intracellularly into the daughter cell. Voltage responses top two traces. Positive calibrating pulses: 10 millivolts, 10 milliseconds. Vertical white bar: 20 millivolts for top two traces, 20×10^{-9} amperes bottom current trace.

(Bottom) Low magnification scanning electron micrograph of same coupled cell pair.

(B) Higher magnification scanning pictures of the coupled cell pair (bottom) and daughter cells (top).

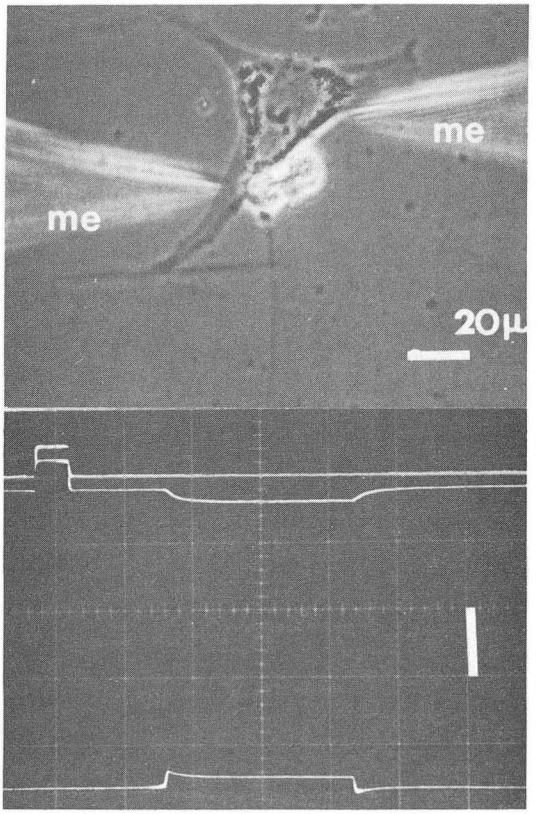

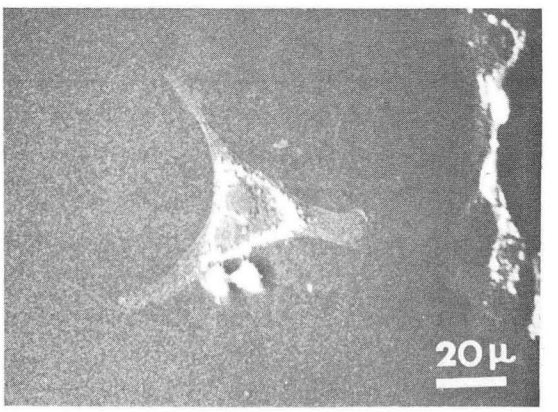

XBB 697-4798

Fig. 27A

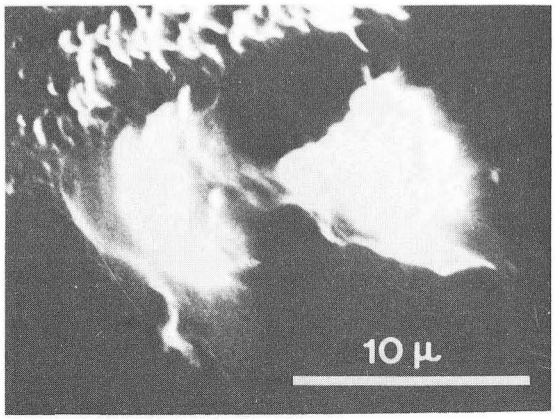

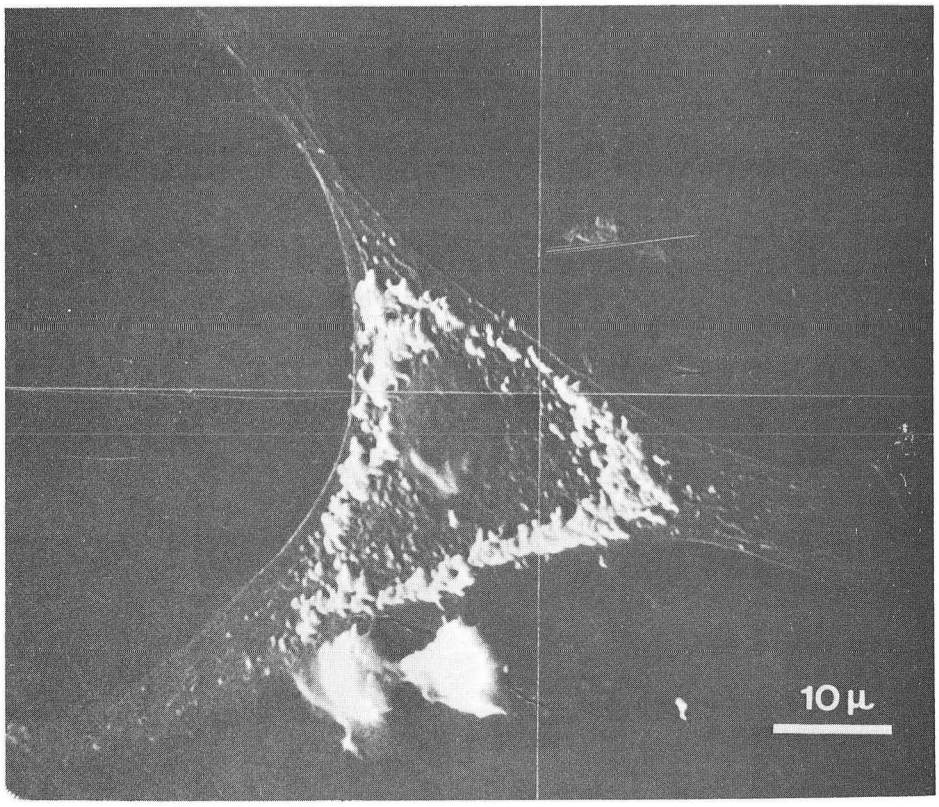

XBB 697-4797

Fig. 27B

FIGURE 28

Scanning electron micrographs of two coupled cells at an early stage of Rous sarcoma virus (RSV) transformation (three days).

A. Phase contrast picture of the two living cells impaled with micreoelctrodes (Me).

B. Electrical record. Middle trace shows that a voltage response is recorded inside cell "b" due to a hyperpolarizing pulse of current - 4×10^{-9} amperes and 56 milliseconds (bottom trace) inside cell "a", but none is recorded when the recording microelectrode is just outside cell "b" (Top trace). Positive calibrating pulses are 10 millivolts and 10 milliseconds. White vertical bar is 20 millivolts for top two traces and 20×10^{-9} amperes for bottom trace.

C. Scanning electron micrograph of same cells a and b. Both the nuclei and nucleoli of the cells are clearly visible.

D. Higher magnification micrograph showing the cytoplasmic extensions originating from cell b. The nucleus of the cell which appears below cells a and b in the phase contrast picture (see A) is clearly visible (see also D).

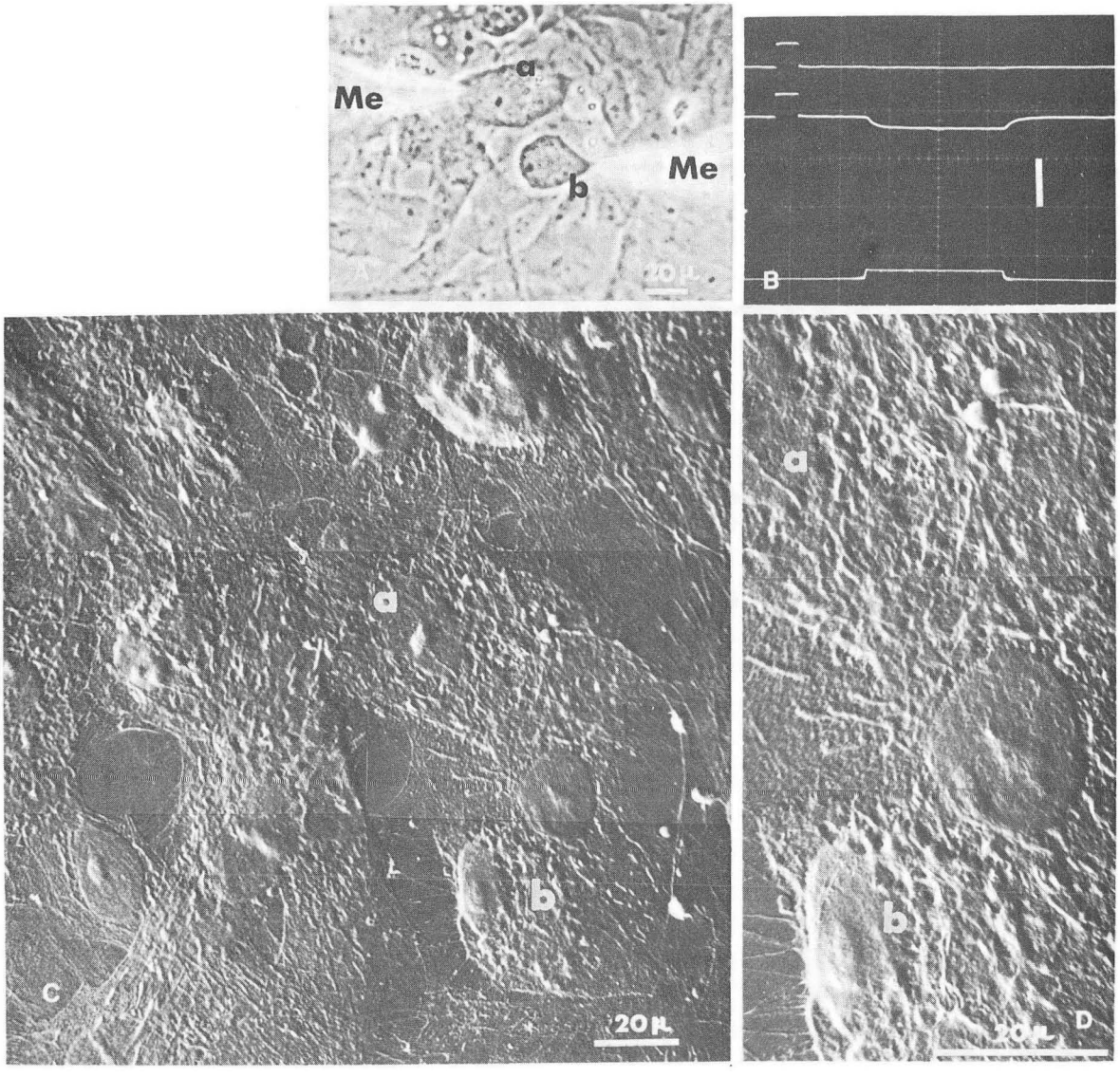

XBB 699-6071

Fig. 28

similar in appearance to those seen in scanning micrographs of metaphase fibroblasts and fibroblasts within a confluent monolayer (compare with Figures 22 and 24, this thesis). The nuclei and nucleoli are clearly visible in both cells, as well as others in the field. Particularly note the nucleus seen between cells 'a' and 'b' in (C). This nucleus appears to belong to the cell seen between, but beneath, these cells in the phase picture. This nucleus is seen in higher magnification in (D).

Figure 29 shows scanning electron micrographs of a Rous transformed cell in a culture infected with Rous four days prior to the electrophysiological measurement. The Rous cell (R) in the phase contrast picture is highly refractile and spherically shaped, the characteristic morphology of Rous transformed cells. The same cell is easily identifiable in the scanning micrographs B, D and E. One intriguing aspect of the Rous cell is its surface architecture shown in Figure 29 (D, E). The numerous convolutions in the surface of the RSV transformed cell were not seen in any other chick fibroblast

FIGURE 29

Scanning electron micrographs of a Rous sarcoma transformed fibroblast in a culture infected four days prior.

A. Phase contrast picture of the living cells. The Rous transformed cell (R) and the untransformed fibroblast (N) are seen impaled with microelectrodes (ME).

B. Scanning electron micrograph of the same cells as in A.

C. Electrical record. A voltage response (middle trace) is recorded by the electrode within the Rous cell (R) due to a hyperpolarizing pulse of current 4×10^{-9} amperes and 56 milliseconds (bottom trace) passed into the other cell (N) but no voltage response is recorded with the recording electrode just outside (R). Positive calibrating pulses: 10 millivolts and 10 milliseconds. Vertical white bar: 20 millivolts for top two traces and 20×10^{-9} amperes for bottom trace.

D.,E. Higher magnification scanning electron micrographs of the same Rous transformed cell showing its highly convoluted surface architecture (see text for further details).

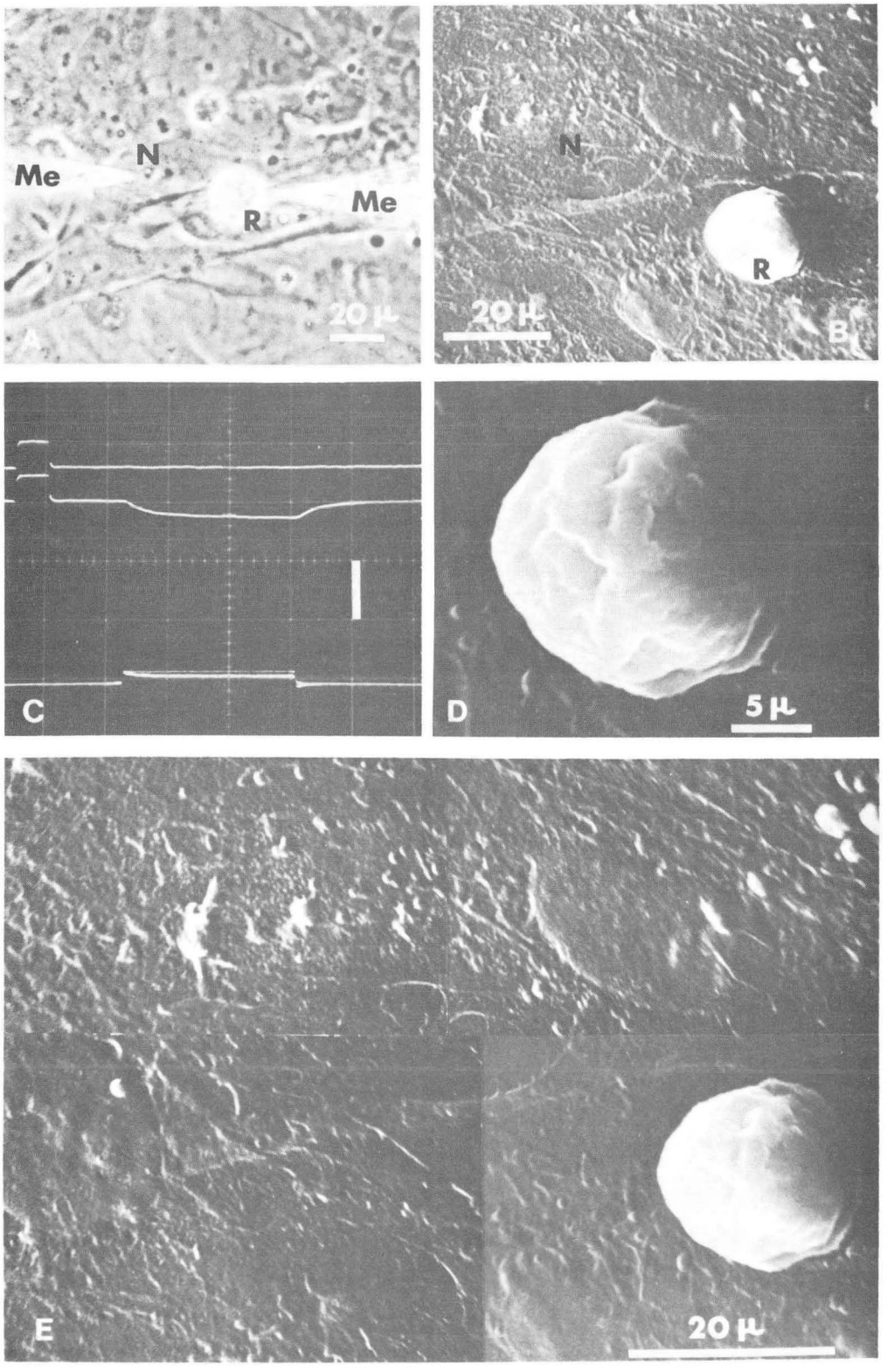

XBB 699-6069

Fig. 29

cells, including the rounded-up mitotic cells, which were studied with the scanning electron microscope. Due to these convolutions, the surface area of a RSV transformed cell is greater than one would guess from looking at the phase contrast picture. It would be interesting to know what role these highly convoluted surfaces play in the behavior of Rous cells in culture. This surface architecture might possibly reflect a change in the rates of uptake and release of metabolic substances from that of normal cells. Similar surface architecture has been observed in scanning micrographs of ascites tumor cells by Williams and Ratcliff, (1969) and in those of macrophages by H. Dalen (unpublished observation).

It should be briefly mentioned that the first attempts to obtain scanning electron micrographs of fully transformed RSV cells were not successful. These cells easily detached from the dish and from other cells due to the usual mechanical disturbance encountered during the preparative procedures. This may be partly explained by the decreased adhesiveness of these sarcoma cells (Rubin, 1966). Only after great care was taken to minimize mechanical disturbances such as very gentle rinsing of the cells

and very careful handling of the dish during fixation procedures did fully transformed cells remain attached.

Tight Junctions in Secondary Fibroblasts

Preliminary evidence that the low-resistance junctions between secondary chicken embryo fibroblasts demonstrated in these experiments correspond to the electron microscopists "tight junctions" is shown in Figures 30 and 31. These transmission electron micrographs were made by Dr. J. Leventhal (unpublished). Figure 30 shows a small area of intercellular contact where the extracellular space between the neighboring cells is apparently obliterated. These "tight junctions" are similar to the tight junctions found in numerous electrically coupled adult tissues (Pappas and Bennett, 1966), and are identical in appearance to those junctions which have been seen in the chick embryo *in vivo* (Trelstad et.al., 1967). Figure 31 is another example of a tight junction seen between these cells. The classical "pentilaminar" structure characteristic of tight junctions is clearly seen in this electron micrograph. The above findings are consistent with the idea that tight junctions may be the structural basis for coupling in these cells.

FIGURE 30.

Transmission electron micrograph of a tight junction between two normal secondary chick embryo fibroblasts in agar. Phosphate buffered glutaraldehyde and osmium fixation. Uranyl acetate and lead citrate staining. Magnification x90.000. (Courtesy of Dr. Jeana Levinthal).

XBB 698-5017

Fig. 30

FIGURE 31.

Transmission electron micrograph of a tight junction between normal secondary fibroblasts in a cell monolayer. Infected with Sendai virus two minutes before fixation. Phosphate buffered glutaraldehyde and osmium fixation. Uranyl acetate and lead citrate staining. Magnification X 40,000.

XBB 698-5021

Fig. 31

RELATED ELECTRICAL PHENOMENA - MEMBRANE POTENTIALS OF SECONDARY FIBROBLASTS

Chemical gradients for different ions provide the major, though possibly not the only, source of bioelectric potentials and, according to the ionic theory of bioelectrogenesis, changes in the relative permeability of the cell membrane for various ions form the basis of the electrical manifestations of cells (Grundfest, 1967). In a similar manner, changes in the ionic gradients across the plasma membrane of cultured cells or changes in the relative ionic permeabilities of these membranes must result in corresponding changes in cellular membrane potentials. Likewise, the converse will necessarily be true.

Preliminary evidence from membrane potential measurements on normal secondary fibroblasts suggests that membrane potentials of cells within a confluent monolayer are significantly greater than those of isolated single cells. Figure 32 shows two histograms of membrane potential measurements, one from isolated fibroblasts (top) and one day in culture and another from cells within a confluent monolayer (bottom) four days in culture. The data for

FIGURE 32.

Histograms of membrane potentials from normal chick embryo secondary fibroblasts (one day, top; four days bottom). Ordinate: number of observations; abscissa: membrane potential in millivolts. Potential measurements from a total of 90 isolated cells from one dish are shown in the one day distribution; and those from 100 cells within a confluent monolayer are shown in the four day distribution. The mean membrane potential of the isolated cells is $10.52 \pm (3.97)$ millivolts, that of the four day cells is $28.13 \pm (7.50)$ millivolts, cell interior being negative in both cases.

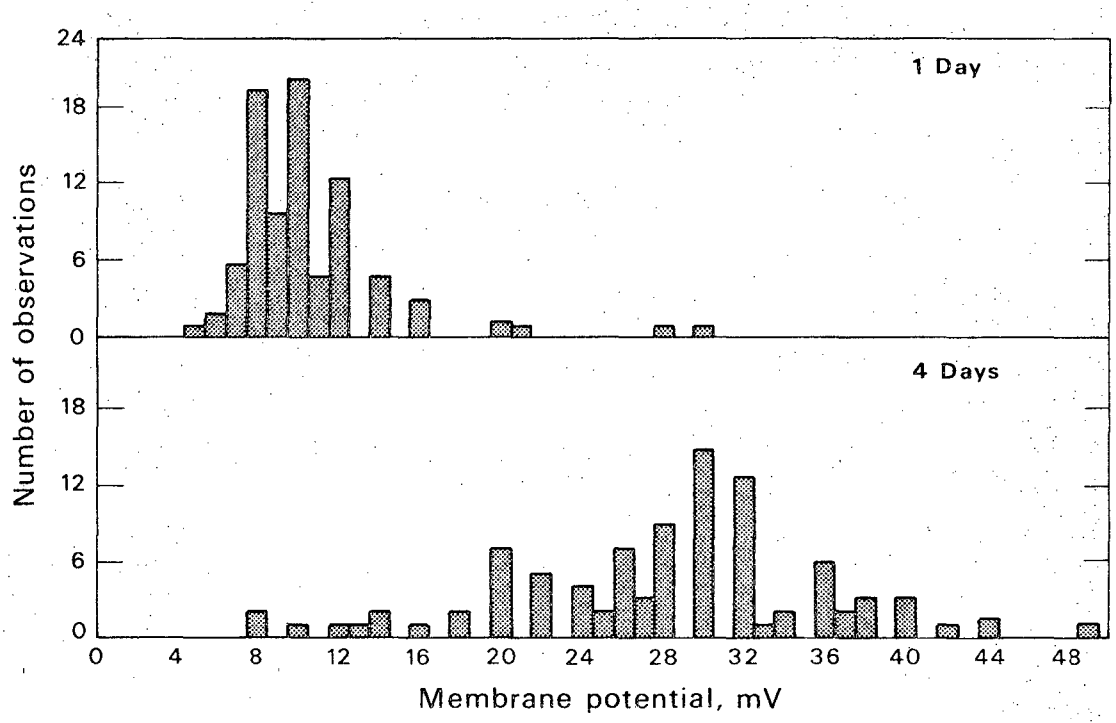
1 Day
4 Days
Number of observations
Membrane potential, mV
0
6
12
18
24
0
4
8
12
16
20
24
28
32
36
40
44
48

XBL 699-5674

the one day sample of potential measurements are all from one dish containing approximately 2×10^5 cells and that of the four day measurements from another dish containing 3×10^6 cells. Both sets of measurements are from experiments lasting approximately two hours and carried out at room temperature 25°C in medium 2-1-1 with the same microelectrode. The mean membrane potential for the isolated cells is 10.52 millivolts, and that for the confluent cells 28.13 ± 7.50 millivolts. The shift in the values of the membrane potentials between one and four day cells was not abrupt, since predominantly intermediate values were found in cells at two and three days in culture. The majority of cells by the second day were in contact and presumably coupled to one or more neighboring cells. Membrane potentials of these cells were similar but, in general, higher than those of isolated cells, but smaller than the potentials of cells in confluent monolayers.

One explanation for this change in membrane potentials towards higher values may be that the isolated cells were trypsinized the day before the measurements and, therefore,

may have been more susceptable to damage from microelectrode penetration than were cells in confluent monolayers some four days removed from the trypsinization process. However, this appears unlikely, since cells seeded at densities of around 10^6 cells and forming a confluent monolayer in one day had membrane potentials similar to cells in culture four days. Another possibility is that isolated cells themselves were more susceptable to electrode damage. This possibility must be considered to contribute some to the results, since in the experiments the ratio of the number of successful penetrations of isolated cells to that of confluent monolayer cells was low. Isolated cells were difficult to penetrate because they were no more than 1 to 5 microns thick. Also, the membrane potentials of isolated cells usually declined with a time constant of seconds after penetration, whereas, the potential decline in confluent monolayer cells after impalement was slow, frequently in the order of minutes. This difference in time constants may be due to the continuous pool of ions shared between coupled cells in a monolayer as compared to isolated cells. In a coupled cell system, ions might readily flow into a very slightly injured cell to maintain the membrane potential, whereas

this could not occur in an isolated cell.

Although electrode damage cannot be excluded as an explanation of the observed difference in membrane potentials between one and four day cells, it is unlikely that it accounts for the total shift. Rather, it appears reasonable to conclude that the shift in the membrane potentials represents a change in cellular permeability or in intracellular concentration, or in both for one or more ions (see discussion).

DISCUSSION

The results of the present study indicate that chick embryo fibroblasts in culture are tightly coupled. That this coupling is not an artifact of the microelectrode technique is shown by the fact that coupling is found between cells separated by as many as ten cells which have not been damaged by microelectrode penetration. Rather, coupling between cells is due to their ability to form low-resistance junctions in culture.

Contact between actively moving fibroblasts results in the formation of a low-resistance junction or junctions between them. In a few cases where both the surface area of the cells and the contact area between them could be estimated from the photographs, the specific resistance of the junctional membranes was approximated using the circuit in Figure 1b. It was found to be serveral orders of magnitude smaller than that of the non-junctional membranes. However, the calculation is very approximate as it has several possible sources of error: the actual input resistances for the cells used in the calculation were not known, but, instead the upper values of those found in other cells were used;and only the upper surface

of the cell facing the medium was considered in the calculation; the internal resistance of the fine processes was estimated as being low and was therefore not included, these values of resistance might actually be larger; the resistance of the contact area was assumed to be uniform. Another source of error was some degree of damage due to microelectrode penetration during coupling measurements. This inevitably reduced the coupling potentials. All these sources of error lead to an underestimate of the degree of coupling.

The role of coupling in the phenomenon of contact inhibition of movement (Abercrombie and Heaysman, 1953) still remains unclear. Evidence presented in the results suggests that the low resistance interconnections between cells may exist throughout the contact period. Thus, cells in a state of contact inhibition of movement are in all probability coupled.

The role of coupling in cell division or in the phenomenon of density dependent inhibition of cell division is also difficult to define for a number of reasons. First, coupling has been demonstrated between contacted fibroblasts in both sparse and dense cultures. Many,

if not all, cells in contact, including those in mitosis, are coupled. Secondly, greater than 80% of secondary fibroblasts are in contact (and coupled?) at a cellular density of approximately 2×10^4 cells/cm^2 but at this density the proliferation rate is maximal and is not inhibited until a density of approximately 10^5 cells/cm^2 or five times greater is attained. Third, and lastly, Rous transformed cells continue to divide, even in very crowded cultures, yet they are coupled. It must be emphasized that the presence of coupling, as shown by electrical measurements, means that there is direct cell-to-cell transfer of small ions that carry the current. Its presence tells nothing about the direct transfer of large particles which might participate in cellular regulatory processes.

The prevalence of low-resistance junctions in tissue culture cells, normal or transformed, as well as in embryonic and adult tissues suggests that these junctions are basic to cell activity. At present, their role is known only in the electrical activity of excitable tissues. What are the possible functions or consequences of low-resistance junctions between the fibroblasts as studied

here? It is reasonable to conclude from the results that inorganic ions move rapidly between fibroblasts in contact. These ions such as K^+, Na^+, Cl^- must, therefore, become part of a common intracellular milieu of the coupled fibroblasts. The low-resistance junctions inevitably distribute the work of pumping ions and buffering. One consequence of this is that all functions subserved by such ions would be stabilized to some degree as each cell in contact acquires an average concentration. Any ionic activity performed by any one member of the coupled fibroblasts would tend to be damped with respect to the activity of the rest of the cells. The degrees of damping would in all likelihood depend on the number of cells in contact.

This damping phenomenon can be compared to that frequently observed in coupled excitable cells. Furshpan and Potter (1968) give the example of cardiac or smooth muscle cells. To stimulate a cell, positive ions are delivered to its interior, but some of these escape into neighboring cells. The consequences of coupling in these cells is not that activity is impossible, but that any member is less likely to perform its characteristic activity in response to a small stimulus.

The ability of ions to pass freely between coupled fibroblasts as described above, appears to present a problem in the case of cell injury. Injury to one or more cells in a coupled system could conceivably lead to the short circuiting of the rest of the cells. However, this was not found to be the case in coupled fibroblasts in culture. The "wounding" experiment described under Results in this thesis is of particular interest in this regard. Injured fibroblasts uncoupled from neighboring cells but coupling between the healthy uninjured cells was unaffected. This uncoupling of injured cells also occurs _in vivo_. Low-resistance connections between cells in the squid embryo were also found to be very labile, sealing off following injury (Potter et.al., 1966) It is likely that the sealing off is related to the influx of extracellular medium into the injured cell (see Loewenstein, 1968).

Direct transfer of substances other than ions between secondary fibroblasts has recently been suggested by the work of Peterson (1969) and Peterson and Rubin (1969). Cells labelled with P^{32}- choline are found to transfer the label preferentially to cells in which they

are in contact. However, the label is likely to be incorporated into phospholipids possibly associated with the cell surface and these molecules need not be transferred from within one cell to within another. It remains to be shown whether this transfer is through the low-resistance junctions between these cells.

Although no evidence yet exists that demonstrates the passage of small metabolic molecules or regulatory substances through low-resistance junctions, these junctions offer a very attractive mechanism for cell-to-cell communication. The spread of dyes of 10^3 MW in coupled cell systems (Furshpan and Potter, 1968) suggests that molecules such as thyroxine and steroid hormones, etc., or other molecules having inductive or repressive as well as nutrient affects on cell behavior might also spread readily through coupled cells. Potter, et.al.(1966) findings that the yolk cell is coupled to possibly all cells in the developing squid embryo suggests that intermediary metabolical and waste products might distribute through low-resistance junctions. Future experiments are needed to determine whether low-resistance junctions provide pathways for intercellular control of complex activities such as movement, division or differentiation (see later).

The transmission electron microscopic examination (Dr. J. Levinthal, unpublished) on chick embryo fibroblasts in culture indicates the presence of tight junctions between these cells which under a variety of conditions were shown in this work to form low-resistance junctions. At present, this finding is consistent with the idea that tight junctions may be the structural basis for low-resistance coupling. However, Katz (1966) has pointed out that only a few cytoplasmic bridges 100Å in diameter between cells can account for electrical coupling. These bridges might be difficult to detect with the electron microscope.

It is evident from the above discussion that the correlation between low-resistance coupling and tight junctions much remain circumstantial until more definitive experiments directly relating coupling and junction morphology can be performed. As a first step in this direction, the experiments using the scanning electron microscope to investigate contact morphology between coupled cells in tissue culture are of interest. The results of experiments presented in this paper indicate that a cell pair in culture may be tested for coupling with microelectrode techniques and the contact morphol-

ogy between the same cell pair may be examined with electron microscopes. Moreover, in many cases the area of contact between cells in culture is very limited, and a large number of morphological junctions within this area is unlikely. The scanning pictures in this thesis show that many of the morphological features possessed by living fibroblasts in culture appear little changed inspite of microelectrode penetration and a method of preparation involving fixation, drying and the application of conducting coatings in vacuo. The only impression gained about shrinkage during preparative procedures is that when fibroblasts are dried they shrink down upon their substrate rather than detaching from it and retracting (see also Boyde et.a., 1969). Hence, cellular configuration in scanning micrographs closely resembles that usually seen in culture. The success of this technique indicates that a transmission electron microscopic study on the contact area between tissue culture cells previously tested for coupling now appears feasible.

Although the scanning electron micrographs reveal little about the actual contact morphology between

coupled cells, they do reveal the relative cell membrane positions between contacted cells. The micrographs of the isolated fibroblast cells show that the ruffled membrane of an approaching cell "under laps", i.e., crosses under the contacted cell rather than "overlaps". This finding and that by Boyde et.al (1969) suggests that at the point of contact the advancing membrane has more adhesion to the substrate than does the contacted cell, since the advancing cell membrane displaces it. It is highly unlikely that the relative positions of an advancing membrane and a "contacted" cell seen in the micrographs become reversed by the methods of preparation employed. In a recent paper Carter (1965) has suggested that contact inhibition is the result of the greater strength of adhesion of a cell to its substratum than to another cell.

Normal secondary fibroblasts in Rous sarcoma virus (RSV) infected cultures are coupled at all stages of cellular transformation which includes cells active in virus production, one to two days after infection (Vogt and Rubin, 1962), and cells at different stages of morphological transformation within Rous foci (Temin

and Rubin, 1958). Coupling between cells in RSV infected cultures appears indistinguishable from normal cells in uninfected cultures. Thus transformation of normal fibroblasts by Rous virus in culture does not appear to cause cellular uncoupling as might be detected by procedures used in this work.

Similar results have been found in long term cultures of 3T3 cells transformed with SV40 many generations removed from the cells originally transformed (Potter et.al.,1966). 3T3 cells (mouse fibroblasts) are similar to the secondary chick cells studied in this thesis in that both cell types are sensitive to contact inhibition of movement and cell division and both types are released from these inhibitions with virus transformation (Green and Todaro, 1967; Rubin and Colby, 1968).

As stated in the introduction, coupling has been observed in some cases (Furshpan and Potter, 1968) and not in others (Loewenstein, 1968). The epithelial cancer studied apparently lack coupling and the transformed fibroblasts many generations removed from those originally transformed in culture do not. The results of this thesis show

coupling is not interrupted during an early phase of fibroblast RSV transformation in the same cells. Coupling is present when the transformation appears in the Rous infected cells and remains present thereafter in these cells. Short breaks in coupling between cells in culture cannot be excluded, since they are difficult to detect with the coupling procedures usually employed. However, this would still be unlike the extensive uncoupling found by Loewenstein in epithelial cancers.

Ultrastructure analyses on normal and transformed cells in culture are few, but generally these studies demonstrate that while tight junctions occur frequently between normal fibroblasts in culture (Devis and James, 1964; A. Martinez-Palomo et.al., 1969), their transformed counterparts lack tight junctions, but frequently exhibit close junctions and desmosome-like structures. In a study by Morgan(1968) on chick embryo fibroblasts transformed with the Bryan strain of RSV, tight junctions were not found between either normal or transformed cells, but close junctions between both cell types were frequently observed. In this respect, it is of interest to note that Revel and Sheridan (1967) could only demonstrate

the presence of close junctions but nottight junctions between mouse brown fat cells which they showed to be coupled.

It has been suggested that virus production leads to a change in cell surface membrane structure (Rubin, 1966). The surface architecture of Rous sarcoma virus transformed fibroblasts as revealed by the scanning electron microscope is interesting in this respect. The highly convoluted surface was seen in all Rous cells, but not in any other chick fibroblast cells, including the rounded-up mitotic cells, It is highly unlikely that this surface architecture of Rous cells is an artifact of fixation. However, this cannot be entirely excluded. Further studies on the Rous cell architecture with scanning electron microscope would appear to be certainly worthwhile. It is of interest to note that even with the apparent morphological change in the Rous cell membrane the low-resistance junction between it and other cells remains. Apparently, these junctions can be very labile (as in the wounding experiment) or they can persist through drastic morphological changes in cell shape, as in the cases of mitotic cells and transformed cells.

The preliminary finding of a difference between the membrane potentials of isolated fibroblasts and fibroblasts within a confluent monolayer may prove interesting. The potentials of proliferating cells (isolated) appear to be significantly lower than those of non-proliferating cells. The low membrane potential of the isolated cells as compared to confluent cells may represent a general leakiness to ions possibly resulting from the mechanical distortion of the isolated cell membrane on the plastic substrate. Mechanical distortion is known to produce depolarization in other cell systems (the pacinian corpusle,for example). Cells in confluent monolayers appear to be much less spread out on the substrate. This might naturally arise from the crowding of the cells in a monolayer. It is interesting that leakiness seems particularly great when the cells are engaged in active synthesis related to growth and division.

Another alternative to the general "leaky" state would be that there is a change in the cellular permeability to one or more specific inorganic ions, especially Na^+ (see below), between the isolated and confluent states.

This alternative is appealing for the following reasons: first, in the very few studies of membrane potential measurements on mammalian cells in culture, a consistent finding is that low membrane potentials are associated with high Na^+ cellular permeability (Aull, 1967; Hempling, 1962; Borle and Loveday, 1969); in one case the permeability ratio P_{Na}/P_K in HeLa cells was found to be fifty times higher than in muscle and nerve cells (Borle and Loveday, 1969). Secondly, there is some evidence that cell concentrations of sodium (Na) and Potassium (K) are functions of the age of the culture. Wickson-Ginzburg and Solomon (1963) found that during the first four days growth of HeLa cells, the intracellular (K^+) increases and the cell (Na^+) decreases. Considering these findings, it is tempting to suggest that the low membrane potentials observed in the one day (proliferating) cells may be a result of high Na^+ permeability and/or high cell (Na^+): and the increase in potential by four days (non-proliferating state) is a result of decrease in Na^+ permeability and/or a subsequent drop in intracellular Na^+.

However, since none of the variables controlling the membrane potential of the chick embryo fibroblasts studied

in this paper are known, speculations on the mechanism shall not be expanded further. Some obvious questions which are of interest are: how does the membrane potential depend on cell density, i.e., cells/cm^2, what are the concentrations of Na^+, K^+, Cl^- within the one day vs. the four day cells, what are the relative cellular permeabilities of each ion at those days and can the potential be shown to follow the Goldman equation for Na^+ and K^+ with Cl^- passively distributed across the cell membrane? Most of these questions are answerable by simple tissue culture experiments with standard electrophysiological tools.

CONCLUDING REMARKS AND FUTURE OUTLOOK

Implicit throughout this work has been the assumption that the use of electrophysiological techniques provides a unique approach to studying the problems of mammalian cell interactions in culture. Support for this assumption is shown by the results of the present investigation. It has been demonstrated in this paper that many, if not all normal or transformed fibroblasts in contact communicate in such a way as to allow the rapid flow of small ions, such as K^+, Na^+ and Cl^- from one cell interior directly to another. This results in these ions becoming part of a common intracellular milieu of the coupled cells in culture. This intercellular communication was shown to be a consequence of the development of low-resistance junctions between these mammalian cells in culture. It appears reasonable to conclude from the prevalence of these low-resistance junctions between cells in culture, as well as in embryonic and adult tissues, that these junctions are basic to cell activity.

The present electrophysiological investigation was limited to the study of ionic flow through the low-

resistance junctions between cultured cells. It is not known at present whether these junctions also provide pathways for larger particles which might be involved in the cellular control of complex activities such as cell movement and cell division in culture. However, these junctions offer a very attractive mechanism for cell-to-cell communication, and future experiments employing electrophysiological techniques should provide more information on the role of these junctions in cellular regulatory processes.

Along these lines, the following types of experiments are a few that might be undertaken: (1) Cells in tissue culture can be injected with radioactive substances passed through fine microelectrodes filled with the radioactive material and cellular coupling checked electrically before, during or after cell contact is made. Subsequent autoradiography studies can then be carried out on these cells to determine if transfer of radioactive material between cells has occurred. Also, from the results of this thesis it appears that an autoradiography study at the transmission microscopic level of cells previously injected with radioactive materials

and checked for coupling might be possible. Experiments of this type would combine the advantages of the fluorescein experiments of Furshpan and Potter (1968) and Loewenstein (1968) and the genetic experiments of Subak-Sharpe et.al. (1969) and Stoker (1967a). (2) Experiments such as those described in (1) could be used with substances (as yet unknown) which might selectively prevent the passage of substances between cells. If a variety of substances could be shown to uncouple cells, then it might be possible to determine the ranges and types of substances which pass through the low-resistance junctions by the injection of a variety of substances into cells and checking for transfer with various techniques such as fluorescence microscopy or autoradiography. (3) As suggested in this thesis, the changes in membrane potential of cells in culture may be related to activities associated with cell growth and cell division. These relationships between cellular membrane potentials and cell growth and division in tissue culture can be determined by simple tissue culture experiments, utilizing standard electrophysiological tools.

From the above discussion it can be concluded that the combined techniques of electrophysiological tissue culture, autoradiography and electron microscopy offer new ways of attacking the problems of mammalian cell interactions.

SUMMARY

1. Intercellular communication or electrical coupling between normal chick embryo fibroblasts and between fibroblasts transformed with Rous sarcoma virus in culture was studied with intracellular microelectrodes.

2. Coupling was present between normal chick embryo fibroblasts in proliferating cultures. Mitotic cells in contact with interphase cells were coupled.

3. Coupling was also present between cells in a confluent monolayer in which further proliferation has been inhibited ('density dependent inhibition').

4. The results showed that between cancer fibroblasts (Rous sarcoma transformed) coupling was present when the transformation appeared in the infected cells and remained present thereafter in these cells.

5. Coupling between the cells was not an artifact of the microelectrode technique, but was shown to be due to the ability of these cells to form low-resistance junctions in culture.

6. The specific membrane resistance in normal fibroblasts was estimated to be several orders of magnitude smaller than that of the non-junctional membranes ($0.12 \Omega\text{-cm}^2$ as compared to $400 \Omega\text{-cm}^2$).

7. The lability of low-resistance junctions between cells was shown in the wounding experiment. This result demonstrated that injured fibroblasts readily uncoupled from neighboring cells without interrupting coupling between the healthy uninjured cells.

8. Tight junctions (photographs of Dr. J. Levinthal) exist between the same type of fibroblasts that were shown to be coupled. This finding is consistent with the idea that tight junctions are the morphological structures of low-resistance junctions.

9. A method was presented to allow the study of the cellular morphology of previously coupled cells with the scanning electron microscope.

10. With this technique, it was shown that in the cases studied when cellular processes eventually reached neighboring cells, they underlapped them and formed low-resistance junctions.

11. The scanning electron micrographs of Rous sarcoma virus transformed cells revealed that the surface morphology of these cancer cells was highly invaginated, a characteristic not found in any of the normal fibroblasts studied.

12. Preliminary studies on the membrane potentials of the normal fibroblasts showed that the values for isolated cells were significantly lower than those for cells within a confluent monolayer. Possible cellular permeability changes to specific ions are discussed as causes for the observed changes in membrane potential values.

13. Finally, it is concluded that electrophysiological tools combined with tissue culture techniques and autoradiography offer new ways of attacking the problems of animal cell interactions.

APPENDIX I

The advent of commercial production of operational amplifiers incorporating field effect transistors (FET)[1] has yielded voltage operated solid-state devices with extremely high input impedance, high gain and wide-band amplifiers of miniature size. One such low cost FET amplifier Model KM-47C (K & M Electronics Corp., Hackensack, New Jersey) has been employed as the basic unit in a high input impedance amplifier built specifically to be used to record biological signals as detected with high impedance electrolyte filled glass microelectrodes.

A highly schematic diagram of the basic amplifier design is shown in Figure 33a. The upper amplifier A_1 in Figure 33a is constrained to unity gain by short circuiting the output e_o of A_1 to the inverted pole of the differential input of A_1. Signals through the microelectrode (ME) are fed into the positive or non-inverted input of A_1 and appear at e_o unchanged. The overall frequency response of A_1 is increased by negative capacitance feedback with the use of amplifier A_2. To achieve this, the

---

[1]W. Shockley, "A Unipolar Field-Effect Transistor," Proc. IRE, Vol. 40, pp. 1365-1367, November 1952.

FIGURE 33

A. Schematic diagram of a high-input impedance Field Effect Transistor operational amplifier. ME - microelectrode (see text for further details).

B. Circuit diagram of actual amplifier design. A bottom view of the pin arrangement on the KM-47C operational amplifiers is shown (see text).

C. Triangular wave generator employing Fairchild μA709C operational amplifier (see text for details).

a. High-input impedance microelectrode amplifiers

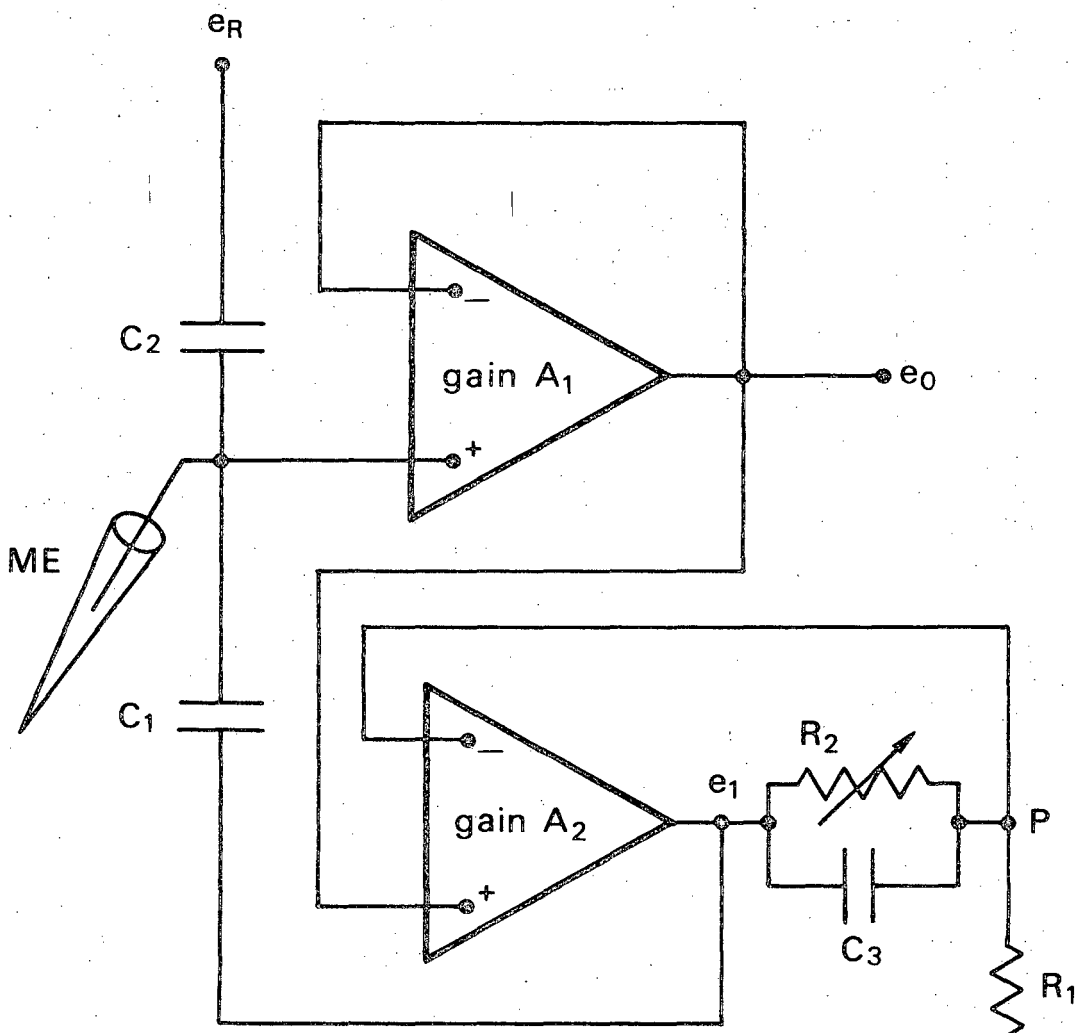

$$A_1 = 1$$

$$A_2 = \frac{R_2 + R_1}{R_1}$$

DBL 698-5010

b. Actual amplifier design

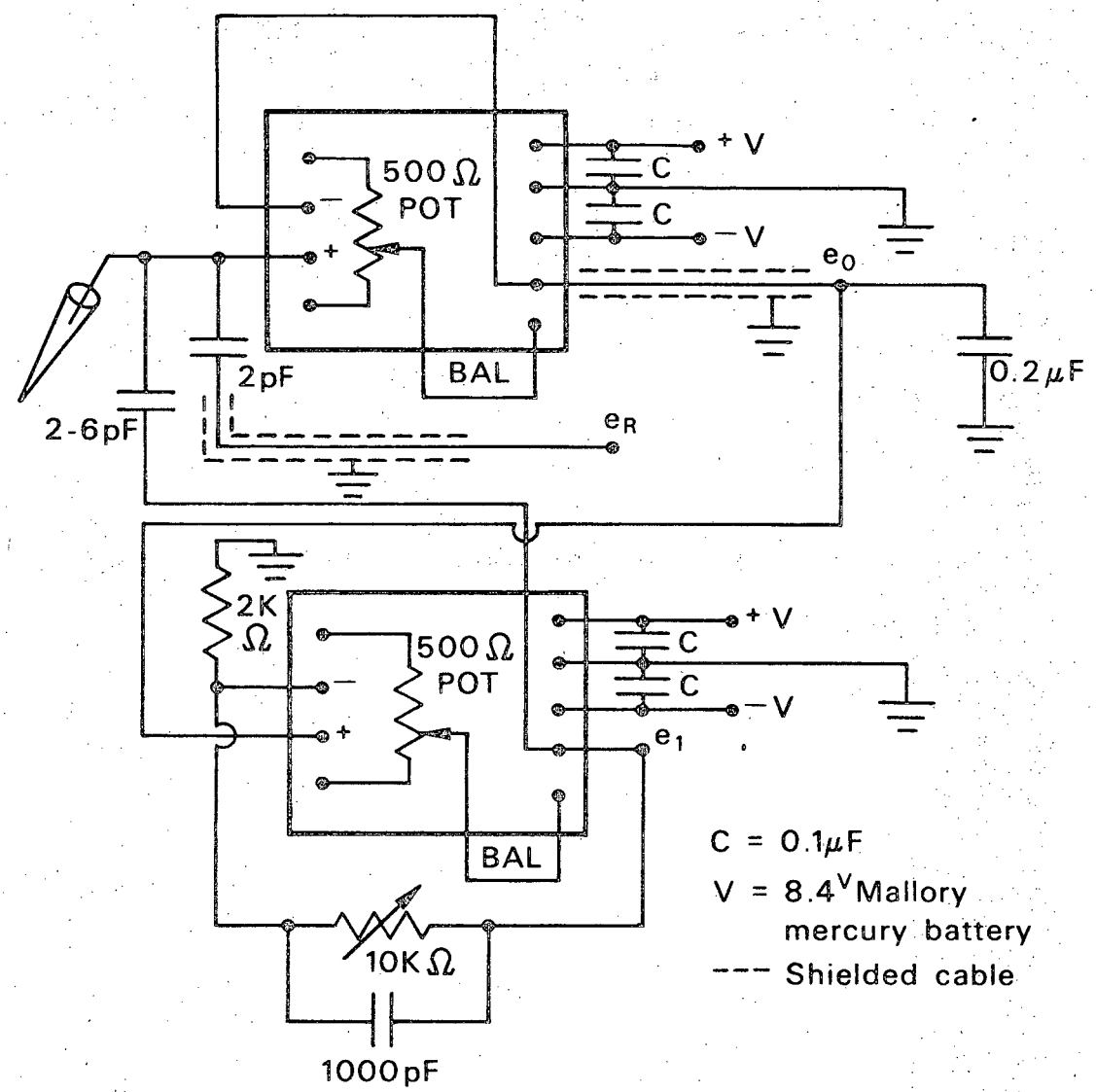

Bottom view of KM47C operational amplifiers

DBL 698-5011

c. Triangular wave generator

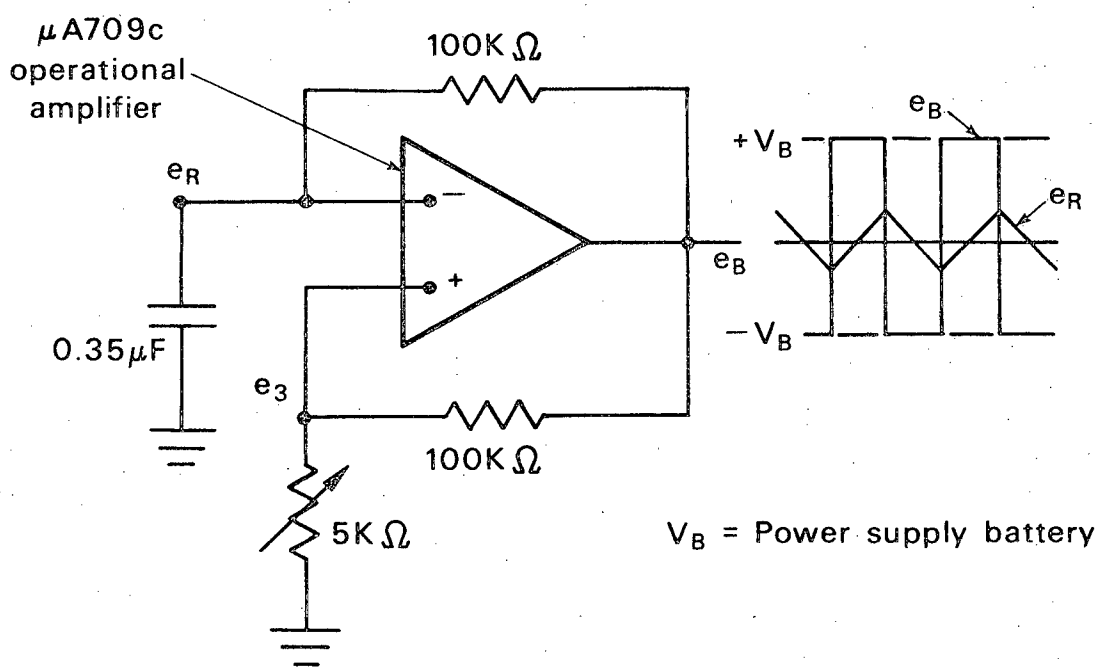

DBL 698-5012

output signal e_o is fed into the non-inverting input of amplifier A_2 whose gain is given by $A_2 = \frac{R_2 + R_1}{R_1}$ and can be changed by adjusting the potentiometer R_2. A negative capacitance feedback loop (see Appendix II for theory) was effected by feeding the output e_1 of A_2 through a small capacitor C_1 (2- 6 pF) to the positive input of A_1. With this negative capacitance scheme, a square voltage pulse which has become degraded by passing through a high impedance probe at the input can be essentially compensated to reproduce the original square pulse.

Whenever high impedance glass microelectrodes are used to record signals from biological tissues, it is highly advantageous to monitor the electrode resistance at any time during an experiment. A resistance check circuit was therefore incorporated into the amplifier design. As is shown in Appendix III, if a triangular wave is applied to the positive input of A_1 through a small capacitor, the output e_o will be proportional to the electrode resistance Re. The circuit which was used to generate a triangular wave is shown in Figure 33c.

The operation of this circuit can be easily seen by noting that a fraction e_3 of the saturation voltage $+V_B$ (for instance) will appear across the 5 KΩ potentiometer in the voltage divider circuit which is applied to the positive input of the μA709C amplifier (Fairchild Electronics). At the same time, the 0.35 μ F capacitor will charge up integrating e_B until $e_R > e_3$ at which time the output e_B switches to $-V_B$. The capacitor will then discharge in a ramp fashion until $e_R < e_3$ when the output e_B will again go to $+V_B$ and the cycle is repeated. This results in a triangular wave at e_R. This voltage e_R shown applied to C_2 in Figure 33a then allows for electrode resistance measurements during the course of the experiments.

The actual amplifier design for the basic recording unit is shown in Figure 33b. Both the DC offset voltages can be nulled to zero by the 500Ω potentiometers and the balance control on the operational amplifiers themselves. The capacitors C across the supply batteries to ground eliminate any voltage fluctuations due to those batteries. The shielded cables reduce most of the interference voltages which are picked up by the leads. The

0.2 μF capacitor at the output e_o is used to limit the band width of the noise voltages. The noise level under fully capacitive compensated conditions was no more than 500 μ when microelectrodes with as high as 100 MΩ impedance were used.

The resulting amplifiers had input impedances of approximately $10^{12}\Omega$, input currents of $< 10^{-11}$ amperes, drift of $<$ 5 mv per one-half hour and compensated frequency response of over 30KC with electrodes whose resistances were as high as 100 MΩ .

APPENDIX II

NEGATIVE CAPACITANCE FEEDBACK

In detecting and amplifying bioelectric signals, distortion of the signal is introduced by the recording equipment. Specifically, bioelectricity detected with very high resistance glass microelectrodes will be distorted if fast voltage fluctuations are contained in the bioelectric signal. As shown below, this is mainly due to the poor frequency response of glass microelectrodes and stray input capacitances of amplifiers. In order to overcome this, negative capacitance feedback may be fruitfully employed to increase the frequency response of the entire recording system. Only a very simple heuristic way of demonstrating the negative capacitance feedback effect is given here.

Consider the schematic diagram (a) which shows a microelectrode (ME) inserted into cell B which generates a biological signal e_B. The amplifier of gain A is an ideal amplifier which introduces no distortion into the system. C_1 is an input capacitance. The loop containing the capacitance C is the negative capacitance feedback loop.

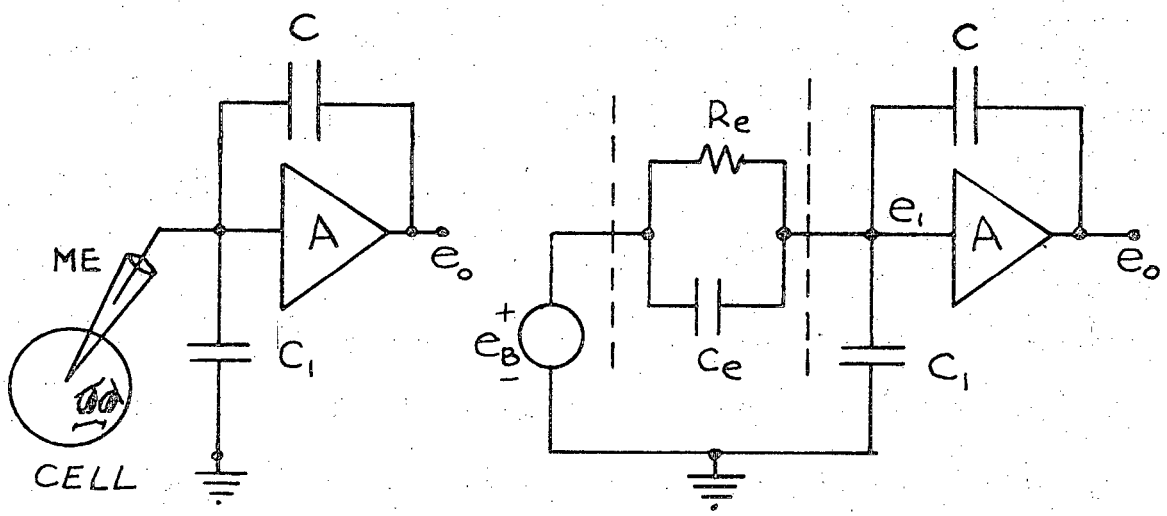

Diagram (a) Diagram (b)

Diagram (b) is a simplified equivalent electrical circuit for the setup in (a). The circuit within the dashed lines represents the microelectrode (ME). Due to the high impedance (Re) and non-zero capacitance (C_e) of the microelectrode and the input capacitance C_1 of the amplifier, the signal e_B will be distorted as it appears at the output e_o. This distortion can be eliminated if one can find conditions in which the output of the system e_o is related to the input e_B by a constant G, i.e., $e_o = Ge_B$. It is now shown that by the use of a capacitive feedback loop (C) from the output to the input of the amplifier, this relationship can be approximately attained with G=A.

The transfer function of the system defined as

$G(s) = \frac{E_o(s)}{E_B(s)}$ ((s) being the complex frequency variable in

the Laplace transformation) will be determined, assuming that the amplifier of gain A draws no appreciable current at its input and essentially has constant gain A over the entire frequency spectrum.

The Laplace transform equivalent of Kirchhoffs current law at node e_1 of diagram b is:

$$\sum I(s) = \frac{E_B(s) - E_1(s)}{R_e} + sC_e\left(E_B(s) - E_1(s)\right) \tag{1}$$

$$+ sC\left(E_o(s) - E_1(s)\right) + sC_1\left(0 - E_1(s)\right) = 0$$

Noting that $E_o(s) = A\ E_1(s)$

and defining $\tau_e = ReCe$, $\tau = ReC$, $\tau_1 = ReC_1$

we substitute $E_o(s)/A$ for $E_1(s)$ in equation (1) and multiply by A x R_e.

Therefore,

$$AE_B(s) - E_o(s) + s\tau_e E_B(s)A - s\tau_e E_o(s) + s\tau AE_o(s) \tag{2}$$

$$-s\tau E_o(s) - s\tau_1 E_o(s) = 0$$

rearranging and collecting like terms:

$$A(1+s\tau_e)E_B(s) = \left(1 + s\tau_e - s\tau A + s\tau + s\tau_1\right)E_o(s) \tag{3}$$

or

$$G_s \equiv \frac{E_o(s)}{E_B(s)} = \frac{A(1+s\tau_e)}{1 + s(\tau_e + \tau_1 + \tau(1-A))} \tag{4}$$

By selecting C and an appropriate gain A, it is clear that $\tau(1-A)$ can be made close to $-\tau_1$ in which case the transfer function G(s) becomes

$$G_s(s) \approx \frac{A(1+s\tau_e)}{(1+s\tau_e)} \approx A \tag{5}$$

Thus, by adjusting the negative capacitance to the input of the amplifier, the distortion due to the microelectrode and stray capacitances is essentially eliminated.

APPENDIX III

ELECTRODE CHECKING METHOD AND CIRCUIT

Consider the following equivalent circuit representation of a microelectrode at the input of an amplifier A with associated circuitry to measure the electrode resistance (Re) (see diagram C). It is shown below that $V_{2max} = R_e(mv)$

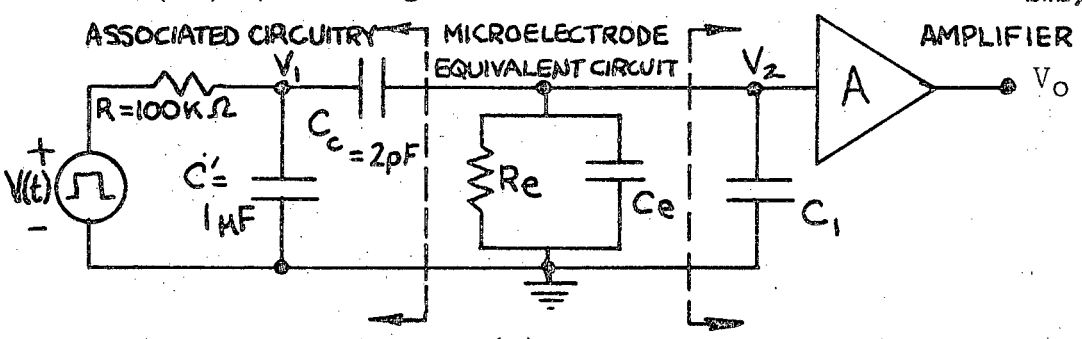

Diagram (c)

Let V(t) be a repetitive square wave as shown in Diagram (d)

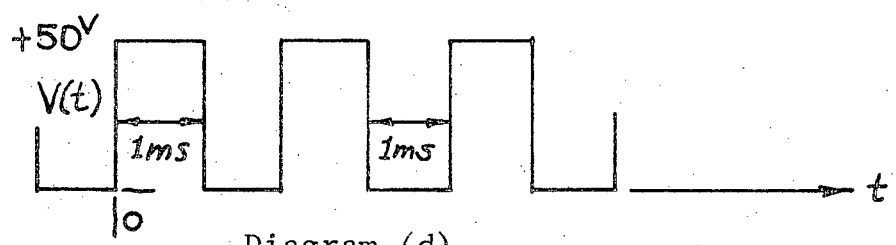

Diagram (d)

Under an applied pulse of $V_{(t)}$, the voltage pulse of $V_1(t)$ will be given approximately by:

$$V_1(t) = 50\,(1 - e^{-t/RC'}) \text{ where } RC' = 100\,ms$$

Therefore, at $t = 1ms$, $V_1(1ms) \equiv V_{peak}$

$$V_1(1ms) \approx 50\,(1 - e^{-1/100}) \approx V_{peak}$$

Hence, $V_{peak} \approx 50\left(1 - 1 + \frac{1}{100}\right) \approx \frac{1}{2}$ Volt, using the first two terms of a Maclaurins series - e^x

$V_1(t)$ is given approximately as shown

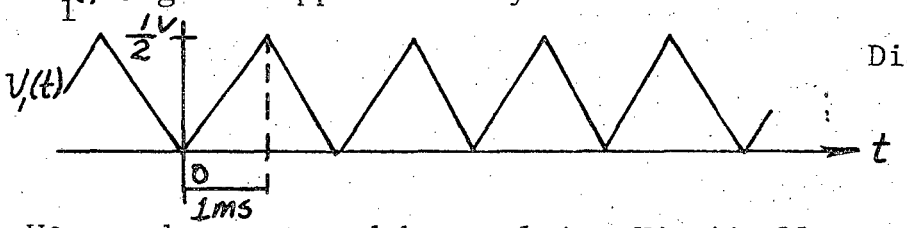

Diagram (e)

V2 can be computed by applying Kirchhoffs current law at node V_2

$$\sum i = -C_c \frac{d}{dt}(V_1 - V_2) + \frac{V_2}{Re} + (Ce + C_1)\frac{dV_2}{dt} = 0 \quad (1)$$

or rearranging

$$\frac{V_2}{Re} + (Ce + C_c + C_1)\frac{dV_2}{dt} = C_c \frac{dV_1}{dt}$$

or, $$V_2 + Re\,(Ce + C_c + C_1)\frac{dV_2}{dt} = ReC_c\frac{dV_1}{dt} \quad (2)$$

$\frac{dV_1}{dt}$ is a square wave:

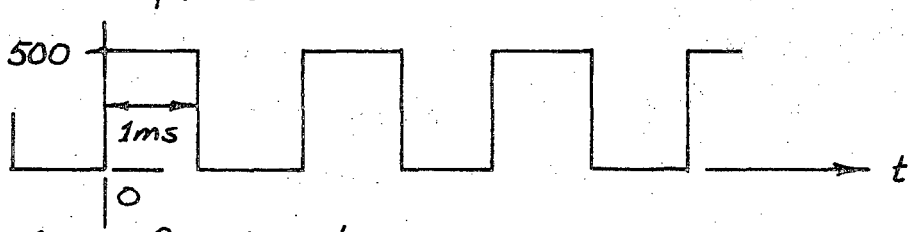

Therefore, for 1 pulse

$$ReC_0\frac{dV_2}{dt} + V_2 = 500C_cRe \text{ where } C_0 = Ce + C_c + C_1$$

So V_2 is as shown in (f):

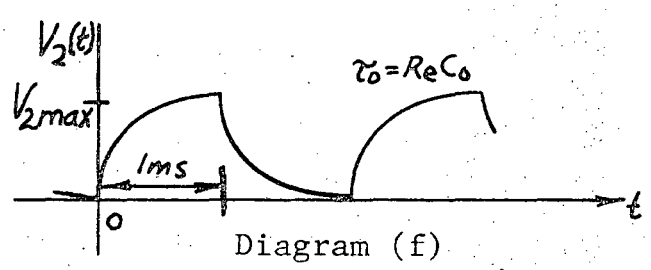

Diagram (f)

where $V_2 max = 500C_cRe$

substituting $C_c \simeq 2pF$ and $Re(M\Omega)$

$$V_2 max = 500 \cdot 2pF \cdot Re \cdot 10^6$$

Therefore, $V_2 max = Re\,(mv)$

and the rounding is given by

$$\tau_o = C_o Re = (C_1 + Ce + C_C)Re$$

which can be resquared by compensation as was shown in Appendix II.

In practice, electrode resistance is checked as follows: the triangular waveform generated by the circuit shown in Figure 33c is applied through the capacitor C_2 (in Figure 33a) to the positive input of amplifier A_1. In the uncompensated state the output e_o is a distorted square wave as shown in diagram (f). This distortion is essentially compensated for by adjusting the potentiometer R_2 (see Figure 33a) to achieve maximum rise time of the waveform. This maximum is judged by maximum "squareness" of the output waveform e_o. The peak amplitude of e_o in millivolts gives the electrode resistance in Megohms.

BIBLIOGRAPHY

Abercrombie, M. and E. J. Ambrose. 1958. Interference microscope studies of cell contacts in tissue culture. Experimental Cell Research, 15: 332-345.

Abercrombie, M. and E. J. Ambrose. 1962. The surface properties of cancer cells: a review. Cancer Research, 22: 525-548.

Abercrombie, M. and E. M. Heaysman. 1953. Observation on the social behavior of cells in tissue culture. I. Speed of movement of chick heart fibroblasts in relation to their mutual contacts. Experimental Cell Research, 5: 111-131.

Abercrombie, M. and E. M. Heaysman. 1954. Observations on the social behavior of cells in tissue culture. II. Monolayering of fibroblasts. Experimental Cell Research, 6: 293-306.

Abercrombie, M. and E. M. Heaysman and H. M. Karthauser. 1957. Social behavior of cells in tissue culture. III. Mutual influence of sarcoma cells and fibroblasts. Experimental Cell Research, 13: 276-292.

Ambrose, E. J. and J. A. Forrester. 1968. Electrical phenomena associated with cell movements. Aspects of cell mobility. XXIInd Symposium on the Society for Experimental Biology, Cambridge University Press. Pp. 237-248.

Asada, Y. and G. D. Pappas and M. V. L. Bennett. 1967. Alteration of resistance at an electrotonic junction and morphological correlates. Federation Proceedings, 26: 330.

Auerbach, R. 1964. Retention of functional differentiation in cultured cells. Defendi V. Ed., Wistar Institute Press, Philadelphia, Pa. Pp. 3-10.

Aull, F. 1967. Measurement of the electrical potential difference across the membrane of the Ehrlich mouse ascites tumor cell. J. Cell Physiology, 69: 21-32.

Baird, I. 1967. A new stimulus isolator for biological preparations. Med. Electron.Biol. Engr., 5: 295-298.

Barski, G. and J. Belehradek. 1965. Étude microcinématographique du mechanisme d'invasion canereuse en cultures de tissu normal associe aux cellules malignes. Experimental Cell Research, 37: 464-480.

Bennett, M.V.L., G.D. Pappas, E. Aljure and Y.Nakajima. 1967. Physiology and ultrastructure of electrotonic junctions. IV. Medullary electromotor nuclei in Gymnotid fish. J. Neurophsyiology, 30: 236-300.

Borle, A.B. and J. Loveday. 1968. Effects of temperature, potassium, and calcium on the electrical potential difference in HeLa cells. Cancer Research, 28: 2401-2405.

Boyde, A., F. Grainger and D.W. James. 1969. Scanning electron microscopic observations of chick embryo fibroblasts in vitro, with particular reference to the movement of cells under others. Z. Zellforsch, 94: 46-55.

Carter, S. B. 1965. Principles of cell motility: the direction of cell movement and cancer invasion. Nature, 208: 1183-1187.

Curtis, A.S.G. and M. Varde. 1964. Control of cell behavior: topological factors. J. National Cancer Institute; 33: 15-26.

Del Castillo, J. and B. Katz. 1954. Changes in end-plate activity produced by pre-synaptic polarization. J. Physiology. (London) 124: 586-604.

Devis, R. and D. W. James. 1964. Close association between adult guinea pig fibroblasts in tissue culture, studied with the electron microscope. J. Anatomy, 98: 63-68.

Eccles, J. C. 1957. The physiology of nerve cells. The John Hopkins Press, Baltimore.

Farquhar, M. G. and G. E. Palade. 1963. Junctional Complexes in various epithelia. J. Cell Biology, 17: 375-412.

Fawcett, D. W. 1961. Intercellular bridges. Experimental Cell Research (Suppl.) 8: 174-187.

Fawcett, D. W. 1966. An atlas of fine structure, the cell. W. B. Sanders Company, Philadelphia and London.

Furshpan, E. J. and D.D. Potter. 1968. Low-resistance junctions between cells in embryos and tissue culture in Current Topics in Developmental Biology 3, Academic Press, New York.

Galtsoff, P. S. 1925. Regeneration after dissociation (an experimental study on sponges). I. Behavior of dissociated cells of Microciona prolifera under normal and altered conditions. J. Experimental Zoology, 42: 183-221.

Green, H. and G. J. Todaro. 1967. The mammalian cell as differentiated micro-organism. Annual Review of Microbiology, 21: 573-600.

Grobstein, C. 1964. Cytodifferentiation and its controls. Science, 143: 643-650.

Grundfest, H. 1967. Some comparative biological aspects of membrane permeability control. Fed.Proc.,26:1613-1626.

Gurr, E. 1960. Encyclopaedia of microscopic stains. Williams and Wilkins, Baltimore.

Hagiwara, S. and I. Tasaki. 1958. A study of the mechanism of impluse transmission across the giant synapse of the squid. J. Physiology (London) 143: 114-137.

Hempling, H. G. 1962. Potassium transport in the Ehrlich mouse ascites tumor cell. J. of Cell & Comp.Physiology, 60: 181-198.

Hodgkin, A. L. and A. F. Huxley. 1952. Currents carried by sodium and potassium ions through the membrane of the giant axon of Loligo. J. Physiology (London) 116: 449-472.

Hodgkin, A. L. and R. D. Keynes. 1957. Movements of labelled calcium in squid giant axons. J. Physiology (London) 138: 253-281.

Hodgkin, A. L. and W. A. H. Rushton. 1946. The electrical constants of a crustacean nerve fibre. Proc. Roy. Soc. Series B, 133: 444-479.

Humphreys, T. 1963. Chemical dissolution and in vitro reconstruction of sponge cell adhesions. I. Isolation and functional demonstration of the components involved. Developmental Biology, 8: 27-47.

Ito, S. and N. Hori. 1966. Electrical characteristics of the Triturus egg cells during cleavage. J. General Physiology, 49: 1019-1027.

Ito, S. and W. R. Loewenstein, 1969. Ionic communication between early embryonic cells. Developmental Biology, 19: 228-243.

Jamakosmanovic, A. and W. R. Loewenstein. 1968. Intercellular communication and tissue growth. III. Thyroid cancer. J. Cell Biology, 38:556-561.

Kanno, Y. and H. Matsui. 1968. Cellular uncoupling in cancerous stomach epithelium. Nature, 218: 775-776.

Kuffler, S. W. J. G. Nicholls and R. K. Orkland. 1966. Physiological properties of glia cells in the nervous system of amphibia. J. Neurophsyiology, 29: 768-787.

Kuffler, S. W. and D. D. Potter. 1964. Glia in the leech central nervous system. Physiological properties and neuron-glia relationships. J. Neurophysiology, 27:290-320.

Lash, J. W. 1963, in Cytodifferentiation and Macromolecular Synthesis, Symp. Soc. Study Develop. Growth, 21st. Pp 235-260 (Locke, M. ed., Academic Press).

Levine, E. M., Y. Becker, C. W. Boone and H. Eagle. 1965. Contact inhibition, macromolecular synthesis and polyribosomes in cultured human diploid fibroblasts. Proc. National Academy of Sciences U.S., 53: 350-356.

Loewenstein. W. R. 1966. Permeability of membrane junctions. Conference Biological Membranes, Recent progress, Annals of New York Academy of Sciences, 137: 441-472

Loewenstein, W. R. 1967. On the genesis of cellular communication. Developmental Biology, 15: 503-520

Loewenstein, W. R. 1967a. Cell surface membranes in close contact. Role of calcium and magnesium ions. J. Colliod Interface Sci. 25: 34-46

Loewenstein, W. R. 1968. III. Emergence of order in tissues and organs communication through cell junctions. Implications in growth control and differentiation. in The Emergence of Order in Developing Systems, 27th Symposium of the Society for Developmental Biology. Developmental Biology Supplement 2: 151-183.

Loewenstein, W. R. and Y. Kanno. 1964. Studies on an epithelial (gland) cell junction. I. Modifications of surface membrane permeability. J. Cell Biology, 22: 565-586.

Loewenstein, W. R. and Kanno, Y. 1966. Intercellular communication and the control of tissue growth. Lack of communication between cancer cells. Nature, 209: 1248-1249.

Loewenstein, W. R. and Y. Kanno. 1967. Intercellular Communication and tissue growth. I. Cancerous growth. J. Cell Biology, 33: 225-235.

Loewenstein, W. R., M. Nakas, and S. J. Socolar. 1967. Junctional membrane uncoupling. Permeability transformations at a cell membrane junction. J. General Physiology, 50: 1865-1891.

Loewenstein, W. R. and R. D. Penn. 1967. Intercellular communication and tissue growth. II. Tissue regeneration. J. Cell Biology, 33: 235-242.

Loewenstein, W.R., S. J. Socolar, S. Higashino, Y. Kanno and N. Davidson. 1965. Intercellular communication: renal, urinary bladder, sensory, and salivary gland cells. Science, 149: 295-298.

Martinez-Palomo, A., C. Braislovsky and W. Bernard. 1969. Ultrastructural modifications of the cell surface and intercellular contacts of some transformed cell strains. Cancer Research 29: 925-937.

Morgan, H. R. 1968. Ultrastructure of the surface of cells infected with Avian Leukosis-Sarcoma-Virues. J. of Virology Z : 1133-1146.

Moscona, A.A. 1963. Studies of cell aggregation: demonstration of materials with selective binding activity. Proc. National Academy of Sciences U.S. 49: 742-747.

Pappas, G.D. and M.V.L. Bennett. 1966. Specialized junctions involved in electrical transmission between neurons. Annals of New York Academy of Sciences 137: 495-508.

Payton, B.W., M. V. L. Bennett and G. D. Pappas. 1969. Temperature-dependence of resistance at an electrotonic synapse. Science 165: 594-597

Penn, R. D. 1966. Ionic communication between liver cells. J. Cell Biology, 29: 171-173.

Peterson, J. 1969. The release and exchange of phospholipids in chick embryo fibroblasts in tissue culture. Ph.D. thesis in Department of Molecular Biology, University of California, Berkeley.

Peterson, J. and H. Rubin. 1969. Exchange of phospholipids between cultured chick embryo fibroblasts as observed with autoradiography. (In preparation).

Politoff, A. L., S. J. Socolar and W. R. Loewenstein. 1967. Metabolism and the permeability of cell membrane junctions. Biochim. Biophys. Acta. 135: 791-793.

Politoff, A. L., S. J. Socolar and W. R. Loewenstein. 1968. Permeability of a cell membrane junction: dependence on energy metabolism. J. General Physiology, 53: 498-515.

Potter, D. D., E. T. Furshpan and E. J. Lennox. 1966. Connections between cells of the developing squid as revealed by electrophysiological methods. Proc. National Academy of Sciences. U.S. 55: 328-335.

Revel, J. P. and J. D. Sheridan. 1968. Electrophysiological and ultrastructural studies of intercellular junctions in brown fat. J. Physiology (London) 194: 34p

Rubin, H. 1960. The suppression of morphological alterations in cells infected with Rous sarcoma virus. Virology, 12: 14-31.

Rubin, H. 1966. Fact and theory about the cell surface in carcinogenesis. In, Major problems in developmental biology, Locke ed.

Rubin, H. 1967. The behavior of cells before and after virus-induced malignant transformation. In, The Harvey Lectures, Series 61.

Rubin, H. and C. Colby. 1968. Early release of growth inhibition in cells infected with Rous sarcoma virus. Proc. National Academy of Sciences U.S. 60: 482-488.

Sheridan, J. D. 1966. Electrophysiological study of special connections between cells in the early chick embryo. J. Cell Biology, 31: C 1.

Sheridan, J. D. 1968. Electrophysiological evidence for low-resistance intercellular junctions in the early chick embryo. J. Cell Biology, 37: 650-659.

Sheridan, J.D. 1968a. Talk given at Gordon Conference on Cell Structure and Metabolism. Meridan, N.H.

Slack, C. and J. F. Palmer. 1969. The permeability of intercellular junctions in the early embryo of Xenopus Laevis studied with a fluorescent tracer. Experimental Cell Research, 55: 416-419.

Stoker, M. 1964. Regulation of growth and orientation in hamster cells transformed by polyoma virus. Virology, 24: 165-174.

Stoker, M. 1967. Contact and short-range interactions affecting growth of animal cells in culture in Current Topics in Developmental Biology, 2 :107-128. (A. Moscona Ed., Academic Press, New York).

Stoker, M. 1967a. Transfer of growth inhibition between normal and virus-transformed cells: radioautographic studies using marked cells. J. Cell Science 2:293-305.

Stoker, M. and I. Macpherson. 1961. Studies on transformation of hamster cells by polyoma virus in vitro. Virology, 14: 359-370.

Stoker, M. and H. Rubin. 1967. Density dependent inhibition of cell growth in culture. Nature, 215: 171-172.

Subak-sharpe, H., R. R. Burk and J. D. Pitts. 1969. Metabolic cooperation between biochemically marked mammalian cells in tissue cuture. J. Cell Science, 4: 353-367.

Temin, H. M. and H. Rubin. 1958. Characteristics of an assay for Rous sarcoma virus and Rous sarcoma cells in tissue culture. Virology, 6: 669-688.

Todaro, G. J., G. K. Lazar and H. Green. 1965. The initiation of cell division in a contact-inhibited mammalian cell line. J. Cellular Comp. Phsyiol. 66 325-333.

Trelstad, R. L., E. D. Hay and J. P. Revel. 1967. Cell contact during early morphogenesis in the chick embryo. Developmental Biology, 16: 78-106.

Vogt, M. and R. Dulbecco. 1960. Virus-cell interaction with a tumor-producing virus. Proc.National Academy of Sciences. U.S., 46: 365-370.

Vogt, P. and H. Rubin. 1962. The cytology of Rous sarcoma virus infection. Cold Spring Harbor Sumposia. Vol. 27: 395-405.

Wickson-Ginzburg, M. and A. K. Solomon. 1963. Electrolyte metabolism in HeLa cells. J. of General Physiology, 46: 1303-1315.

Williams, A.E. and N. A. Ratcliffe. 1969. Attachment of ascites tumor cells to rat diaphragm as seen by scanning electron microscopy. Nature, 222: 893-895.

Woodward, D. J. 1968. Electrical signs of new membrane production during cleavage of *Rana pipiens* eggs. J. General Physiology, 52: 509-531.

LEGAL NOTICE

This report was prepared as an account of Government sponsored work. Neither the United States, nor the Commission, nor any person acting on behalf of the Commission:

A. Makes any warranty or representation, expressed or implied, with respect to the accuracy, completeness, or usefulness of the information contained in this report, or that the use of any information, apparatus, method, or process disclosed in this report may not infringe privately owned rights; or

B. Assumes any liabilities with respect to the use of, or for damages resulting from the use of any information, apparatus, method, or process disclosed in this report.

As used in the above, "person acting on behalf of the Commission" includes any employee or contractor of the Commission, or employee of such contractor, to the extent that such employee or contractor of the Commission, or employee of such contractor prepares, disseminates, or provides access to, any information pursuant to his employment or contract with the Commission, or his employment with such contractor.

TECHNICAL INFORMATION DIVISION
LAWRENCE RADIATION LABORATORY
UNIVERSITY OF CALIFORNIA
BERKELEY, CALIFORNIA 94720